National Library
of Canada

Acquisitions and
Bibliographic Services Branch

395 Wellington Street
Ottawa, Ontario
K1A 0N4

Bibliothèque nationale
du Canada

Direction des acquisitions et
des services bibliographiques

395, rue Wellington
Ottawa (Ontario)
K1A 0N4

Your file Votre référence

Our file Notre référence

NOTICE

The quality of this microform is heavily dependent upon the quality of the original thesis submitted for microfilming. Every effort has been made to ensure the highest quality of reproduction possible.

If pages are missing, contact the university which granted the degree.

Some pages may have indistinct print especially if the original pages were typed with a poor typewriter ribbon or if the university sent us an inferior photocopy.

Reproduction in full or in part of this microform is governed by the Canadian Copyright Act, R.S.C. 1970, c. C-30, and subsequent amendments.

AVIS

La qualité de cette microforme dépend grandement de la qualité de la thèse soumise au microfilmage. Nous avons tout fait pour assurer une qualité supérieure de reproduction.

S'il manque des pages, veuillez communiquer avec l'université qui a conféré le grade.

La qualité d'impression de certaines pages peut laisser à désirer, surtout si les pages originales ont été dactylographiées à l'aide d'un ruban usé ou si l'université nous a fait parvenir une photocopie de qualité inférieure.

La reproduction, même partielle, de cette microforme est soumise à la Loi canadienne sur le droit d'auteur, SRC 1970, c. C-30, et ses amendements subséquents.

Canada

Physical and electrochemical investigation of novel ultrathin films

Roberta Back

Department of Chemistry
McGill University, Montreal

November, 1992

A thesis submitted to the Faculty of Graduate Studies and
Research in partial fulfillment of the requirements of the
degree of Ph.D.

National Library
of Canada

Bibliothèque nationale
du Canada

Acquisitions and
Bibliographic Services Branch

Direction des acquisitions et
des services bibliographiques

395 Wellington Street
Ottawa, Ontario
K1A 0N4

395, rue Wellington
Ottawa (Ontario)
K1A 0N4

Your file Votre référence

Our file Notre référence

ISBN 0-315-87610-7

Canada

ACKNOWLEDGMENTS

I wish to thank all those who have helped at various stages in the development of this thesis. My supervisor, Professor Bruce Lennox, has been an endless source of inspiration and support, and working under his guidance has taught me much about science and about myself.

I am grateful to Drs. A.S. Hay and M. Strukelj, McGill University, Chemistry, for providing a marvelous series of polyimides.

I am also grateful to Drs. T.X. Neenan and T.M. Miller, AT&T Bell labs, for sending us the beautiful dendrimer molecules.

Mass spectral data and analysis were kindly provided by Dr. O. Mamer, McGill Biomedical Mass Spectrometry Unit, and Dr. J. Finkenbine, McGill University, Chemistry. Invaluable assistance in the use of the Atomic Force Microscope was cheerfully provided by Shaune Hanley.

The UV-vis spectrum of the fullerene mixture was measured by Antonella Badia.

All the people in my lab deserve a very special thanks for their discussions and their friendship. These include Zhao, Louis, Antonella, Michelle, Ling, Li, Tara, Jiaiyi, Mala, Susan, and Fuyuan. I am particularly grateful to Louis and Antonella for the very <u>thorough</u> job of proof-reading. The abstract was kindly translated by Christine Carbonneau.

I am forever indebted to Marko, who has helped me keep body and soul together when I felt like they were flying apart.

Finally, I acknowledge with deep gratitude the love and support of my parents and my brother.

This thesis is lovingly dedicated to the memory of
my father,

Robert Arthur Back
Aug.1929-Dec.1991

Great is truth, and mighty above all things: it endureth,
and is always strong: it liveth and conquereth forevermore.
The more thou searchest, the more thou shalt marvel.

First and Second Books of Ezra,
The Apocrypha

ABSTRACT

A study of novel ultrathin films is presented in two sections. The first section presents an investigation of several unconventional film-forming molecules at the air/water interface using the surface film balance apparatus. Strongly hydrophobic fullerenes (C_{60} and C_{70}) were found to spread at the air/water interface to form Langmuir films of multilayer rather than monolayer thicknesses. The formation of these well-defined multilayers is independent of the initial surface density of the fullerene. The films adopt discrete thicknesses of 4-5 monolayer equivalents. The multilayer of the non-spherical C_{70} exhibited a transition attributed to a reorientational process that was not observed with the C_{60} multilayer. A calculation of the work of compression for the two fullerene films confirmed important differences between the C_{60} and C_{70} films. 1,3,5-Phenylene-based hydrocarbon starburst dendrimers were also found to form multilayer Langmuir films at the air/water interface. The formation of these multilayers, however, is dependent on the initial surface density of dendrimer, and believed to rely upon interpenetration amongst dendrimer molecules. Langmuir-Blodgett films of dendrimer co-spread with fatty acid were examined by Atomic Force Microscopy. A series of amorphous polyimides also appear to form multilayer Langmuir films, possibly because they adopt a conformation on the water surface that renders them more rigid than in the bulk material.

The second section describes the electrochemical and interfacial properties of two series of thiophene/ferrocene conjugates. The detailed electrochemistry of these compounds is described, including their electro-oxidative polymerization and the subsequent characterization of the polymer film. Their unique bifunctional nature leads to the formation of a polymer material that is intrinsically limited to the formation of monolayers. At the air/water interface, these molecules have a well-defined phase transition from a disordered state to an ordered state. Their oxidative polymerization was effected chemically at the air/water interface in both their expanded form, in which they

are extended on the water surface, and a more condensed form, although it was observed to proceed more rapidly in the expanded form.

In both studies, the properties of the ultrathin films that are formed are discussed in the context of the transition from aggregates to bulk material. The implication of the present results is also discussed with respect to the nature of the surface tension measurement in the surface film balance experiment. Finally, the importance of an architecture imposed by the properties of the molecules such as that observed in the electropolymerization of the thiophene/ferrocene compounds is discussed.

RESUME

Une étude sur des nouvelles pellicules ultra-fines est présentée en deux sections. La première section présente une étude de plusieurs molécules non-conventionelles capables de former des pellicules à l'interface air/eau en utilisant la balance de pellicule surface. Des fullèrenes fortement hydrophobes (C_{60} and C_{70}) s'étendent à l'interface air/eau, formant des pellicules multi-couches de Langmuir et non des pellicules ayant une seule couche d'épaisseur. La formation de ces multi-couches bien définies est indépendente de la densité de surface initiale des fullèrenes. Les films adoptent une épaisseur équivalente à 4-5 monocouches. Les multi-couches des fullèrenes C_{70} non-sphériques démontrent une transition de phase orientationnelle qui n'a pas été observée avec les multi-couches C_{60}. Les calculs des travaux de compression sur les deux pellicules de fullèrenes ont confirmé des différences importantes entre les pellicules C_{60} et C_{70}. Les dendrimères "Starburst" d'aryle benzène forment également des pellicules multi-couches de Langmuir à l'interface air/eau. La formation de ces multi-couches dépend cependent de la densité de surface initiale des dendrimères, et semble dépendre de l'interpénétration entre les dendrimères. Les pellicules Langmuir-Blodgett constituées de dendrimères et d'acides gras ont été examinées par la Microscopie de Force Atomique. Plusieurs polyimides amorphes ont été étalées à l'interface air/eau. Ceux-ci semblent former des pellicules multi-couches de Langmuir. La formation de ces multi-couches semble cependent dépendre de la structure secondaire du squelette polymérique, laquelle rend les molécules plus rigides.

La deuxième section décrit les propriétés électrochimiques et interfaciales de deux séries de nouvelles supramolécules thiophène/ferrocènes. L'électrochimie de ces composés est décrite en détail, de même que leur électropolymérisation anodique et la caractérisation des pellicules polymériques formées. La nature bifoncttionnelle unique de ces composés entraîne la formation de matériaux polymériques, qui sont limités intrinsèquement à la formation de monocouches. A l'interface air/eau, ces molécules

exécutent une transition de phase bien définie, d'un état de désordre à un état d'ordre. La polymérisation oxidative de ces composés a été effectuée chimiquement à l'interface air/eau à partir de ces deux états; il a été observé que la polymérisation a lieu plus rapidement à partir de l'état de désordre. Dans les deux sections, les propriétés des pellicules ultra-fines formées sont discutées dans le contexte de la transition: agrégats à l'état solide. L'implication des résultats présentés est aussi discuté par rapport à la nature des tensions de surface mesurées avec le balance de pellicules surface. Finallement, l'importance de l'architecture moléculaire, observée par example dans l'électropolymérisation des composés de thiopènes et de ferrocènes est discutée.

TABLE OF CONTENTS

SECTION II

INTRODUCTION

"Nanotechnology": it has the ring of a "buzzword", or jargon, but it arises from a new multidisciplinary field that considers the realm of "nanostructures", that is, a world on the nanometer scale.

This new-found field is a symptom of our desire to miniaturize our surroundings, to enable us to conquer more and more of our technological advances at once. Nanotechnology is the means to this miniaturization of the future. To date, much of our miniaturization has been brought about by old technology, but we have reached several limits imposed by this technology. In order to further condense and streamline the operation of our devices, we must peer further down, into the depths where atoms and electrons behave as individual entities, large and distinct, with properties unique to the atomic scale. It is indeed this collection of properties that atoms exhibit when considered individually or in small aggregates, as opposed to in the bulk, that determines many of the principles of nanotechnology.

Aggregates of individual atoms exhibit electronic and optical properties that are a result of their size and in some cases are the result of quantum effects. Once amassed into the bulk, many of these properties are no longer accessible. These properties have been known for some time, from both theoretical and experimental results. Our ability to observe these properties directly, however, and to consider harnessing them for our own use, is new. The advances made in techniques designed to create structures on the nanoscale have been accompanied by the advances made in lasers, microsopy and spectroscopy, to give us a rich and informative view of the nanostructures we create.

Monolayers can be thought of as pseudo-nanostructures. Whereas they may extend over a region visible to the naked eye, they are defined as being one molecule in thickness. They may be assembled in several ways. Deposition techniques such as chemical vapour deposition and sputter coating produce films that are largely isotropic and often the thickness of such films is difficult to control. Langmuir-Blodgett (LB) films, on the other hand, are intrinsically limited to increments of monolayer thickness. LB monolayer films involve the orientation of molecules at an interface, resulting in a highly anisotropic structure. The interface acts as a template, and is responsible for imposing the order amongst the oriented molecules. The anisotropy and the molecular thickness of these films lead to unique electrical and optical properties.

The conductivity of a material in a monolayer may be quite different from the conductivity of the same material in the bulk. Furthermore, conductivities of monolayers will often be anisotropic. The conductivity perpendicular to the film will be affected by, among other things, the rate of electron tunnelling through the film. This rate may be significant for highly resistive materials in ultrathin films [1], where the tunneling is through space, and unaided by the molecular structure of the film. If the material is highly conducting, however, exceptionally high conductivities may be observed along the plane of the film [2].

The optical properties of certain materials in an ultrathin film are quite different from the optical properties of the bulk material. When several monolayers are combined to form an ultrathin film with a thickness on the order of optical wavelengths, the reflective and refractive properties of the film may be quite distinct [1]. Furthermore, the high degree of orientation in LB films and self-assembled monolayers leads to films with anisotropic polarizability, and thus nonlinear optical behaviour. It must be stressed that this behaviour can be as much a function of the physical structure of the monolayer as it is of the chemical structure of the monolayer. Finally, some LB films have additional orientation within the plane of the film [3]. This arises from the dipping method of LB film formation, in which the molecules may align themselves in the direction of dipping,

---

1. Roberts, G.G., in *Electronic and Photonic Applications of Polymers*, Ed. Bowden, M.J.; Turner, S.R., ACS series 218, **1988**, p.225.
2. Yassar, A.; Roncali, J.; Garnier, F., *Macromolecules*, **1989**, *22*, 804.
3. Wegner, G. *Ber. Bunsenges. Phys. Chem.* **1991**, *95*, 1326.

due to sheer forces, and is observed particularly in rigid rod materials [3]. This lends another dimension to the anisotropic polarizability of the films.

It was put forward by Don Eigler at *Nature*'s conference, *Nanotechnology: Science at the Atomic Scale*, Tokyo, 1992 [4], that nanotechnology does not yet exist. What we have at present is the potential for a powerful technology, based on the growing field of "nanoscience". The distinction is an important one. The results of basic science dealing with things and events on the nanoscale have yet to be translated into what can fairly be called technology. Yes, the potential is immensely attractive, but the bridge needed to span the divide between nanoscience and nanotechnology is far from complete, and until this bridge exists, nanotechnology remains simply uncharted territory. One of the present needs is for a better understanding of basic nanoscience, which will be achieved only through basic studies of structure/property relationships in nanostructures such as the ones described in the following pages.

This thesis is largely concerned with the properties of molecules at interfaces. The approaches are varied: a specific technique (the surface film balance) is studied under a range of conditions using a diverse group of molecules, and a coherent series of thiophene/ferrocene conjugates is examined in several monolayer formations using various techniques. In both approaches, however, the underlying goal is to elicit information about interfacial phenomena, to probe films of molecular thickness, and to gain some understanding of their oftentimes unique behaviour. It is from this depth of understanding that a true nanotechnology may emerge.

---

4. Ball, P.; Garwin, L., *Nature*, **1992**, 355, 761.

SECTION I
Studies of Unconventional Langmuir Film- Forming Materials at the Air/Water Interface

I.1. INTRODUCTION

I.1.1. Historical Perspective

In 1889 Fraulein Agnes Pockels wrote to Lord Rayleigh: "My Lord, - Will you kindly excuse my venturing to trouble you with a German letter on a scientific subject?" [5]. She then went on to describe her extensive studies of water surfaces that she had been persuing for more than a decade. Although her words were modest, the work was so significant that Lord Rayleigh eventually forwarded these results to *Nature*, leading to their publication in 1891 [6]. In this first paper she discussed the effects of contaminants, such as waxes, oils and other easily available substances, on the surface tension and mobility of water surfaces. More details of her biography are included in a paper by Laidler [7].

Pockels had a very rudimentary but elegant apparatus set up in her kitchen, consisting of a shallow pan filled to the brim with water in which she could change the surface area of the water using a strip of tin placed across the edges of the pan. She first measured the surface tension with a small button to which a sliding weight balance was attached. The button was allowed to rest just at the water surface, and the balance was loaded to the maximum mass the surface tension of the water could bear before the button broke away. Then the area on the pan was varied and the resulting decrease in surface tension was observed as the button was released from the water surface. The general principle involving the measurement of the force of the surface tension of clean

---

5. Letter from Agnes Pockels to Lord Rayleigh, translated by Lady Rayleigh, which he forwarded to Nature, to be published in the following reference.
6. Pockels, A., *Nature*, **1891**, *43*, 437.
7. Laidler, K.J., *Chem 13 News*, **1991**, 11.

water on an object, and comparison of this force with that exerted on the same object by a water surface modified by some surface active material, is known as the Wilhelmy method [8]. A testament to the elegance of Pockels' technique is that much of the work on monolayers at the air/water interface today uses the same type of surface film balance apparatus, or modified versions thereof.

The most significant feature noted by Pockels was that a clean water surface had a surface tension that was invariant with surface area, but a contaminated water surface exhibited two distinct types of behaviour. The first, at large areas, was like that of a clean water surface, for which the surface tension is invariant with area. However, as the area of the contaminated surface was decreased, (by moving the tin strip along the pan), a critical area was reached beyond which the surface tension dropped dramatically with further decrease in area, as signified by the breaking away of the button from the water surface. She named the former behaviour "normal" (that is, like a clean water surface), and the latter behaviour "anomalous".

Pockels continued her work for several years [9], making extensive studies on various aspects of surface tension, including techniques to measure it [9d], time resolved surface tension [9f] and a very thorough study of the wetting properties of several liquids (water, glycerol, olive oil, oleic acid, benzene, petroleum, turpentine, carbon disulfide, diethyl ether and ethanol) on a range of surfaces (ice, glass, carbon, fats, gums, sugar and various metals) [9e]. Her research was methodical and carefully done, and broke ground for further studies on the surface tension of water, and how it can be altered by what we now think of as surface active materials. It was Lord Rayleigh himself, (having been engaged in similar but less extensive studies on the surface tension of water when he

---

8. Wilhelmy, L., *Ann. Physik*, **1863**, *119*, 177.
9. a) Pockels, A., *Nature*, **1892**, *46*, 418. b) Pockels, A., *Nature*, **1893**, *48*, 152. c) Pockels, A., *Weid. Ann.*, **1899**, *67*, 668. d) Pockels, A., *Ann. D. Physik*, **1902**, *8*, 855. e) Pockels, A., *Physik. Z.*, **1914**, *15*, 39. f) Pockels, A., *Physik. Z.*, **1916**, *17*, 441. g) Pockels, A., *Science*, **1926**, *64*, 304. h) Pockels, A., *Kolloid Z.*, **1933**, *62*, 1.

received her initial correspondance), who eventually calculated that the films of contaminants on the water surface were one molecule thick [10].

Irving Langmuir at General Electric Company was a later pioneer in the field of interfacial behaviour, developing the Langmuir film balance on which many surface studies are now performed. It consists of a pan of water like that of Pockels, but with one floating barrier in addition to the moving one in her arrangement. Displacement of the float is correlated to the surface tension, replacing the Wilhelmy method. Langmuir used the film balance to make numerous studies from 1917, when he published his first major work on molecules in insoluble monolayers [11], until well into the 1940's. One of Langmuir's collaborators, Katherine Blodgett, worked with him to devise the deposition method of monolayer films from the water surface (where they are known as "**Langmuir films**") to a solid substrate (where they are known as "**Langmuir-Blodgett (LB) films**") [12].

Much important work in the field followed, particularly in the two decades preceeding the Second World War, triggered largely by Langmuir's work. Key publications such as Adam's *Physics and Chemistry of Surfaces* [13] appeared at that time.

Later, additional surface science books appeared that devoted some space to the behaviour of monolayers at the air/water interface. However, the most useful and thorough publication on this subject was by Gaines [14]. In his monograph, Gaines succeeded in uniting a huge portion of the work, up to 1966, on monolayers at the liquid/gas interface in a very readable and comprehensive way. Historically, his timing

---

10. Rayleigh, Lord, *Phil. Mag.*, **1899**, *43*, 437.
11. Langmuir, I., *J. Am. Chem. Soc.*, **1917**, *39*, 1848.
12. a) Blodgett, K., *J. Am. Chem. Soc.*, **1934**, *56*, 495. b) Blodgett, K., *J. Am. Chem. Soc.*, **1935**, *57*, 1007.
13. Adam, N.K., *The Physics and Chemistry of Surfaces*, 3rd ed. Oxford University Press, London, **1941**.
14. Gaines, G.L. Jr., *Insoluble Monolayers at Liquid-Gas Interfaces*, Interscience Publishers, John Wiley & Sons, Inc. New York, **1966**.

was perfect; at that point there was a lull in the field, allowing him to write a very up to date account. However, (and how could he have known?) monolayers at the air/water interface were poised for a renaissance, beginning around 1980. This renaissance was due in part to the availability of such materials as Teflon, allowing for ultraclean conditions in troughs. Contamination had always been a problem in this work, as any surfactant contaminant, no matter how dilute, was immediately concentrated at the surface, exactly where the vital measurements were being made! Furthermore, interest in thin films was growing, spurred in part by the electronics industry, which was trying to miniaturize components dramatically, and in part by the biological and medical sciences, whose interest in membranes had reached the molecular level. Whatever the impetus for this rebirth, work with the surface film balance experiment is still burgeoning, and new reviews and monographs appear constantly [15]. The monograph by Gaines, however, provides an excellent starting point from which to approach the field, and when carefully examined, often prevents the proverbial reinvention of the wheel in the design of new experiments.

I.1.2. Surface Film Balance Apparatus

The technique for establishing monolayer Langmuir films at the air/water interface employs a shallow rectangular Teflon-lined pan filled to the top of the edges with water, as depicted in Figure 1. One or two moving barriers change the area of the water surface on which the sample has been deposited. As this area is changed, the surface pressure, π, of the water is monitored. This apparatus is known as a surface film balance.

---

15. a) Ulman, A., *An Introduction to Ultrathin Organic Films*, Academic Press Inc. Toronto, **1991**. b) Kuhn, H., *Thin Solid Films*, **1989**, *178*, 1.

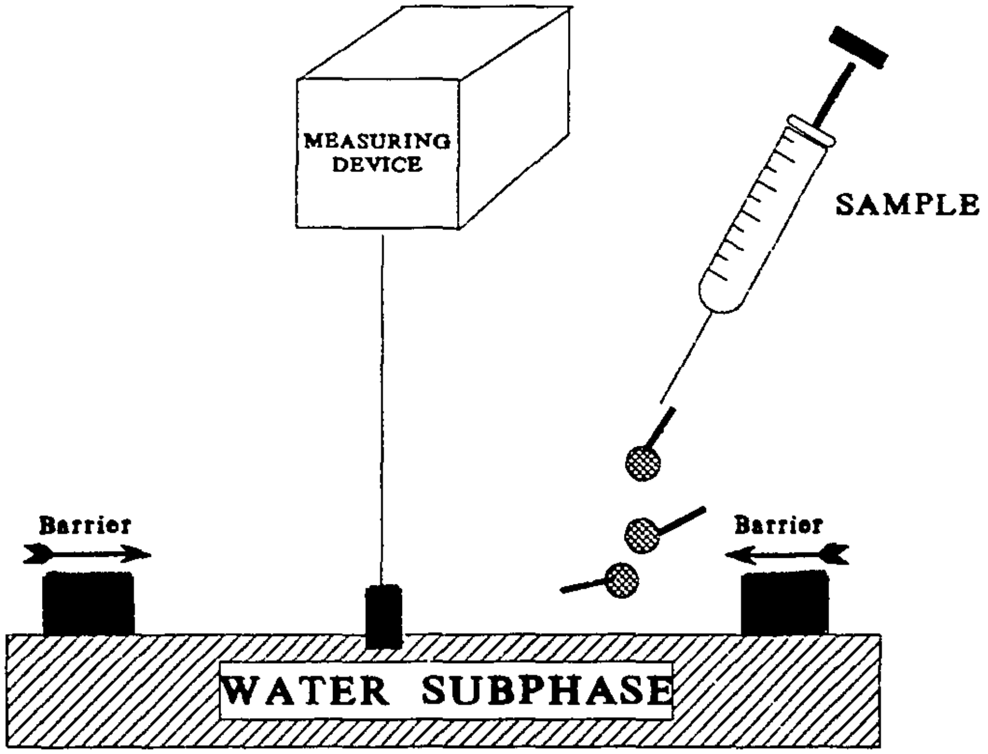

Figure 1. A typical surface film balance apparatus, with two moving barriers.

Surface pressure, π, is defined as the difference between the surface tension of pure water, γ_o, and the surface tension of water modified by some sample molecule, γ, in the following equation:

$$\pi = \gamma_o - \gamma \qquad (1)$$

When the surface of water is uncontaminated it establishes the maximum surface tension (71.97mN/m at 25°C [16]) through strong intermolecular bonding of the surface water molecules, which creates a highly ordered surface. This value corresponds to γ_o in equation (1). Surface active molecules are described as those which cause a change in the surface tension of water, usually by orienting themselves at the air/water interface. These molecules are typically amphiphilic, and the hydrophilic end will affiliate itself with the water surface while the hydrophobic end will prefer the air, thus providing the driving force for the orientation. By achieving this orientation, surface active molecules lower the surface tension of the water by disrupting the order and hence the intermolecular bonding of the surface water molecules. This lowered surface tension corresponds to γ in equation (1). It is important to note here that by definition, π can never be larger than γ_o, which at 25°C is 71.97mN/m.

There are two popular methods for measuring the surface pressure, both dating back to the origins of monolayer work at the air/water interface. These are both illustrated in Figure 2. The first is the Wilhelmy plate technique, a modification of which was used by Pockels. It involves a small sheet of material, suspended from a mass balance so that it is partially submerged in the water. Theory states that the mass of the plate will vary with the surface tension, as the surface tension exerts more (or less) force on the plate. The plate is therefore weighed both before deposition of the sample at the interface and after. The surface tension values of the clean and contaminated water surfaces are derived directly from these measurements, and the surface pressure is

---

16. *CRC Handbook of Chemistry and Physics*, Ed. Weast, R.C., *61st ed.*, CRC Press Inc., Florida, **1980**.

I Wilhelmy Plate

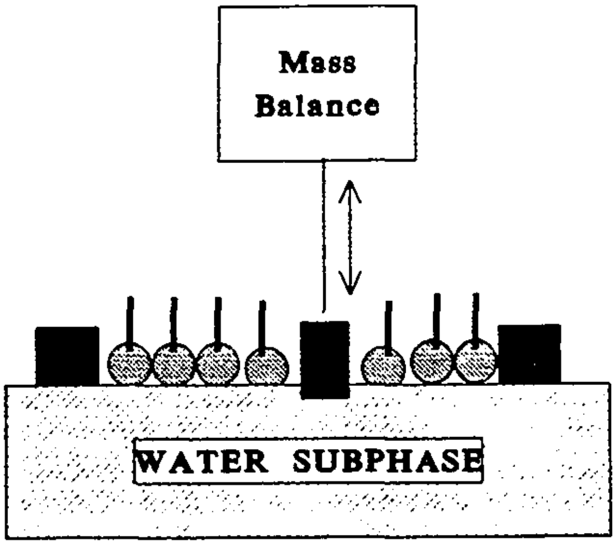

II Langmuir Film Balance

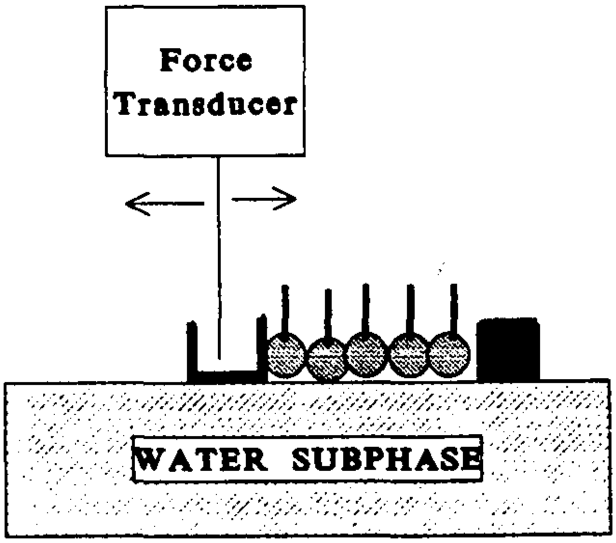

Figure 2. Two methods for measuring surface pressure. I) The Wilhelmy plate technique. II) The Langmuir film balance.

calculated from the difference. Some problems with the technique include the requirement that the contact angle between the water surface and the sheet be invariant before and after the sample is deposited on the water surface, and during compression of the sample on the water surface. If the sample contaminates the sheet, altering the nature of the sheet surface, the contact angle will change, decreasing the validity of the measurement. Thus a very clean sheet of material is of upmost importance. The sheet may be made of many materials, sand-blasted platinum being the most common, as it is relatively easy to clean (by flaming). Filter paper has also been used, having the benefit of a zero contact angle with the water surface. It must be used in a disposable fashion, however, as it is virtually impossible to clean. Glass is also used, but is prone to contamination.

The other popular method for the measurement of surface tension illustrated in Figure 2 is the aforementioned Langmuir film balance. In this technique, a floating barrier fixed across the width of the trough replaces one of the moving ones in Figure 1, in such a way as to separate a pure water surface on one side of the float from the contaminated water surface on the other side of the float. The theory states that the difference in surface tension between these two surfaces will cause the lateral displacement of the float in a way that is quantitatively proportional to the surface pressure. A force transducer is attached to the float to detect this lateral displacement. This measurement of the surface pressure is a direct differential method, whereas the Wilhelmy method involves the comparison of two absolute measurements to obtain the surface pressure. An excellent description of the two techniques can be found in Gaines' book [14].

I.1.3. Langmuir Films of Conventional Film-Forming Molecules

In Langmuir film experiments, data is typically collected in an isotherm, in which surface pressure is plotted as a function of the area available per molecule on the water surface between the barriers (moving and/or floating). A compression isotherm of palmitic acid, a typical molecule for Langmuir film studies, is shown in Figure 3 [17]. The surface pressure is measured as the barriers are compressed to decrease the area available to the individual palmitic acid molecules. At large areas (>50Å^2 per molecule) the surface pressure is zero, indicating that the surface density of the palmitic acid molecules is not high enough to change the surface tension. This is the "normal" behaviour observed by Pockels above the critical area (I.1.1.), and may be described as a gas-analagous state, in which the molecules are isolated from one another. As the barriers are compressed, the critical or onset area, A_{on}, is reached (45Å^2 per molecule), where the surface pressure begins to rise. This indicates that the surface tension is beginning to drop, (as in the "anomalous" behaviour observed by Pockels (I.1.1.)), as a result of the orientation of polar head groups of the palmitic acid molecules at the water surface, where they disrupt the intermolecular bonding and order of the surface water molecules. At 39Å^2 per molecule, $A_{t(1)}$, a discontinuity is observed in the curve, as the molecules relieve the rising surface pressure by removing the hydrocarbon tails from the water surface. This point can be thought of as a phase change or transition, where the film has gone from the gas-analagous state to a condensed state or liquid-analagous state, in which the molecules are now interacting with one another, but are still compressible. A further phase transition occurs at $A_{t(2)}$, which corresponds to the transition from the liquid-analagous state to a solid-analagous state, in which the molecules are in a highly ordered arrangement which is virtually incompressible. This phase is also marked by a discontinuity in the curve. The limiting area, A_{lim}, may be defined as the x-intercept of the tangent to the part of the curve that corresponds to the solid-analagous phase (22Å^2 per molecule here). This is an indication of the area required per molecule when the film

---

[17] The Angström is used to define the molecular areas in this thesis, as this is the traditional unit used in surface film balance studies.

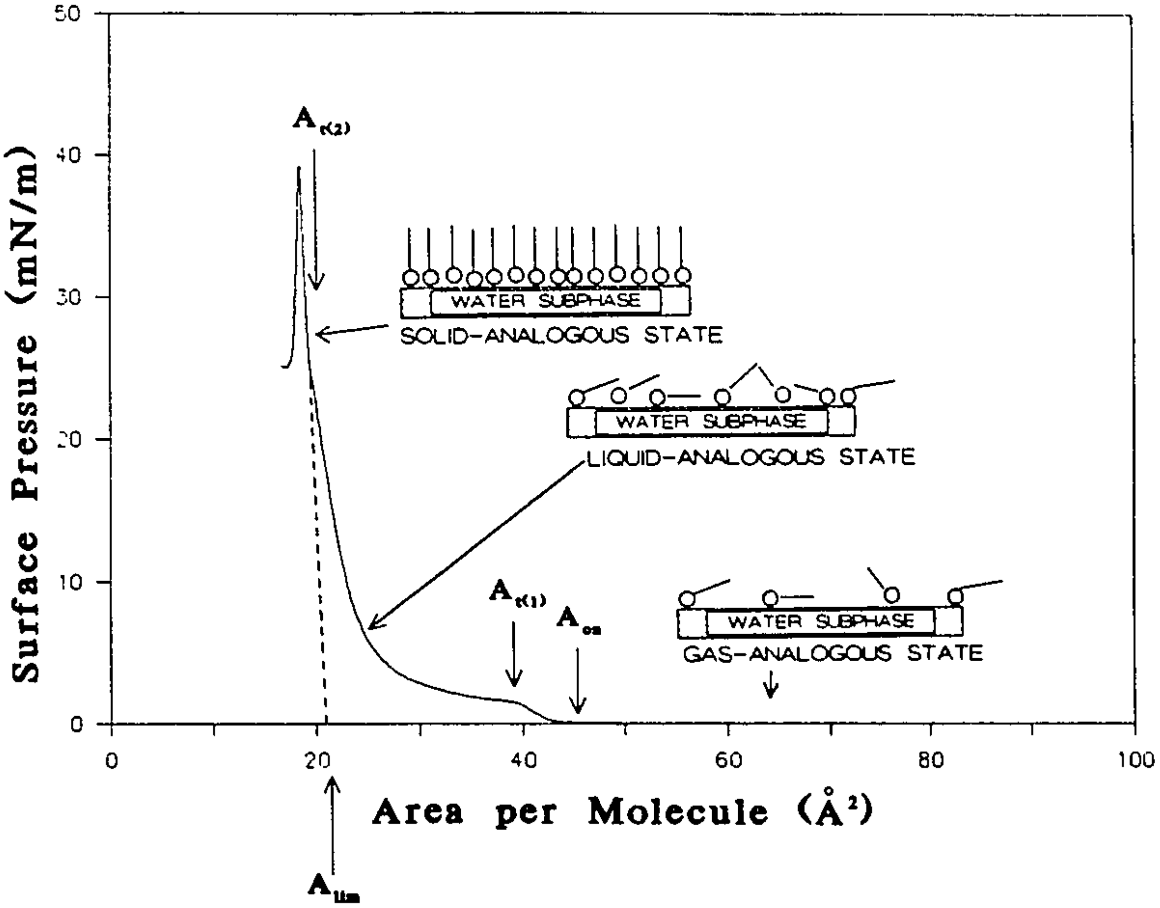

Figure 3. A compression isotherm of palmitic acid, showing the gas-analogous state, the liquid-analogous state, and the solid-analogous state. The onset area (A_{on}), the limiting area (A_{lim}) and the two phase transition areas ($A_{t(1)}$ and $A_{t(2)}$) are also noted.

is in its close-packed form. Thus from the isotherm, one may determine the area occupied by each molecule in the close-packed form, to 0.1Å^2 accuracy.

It was Langmuir, in his first important work (I.1.1.) on the subject of insoluble monolayers at the air/water interface [11] who put forward the notion of surface active molecules being highly oriented at the water surface. In the isotherms he collected for a series of fatty acids, the limiting areas were invariant with the chain length of these molecules. From this he deduced that the molecules must achieve an orientation in which the hydrophobic chains are perpendicular to the air/water interface, and hence do not figure in the limiting area. In this way, the theory was further extended to include the concept of a highly oriented monolayer, at high compressions, for such surface active molecules as the fatty acids.

A plethora of molecules have since been studied at the air/water interface, and even by 1966 the list in Gaines' book [14] is extensive. Typical molecules used to spread and form films on water are those with hydrophilic polar head groups and hydrophobic hydrocarbon tails. There are a range of film-forming abilities amongst the head groups, based on their polarity. The integrity of the films will also depend on the hydrocarbon tail, and its ability to impart stability to the film through strong intermolecular lipophilic interactions. Amongst the polar head groups, ionic groups such as sulfate, sulfonate, and quaternary ammonium ions are so water soluble that they cause the entire molecule to dissolve, even with an alkyl chain of 16 carbons. Aliphatic alcohols, phenol, carboxylic acids (undissociated), methyl ketones, amides, and nitrile all form stable films with an alkyl chain of 16 carbons or greater. Methyl ethers and methyl esters form unstable films and methyl halides and nitro compounds do not form films [13], regardless of the hydrocarbon chain attached. It should be noted that interfaces other than the air/water interface, such as the water/oil interface, have been studied as well. These will not be discussed further in this work, but the reader is referred to Gaines' book [14] for further information.

One group of molecules that have generated much interest are the phospholipids, which assemble in a bilayer formation to make up the membranes in living systems. The research using these compounds at the air/water interface with a surface film balance is a good example of the far-reaching potential of the technique. By assembling the Langmuir films of these molecules at the air/water interface, half of the lipid bilayer is mimicked. Thus by studying these Langmuir films a great deal can be learned about the molecular workings of lipid bilayers in biological systems. Furthermore, co-spreading phospholipids with other molecules may give valuable information regarding the biocompatability of the added species.

Another category of film-forming molecule is that of polymers. These are particularly interesting when considering Langmuir-Blodgett (LB) films, and their applications, which will be discussed in the next two sections. However, before polymeric LB films can be considered, the behaviour of macromolecules at the air/water interface must be studied and understood. Polymer molecules were first examined at the air/water interface by Pockels, although she was not aware of the concept of polymers. A set of papers by Crisp in 1946 [18] clearly summarizes a large quantity of data regarding the formation of Langmuir films from polymer molecules. It was generally observed that in order for a polymer to spread at the water surface, it must contain the proper balance of polar groups and lipophilic groups, as is required for small molecules. As will be discussed in subsequent sections, Wegner and coworkers have recently proposed a modified version of this requirement [19]. In a recent paper, Gaines [20] examines the interesting point regarding the conformation of polymer molecules at the air/water interface. In particular, he considers the important question of whether a monolayer of polymer molecules is only truly a monolayer in the case where each monomer unit of the

---

18. a) Crisp, D.J., *J. Colloid Sci.* **1946**, *1*, 49. b) Crisp, D.J., *J. Colloid Sci.* **1946**, *1*, 161.
19. a) Sauer, T.; Arndt, T.; Batchelder, D.N.; Kalachev, A.A.; Wegner, G. *Thin Solid Films*, **1990**, *187*, 357. b) Embs, F.W.; Wegner, G.; Neher, D.; Albouy, P.; Miller, R.D.; Willson, C.G.; Schrepp, W. *Macromolecules*, **1991**, *24*, 5068.
20. Gaines, G.L. Jr. *Langmuir*, **1991**, *7*, 834.

polymer is in contact with the water surface. Obviously, not all polymers will adopt this highly extended configuration at the air/water interface, with such high energy costs. Most polymer chains are more likely to take on some structure in which only a fraction of the monomer units are actually at the air/water interface. In an extreme case, this may result in a conformation as ordered as a helix. Not surprisingly, this is the structure observed for some polypeptides at the air/water interface [21]. The difficulty is thus in differentiating between a two-dimensional film and a three-dimensional film.

The work in this thesis is concerned with unconventional molecules in Langmuir films, that is non-amphiphiles or atypical amphiphiles. Some unconventional molecules have already been studied at the air/water interface. These include rigid polycyclics [22], hydrophobic polymers such as polystyrene [23], large macrocycles such as phthalocyanines, [24], enzymes [25], "octopus molecules", with hydrophobic "bodies" and hydrophilic "tentacles" [26], block copolymers with one ionic moiety that form surface micelles [27], hydrophobic rigid "hairy-rod" polymers [3] and even Buckminsterfullerene [28]. Often these molecules exhibit extremely interesting electronic or optical properties when ordered at the air/water interface, and thus are the source of much interest.

---

21. Malcom, B.R., *Proc. R. Soc. London, Ser. A,* **1968**, *305*, 363.
22. Kenny, P.W.; Miller, L.L.; Rak, S.F.; Jozefiak, T.H.; Christopfel, W.C., *J. Am. Chem. Soc.*, **1988**, *110*, 4445.
23. Kumaki, J., *Macromolecules*, **1988**, *21*, 749.
24. a) Aroca, R.; Jennings, C.; Kovacs, G.J.; Loutfy, R.O.; Vincett, P.S., *J. Phys. Chem.*, **1985**, *89*, 4051. b) Baker, S.; Petty, M.C.; Roberts, G.G.; Twigg, M.V.; *Thin Solid Films*, **1983**, *99*, 53.
25. a) Sun, S.; Ho-Si, P.-H.; Harrison, D.J., *Langmuir*, **1991**, *7*, 727. b) Sriyudthsak, M.; Yamagishi, H.; Moriizumi, T., *Thin Solid Films*, **1988**, *160*, 463.
26. Conner, M.; Kudelka, I.; Regen, S.L., *Langmuir*, **1991**, *7*, 782.
27. Zhu, J.; Eisenberg, A.; Lennox, R.B., *J. Am. Chem. Soc.*, **1991**, *113*, 5583.
28. a) Obeng, Y.S.; Bard, A.J., *J. Am. Chem. Soc.*, **1991**, 113, 6279. b) Nakamura, T.; Tachibana, H.; Yumura, M.; Matsumoto, M.; Azumi, R.; Tanaka, M.; Kawabata, Y.; *Langmuir*, **1992**, *8*, 4. c) Milliken, J.; Dominguez, D.D.; Nelson, H.H.; Barger, W.R., *Chem. Mater.*, **1992**, *4*, 252. d) Back, R.; Lennox, R.B., *J. Phys. Chem.*, **1992**, *96*, 8149. e) Ganguly, P.; Paranjape, D.V.; Patil, K.R.; Chaudhari, S.K.; Kshirsagar, S.T., *Indian Jounal of Chemistry*, **1992**, *31*, F42.

Particular effort goes into making LB films of these materials, as the LB film is a good vehicle for many applications, but this often poses difficulties, particularly with very hydrophobic molecules. Aside from the practical interest, however, there is much to learn from the behaviour of these molecules at the air/water interface. By examining these molecules in this manner, the ideas behind the surface film balance experiment can be refined, and the methods for measuring the surface pressure in this experiment can be re-examined. Several questions which arise in this work include: (i) what is the origin of the driving force behind the spreading of such compounds on the water surface, (ii) how does a nonpolar compound change the surface tension of water and (iii) do the Wilhelmy plate and the Langmuir film balance both measure changes in the surface tension of the air/water interface exclusively? These and other questions must be addressed as people begin to investigate such molecules, in order that some sense may be made of the results on a fundamental level.

I.1.4. Langmuir-Blodgett Films

I.1.4.1. General Principles

An important advance in the field of Langmuir films was made when Katherine Blodgett, working at General Electric Company with Langmuir, demonstrated that these films could be transferred to a suitable solid substrate (I.1.1.). Indeed, the resulting films are called Langmuir-Blodgett (LB) films. They can be deposited singly to give a monolayer, or consecutively to form a multilayered film.

The deposition of these films is illustrated in Figure 4 for a hydrophilic substrate. Polar head groups are represented by circles, and hydrophobic tails are represented by sticks. The substrate is submerged into the water subphase, at right angles to the interface, before the sample molecules have been spread. The sample solution is then deposited at the air/water interface, and compressed to the specific surface pressure at which the sample molecules achieve their highly ordered solid-analagous phase. The

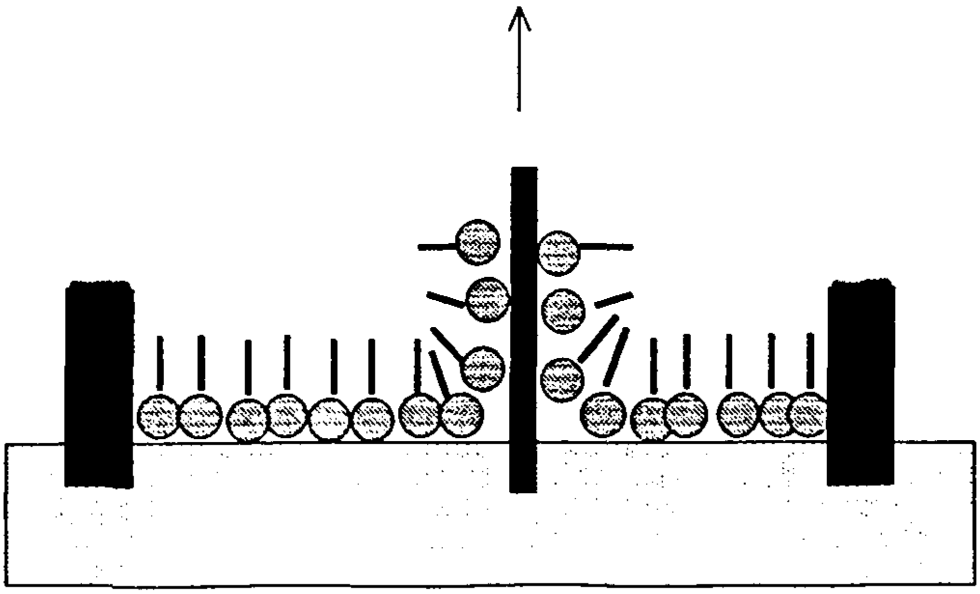

Figure 4. Deposition of an LB film onto a hydrophilic substrate. Polar head groups are represented by circles. Hydrophobic tails are respresented by sticks.

pressure required to create this highly ordered phase is then maintained while the substrate is withdrawn from the subphase, in order that the surface density and hence the molecular configuration in the Langmuir film is maintained to be transferred to the solid substrate. Ideally, as withdrawal of the substrate occurs, the Langmuir film is transferred to the substrate exactly as it exists on the water surface. Once transferred to the solid substrate, the integrity of the LB monolayer film is preserved in part by the interaction of the polar head group with the hydrophilic substrate, and in part from the lipophilic interactions between the hydrophobic tails. This deposition process may be repeated in a variety of ways to achieve multilayered LB films.

An important quantity in LB film formation is the **Transfer Ratio** (**TR**). While immersion and/or withdrawal takes place, and a constant surface pressure is maintained, the motion of the moving barriers required to maintain this surface pressure is recorded. If the transfer proceeds properly, the barriers will move to reduce the surface area between them. The total reduction in surface area between the barriers during the course of one pass through the Langmuir film can be calculated from the net movement of the barriers to give an indication of how much of the Langmuir film was transferred in its original form from the water surface to the solid substrate. This quantity is then divided by the total area of the substrate that was submerged in the subphase (including both sides and all edges), to give the Transfer Ratio.

This quantity represents the efficiency of the transfer, with a value of 1.0 indicating perfect transfer of the Langmuir film to the solid substrate, most likely with no loss or change of configuration. Values of less than 1.0 indicate either incomplete transfer of the Langmuir film to the solid substrate, or rearrangement of the molecules in the film upon deposition onto the solid substrate to a more expanded configuration. Further experiments are required to distinguish between these two possibilities. Finally, a value of greater than 1.0 usually indicates that the film has collapsed during deposition onto the solid substrate.

If more than one layer is desired, there are several possible arrangements. These are all illustrated in Figure 5. The **X** type of film is always deposited onto a hydrophobic substrate, and deposition only occurs upon immersion. The **Z** type, on the other hand, is always deposited onto a hydrophilic substrate, and deposition only occurs upon withdrawal. The **Y** type of film may be deposited onto a hydrophobic or hydrophilic substrate (a hydrophilic substrate is shown in Figure 5) and deposition occurs both upon immersion and withdrawal of the substrate.

The type of film observed is largely dictated by the molecules in the film, the substrate used, and the nature of the interaction between these. These factors are also important in determining the quality of single layer films. A further measure of control may be achieved over deposition by such experimental parameters as temperature and deposition rate. The **Y** type of film is the more stable of the three, as it relies upon hydrophobic-hydrophobic and hydrophilic-hydrophilic interactions. On the other hand, the noncentrosymmetric nature of the **X** and **Z** types of films can lead to interesting nonlinear optical effects.

Sometimes, it is desired to make an LB film from "uncooperative" molecules, such as those unconventional film-forming molecules mentioned earlier. This situation may arise when attempting to incorporate a molecule with particular properties into an LB film, for a specialized application. A strategy to aid in the formation of such LB films is to co-spread the molecules of interest with some well-behaved surfactant such as a fatty acid or a phospholipid. The well-ordered Langmuir film of the surfactant provides a matrix in which the non-spreading molecules may dissolve and distribute themselves. If the non-spreading molecules incorporate themselves sufficiently into this matrix, then it is sometimes possible to make LB films of the whole network, which will contain both the surfactant and the molecule of interest.

Another problem encountered in the formation and application of LB films is their delicate nature and relative instability. Although many interesting applications

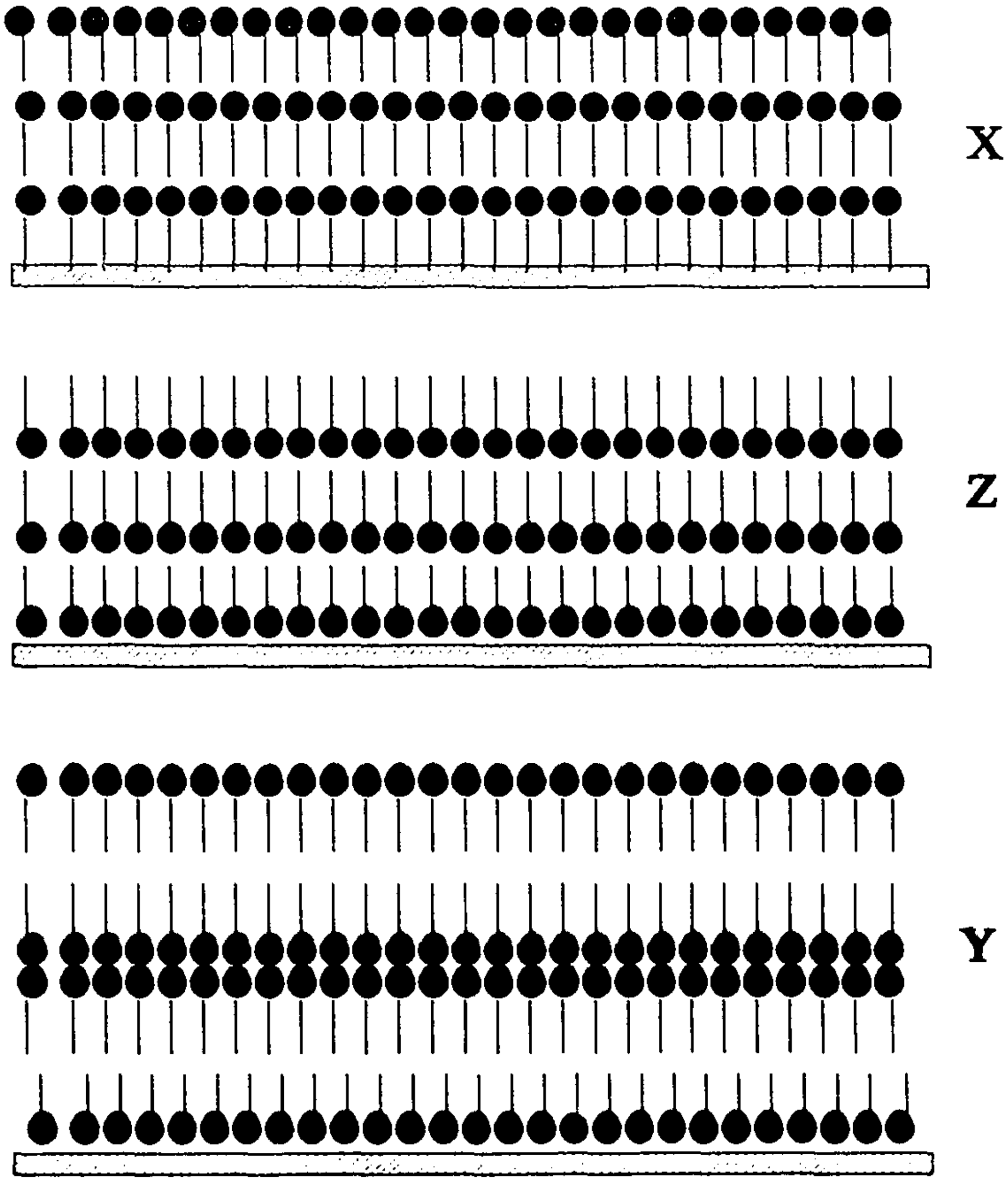

Figure 5. Three possible types of multilayer LB films (X, Y, Z). Polar head groups are represented by circles. Hydrophobic tails are represented by sticks.

suggest themselves in theory for LB films (which will be discussed in the Section I.1.4.2.), they are often thwarted by the practical requirement of durability. One approach to improve the mechanical properties of LB films is to use polymeric materials. There are several ways to achieve this. One method involves spreading amphiphilic monomers on the water surface, and depositing the LB films of these polymerizable materials onto suitable substrates. Polymerization is then initiated within the LB film. This has been successful using several different monomers, particularly the diacetylenes [29]. Their polymerization is usually initiated by UV irradiation, although visible irradiation is adequate with the proper photosensitizers. Thermal polymerizations and gas phase chemically initiated polymerizations are also possible. There are disadvantages to this method, however. Polymers made in this way often give highly strained LB films that crack or craze, as polymerization within the highly ordered LB film often produces a material with a different (usually higher) density than the originally deposited LB film. At the very least, the order of the LB film is usually disrupted upon polymerization, whereas the end application often requires the high degree of order that was present in the monomer film.

Another way to incorporate polymeric materials into LB films is to spread polymerizable molecules on the water surface, compress them to the desired surface density and orientation, and then to polymerize them on the water surface. Again, this could be effected by any sort of suitable irradiation. There is also the possibility of adding a polymerizing agent to the water subphase. However, thermal polymerization on the water surface is not practical. These polymers, made *in situ*, are then deposited on a solid substrate to form the required LB film. This technique is useful, and deserves to be explored further. The resulting materials may not be as highly strained as those produced by the previous strategy, if the conformational changes and density fluctuations can be accomodated by barrier motion prior to LB film deposition.

---

29. Tieke, B.; Lieser, G.; Wegner, G., *J. Polym. Sci.*, **1979**, *17*, 1631.

Finally, when polymers themselves can be spread at the air/water interface, as discussed in Section I.1.3., LB films may then be deposited from the resulting Langmuir films. These films do not exhibit the strain of the films that are polymerized in the Langmuir or LB film form, but are less ordered due to the resistance of the polymer backbone to alignment with other polymer backbones. This recalls the question addressed by Gaines [20] as to whether polymer chains are truly extended on the water surface in two dimensions. The other restriction to this approach is that there is only a limited number of polymer molecules that will spread at the air/water interface and form LB films.

I.1.4.2. **Applications**

Some applications of LB films will now be described, although the purpose of this thesis is not to develop LB films for a particular application, but rather to explore fundamental questions regarding the nature of Langmuir and LB films. The following is by no means an exhaustive list, but rather a sampling of applications, to give the reader an idea of the types of devices that may be designed using LB film technology. These applications, chosen from many examples, are deemed to use the features of LB films to particular advantage.

LB films have two inherently "useful" properties, regardless of their particular molecular composition. The first is their thickness, which can be reduced to the thickness of one molecule, and controlled even more precisely by judicious choice of carbon chain length. Spin coating, another method used in the preparation of thin films, is generally only reliable to approximately 1μm [30], due to the appearance of pinholes at that thickness. The second "useful" property of LB films is their high degree of organization, which can lead to novel electronic and optical properties. The applications of LB films

---

30. Petty, M.C. in *Polymer Surfaces and Interfaces*, Ed. Feast, W.J.; Munro, H.S., John Wiley and Sons, Ltd., Toronto, **1987**, p. 163.

usually exploit one or both of these features, in addition to the possibility of precise control of the composition of the films on a molecular level.

Chemical sensors are one promising application of LB films [31]. They may be designed so that the molecular recognition site, the reaction centre, the transducer of the sensor, or any combination of these is contained in the LB film. It is the ability to design the film on a molecular level that allows for specific functionalities which are required for the sensing device to be incorporated into the film in the desired geometry. Furthermore, the high ratio of surface area to volume in LB films allows for a quick and large response to the analyte solution, relative to a thicker film.

LB films have been used to make both gas sensors and biosensors. Baker *et al* [32] have made a sensor for NO_2 from copper phthalocyanine. The films are deposited onto an aluminum electrode, and the conductivity of the phthalocyanine molecules, which changes in the presence of NO_2, is monitored. The response allows for the detection of ppm concentrations of NO_2 in N_2.

Sriyudthsak *et al* [25b] have developed a glucose sensor with an LB film containing glucose oxidase. The enzyme is adsorbed in a lipid monolayer which is assembled on the water surface, and then the whole film is deposited onto a hydrogen peroxide electrode. Glucose may be detected in various sample matrices with this enzyme sensor.

Another possible type of biosensor is described by Ahlers *et al* [33]. It relies upon the strong binding observed between the protein, biotin, and the ligand, streptavidin. By forming a monolayer with biotin-functionalized molecules, a two-dimensional crystal of streptavidin may be formed through the adsorption of the latter from the subphase into the monolayer at the air/water interface. If this two-dimensional crystal of streptavidin

---

31. Moriizumi, T., *Thin Solid Films*, **1988**, *160*, 413.
32. Baker, S.; Roberts, G.G.; Petty, M.C., *Proc. Inst. Electr. Eng. Part I*, **1983**, *130*, 260.
33. Ahlers, M.; Müller, W.; Reichert, A.; Ringsdorf, H.; Venzmer, J., *Angew. Chem. Int. Ed. Engl.* **1990**, *29*, 1269.

were deposited in the form of an LB film, it could then selectively bind such species as biotinylated proteins and nucleic acids in a sensing fashion.

Besides sensors, LB films may be involved in electronic and optical devices in a variety of ways. One example of this is in microlithography [30]. The molecular thickness of the LB films has the potential to aid in the quest for thinner linewidths and improved resolution in this field. Although optical radiation limited the linewidths in microlithography to a few mm, by employing X-ray radiation or electron beams with wavelengths of <0.1nm, linewidth resolution has now become limited by the degree of electron scatter in the resist material. This may be reduced by careful molecular design of the resist materials, but is vastly improved by decreasing the thickness of the resist film. Hence LB films are an attractive possibility for resist technology. Although LB films may be designed as both positive (photodegrading) or negative (photopolymerizing) resists, the most successful work has been in the photopolymerizable films, as these take on the robust mechanical properties of polymers upon processing. One example of such a film is made of 22-tricosenoic acid [34]. LB films of this fatty acid are photopolymerizable through the double bond functionality to give films that are resistant to plasmas and chemical etching agents, important features for a resist. Linewidths of 60nm have been achieved with this system.

In all of these and other applications, a limiting factor is often the ability of the desired molecules to be incorporated into the LB film. The phthalocyanines are one example of an unconventional film-forming molecule (Section I.1.3.) that has been "forced" into an LB film for the sake of a biosensor design [32]. As LB film technology is further developed, more and more challenging molecules will be introduced into LB films by various routes. The problem is no longer to find a molecule that is known to form an LB film, and that suits one's purposes, but rather to find a way to incorporate the desired molecules into an LB film. With this strategy in mind, the study of

---

34. Barraud, A.; Rosilio, C.; Ruaudel-Teixier, A., *Thin Solid Films*, **1980**, *68*, 91.

unconventional film-forming molecules at the air/water interface takes on a new significance. Although the focus of the following work is to explore the fundamental aspects of Langmuir and LB film formation of unconventional molecules, the implications of this work regarding future applications of LB films is evident.

I.1.5. Unconventional Langmuir Film-Forming Compounds

I.1.5.1. Fullerenes

The discovery in 1985 of the third form of elemental carbon, C_{60}, or Buckminsterfullerene [35], was a momentous event. During carbon vapourization experiments instigated by H.W. Kroto, and performed at Rice University, Texas, in the laboratory of R.E. Smalley, there appeared in the data a mysterious molecular ion at 720 atomic mass units. After intensive work, the structure was revealed to be a beautiful spherical cage of icosahedral symmetry, with 60 carbon units making up the shell. A whole family of these cage-like molecules was suspected to exist, based on the discovery and identification of the next member of the family, C_{70}, in the carbon vapourization experiments. An excellent account of this discovery can be found in *Angewandte Chemie, Int. Ed. Engl.*, in an article by Kroto [36].

The molecule was named **Buckminsterfullerene**, and the extended family, **fullerenes**, after Buckminster Fuller, the architect whose geodesic domes with structures similar to that of C_{60} can be found around the world [37]. Each carbon unit in C_{60} is bonded to three others, forming an sp^2 bonding network. The network consists of 20 hexagons and 12 pentagons, arranged so that each carbon atom is connected to two

---

35. Kroto, H.W.; Heath, J.R.; O'Brien, S.C.; Curl, R.F.; Smalley, R.E., *Nature*, **1985**, *318*, 162.
36. Kroto, H.W., *Angew. Chem., Int. Ed. Engl.*, **1992**, *31*, 111.
37. One such structure graces the 1967 Expo site in Montreal, as part of the American pavillion.

hexagons and one pentagon, with a total diameter of 10.02Å [38]. Figure 6 illustrates the molecular structures of C_{60} and C_{70}.

Since its discovery, the beauty of this symmetrical structure has captured the imagination of scientists from a variety of disciplines. As soon as C_{60} became readily available [38] an explosion of research resulted, with each group wishing to apply "their" technique to the seductive molecule, in an attempt to expose its often elusive or surprising characteristics. The number of papers published on C_{60} is now increasing exponentially, and it is virtually impossible to include an up to date review of the field in this thesis. The following is thus an attempt to collect salient features of current research efforts, in order to present a representative, if not complete, picture of the field.

One of the difficulties encountered in C_{60} work is in forming good crystals of C_{60}. Several papers appeared describing a general lack of success in growing large or regular crystals from solution [39]. For the most part, disordered structures were obtained. Growth from the vapour phase, on the other hand, gave better crystals with a cubic close-packed configuration [40]. Another difficulty encountered in fullerene studies is obtaining reproducible and reliable samples of C_{60}. Werner *et al* [41] have found samples of C_{60} to be prone to contamination by various means. In particular, they compare C_{60} to the highly adsorbant active charcoal. This must be considered when reporting results of C_{60} experiments.

---

38. Krätschmer, W.; Lamb, L.D.; Fostiropoulos, K.; Huffman, D.R., *Nature*, **1990**, *347*, 354.
39. a) Fleming, R.M.; Kortan, A.R.; Hessen, B.; Siegrist, T.; Thiel, F.A.; Marsh, P.; Haddon, R.C.; Tycko, R.; Dabbagh, G.; Kaplan, M.L.; Mujsce, A.M., *Phys. Rev. B*, **1991**, *44*, 888. b) Hawkins, J.M.; Lewis, T.A.; Loren, S.D.; Meyer, A.; Heath, J.R.; Saykally, R.J.; Hollander, F.J., *J. Chem. Soc. Chem. Commun.*, **1991**, 775. c) Gorun, S.M.; Creegan, K.M.; Sherwood, R.D.; Cox, D.M.; Day, V.W.; Day, C.S.; Upton, R.M.; Briant, C.E., *J. Chem. Soc. Chem. Commun.*, **1991**, 1156.
40. Fleming, R.M.; Siegrist, T.; Marsh, P.; Hessen, B.; Kortan, A.R.; Murphy, D.W.;Haddon, R.C.; Tycko, R.; Dabbagh, G.; Mujsce, A.M.; Kaplan, M.L.; Zahurak, S.H., *Mater. Res. Soc. Symp. Proc.*, **1991**, *206*, 691.
41. Werner, H.; Bublak, D.; Göbel, U.; Henschke, B.; Bensch, W.; Schlögl, R., *Angew. Chem. Int. Ed. Engl.*, **1992**, *31* ,868.

C_{60}

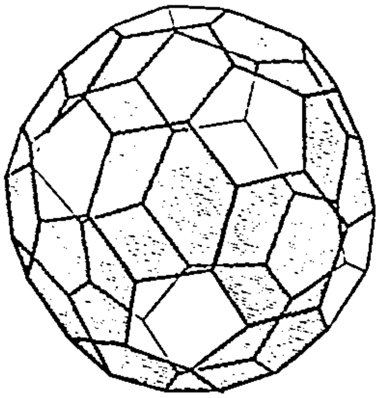

C_{70}

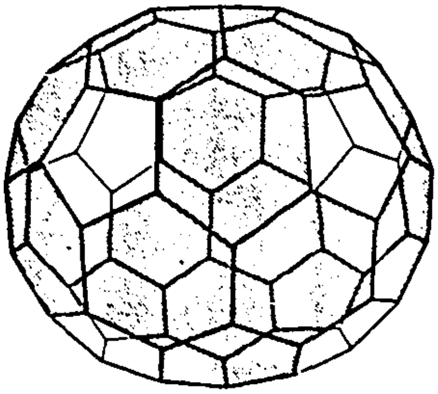

Figure 6. Molecular structures of C_{60} and C_{70}.

The reactivity of C_{60} has been quickly investigated to some extent, with some puzzling results. At first glance, the molecule appears aromatic, with delocalized electrons throughout its structure of sp^2 bonded carbon. However, its reactivity was not like that of benzene, disqualifying it from the aromatic category. This has been attributed to the instability created in the pentagon structures by the double bonds [42]. For example, the reduced species, ($C_{60}H_{36}$) has been formed [43], the radical anion has been polymethylated [44], osmium and platinum complexes have been made [45,46], brominated C_{60} has been formed [47], but no facile electrophilic aromatic substitution-type of reactions have been observed. In fact C_{60} behaves more like an alkene, albeit a moderately unreactive one. Thus it may be concluded that the π electrons of C_{60} are not as readily available for reaction as those of benzene.

The electrochemical investigations of C_{60} provide some insights into the reactivity of C_{60} [48]. Three reversible reduction peaks were found with $E_{1/2}$ values strongly dependent on the solvent. In tetrahydrofuran, these values are -0.21V, -0.81V and -1.39V vs Ag/AgCl, suggesting that indeed reductions should be relatively accessible. However, no oxidation was detected, which to some extent explains the reactivity studies.

From the point of view of surface film balance studies, the symmetry of C_{60} is indeed enticing. All too often, the Langmuir films under investigation consist of large molecules with numerous degrees of freedom, and isotherms that are hence difficult to

---

42. Taylor, R., *Tetrahedron Lett.*, **1991**, 3731.
43. Haufler, E.E.; Concecao, J.; Chibante, L.P.F.; Chai, Y.; Byrne, N.E.; Flanagan, S.; Haley, M.M.; O'Brien, S.C.; Pan, C.; Xiao, Z.; Billups, W.E.; Ciufolini, M.A.; Hauge, R.H.; Margrave, J.L.; Wilson, L.J.; Curl, R.F.; Smalley, R.E., *J. Phys. Chem.*, **1990**, *94*, 8634.
44. Bausch, J.W.; Prakash, S.G.K.; Olah, G.A.; Tse, D.S.; Lorents, D.C.; Bae, Y.K.; Malhotra, R., *J. Am. Chem. Soc.*, **1991**, *113*, 3205.
45. Hawkins, J.M.; Meyer, A.; Lewis, T.A.; Loren, S.D.; Hollander, F.J., *Science*, **1991**, *252*, 312.
46. Fagan, P.J.; Calabrese, J.C.; Malone, B., *Science*, **1991**, *252*, 1160.
47. Birkett, P.R.; Hitchcock, P.B.; Kroto, H.W.; Taylor, R.; Walton, D.R.M., *Nature*, **1992**, *357*, 479.
48. Allemand, P.-M.; Koch, A.; Wudl, F.; Rubin, Y.; Diederich, F.; Alvarez, M.M.; Anz, S.J.; Whetten, R.L., *J. Am. Chem. Soc.*, **1991**, *113*, 1050.

interpret, except in an empirical way. Here is a molecule that has no preferred orientation at the air/water interface, no strong affinity for the water and no tendancy to leave the interface, given its low propensity for sublimation and extremely low water solubility. The possibility therefore exists that it will provide a monolayer whose isotherm may be interpreted in a quantitative way.

Furthermore, if indeed the fullerenes affect the surface tension of the water in the film balance experiment, then aspects of the film balance experiment will have to be reassessed. Classically, the film balance experiment was employed to measure the decrease in surface tension observed when the polar head groups of amphiphilic molecules disturbed the order of the water molecules at the surface (Section I.1.2.). Obviously hydrophobic fullerenes, which have no polar head groups, will not have the same type of influence on the water surface. Thus, if the film balance experiment detects a change in the surface tension of water in the presence of C_{60}, a new type of measurement is being made.

I.1.5.2. Dendrimers

Although traditional polymer studies are concerned with linear molecules, a new class of macromolecules has emerged, called starburst dendrimers, or hyperbranched polymers [49]. Strictly speaking, these are polymer molecules in which all monomer units are branch sites except the terminal monomer units. Although at the present time the only commercial application of these molecules is as size standards for such techniques as Gel Permeation Chromatography (GPC) and X-ray scattering [50], they have many potentially exciting applications. In particular, because of the extensive

---

49. See for example Tomalia, D.A.; Naylor, A.M.; Goddard III, W.A., *Angew. Chem. Int. Ed. Engl.* **1990**, *29*, 138.
50. Starburst dendrimers based upon poly(alkylamides) are available from Polysciences, Warrington, PA, under licence from the Dow Chemical Co.

degree of control with which they may be synthesized, they appear to be ideal building blocks for designing structures on the molecular level to serve the new nanotechnology.

The first such molecules were synthesized by a divergent route, which begins with what will become the centre of the molecule and works outwards by generations. The drawback to such a methodology is that as the molecule becomes larger, and reaction sites more numerous, it is impossible to ensure quantitative reaction at all of these reaction sites, as some sites may become hidden in the expanding structure. Thus, precise control over molecular weight is gradually sacrificed to size in the divergent route.

The molecules that will be used in the surface film balance studies described in this thesis are synthesized by a novel, convergent route [51]. To date, only one other group, besides the supplier of the dendrimers used here, has reported a convergent synthesis of starburst dendrimers [52]. To begin this synthesis, two primary building blocks of the dendrimer, each with a functionality labelled **Z**, are reacted with a trifunctional molecule with two identical functionalities labelled **X**, and one functionality labelled **Y**. The **Z** and **X** groups couple, leaving a product molecule with a **Y** group, which is then converted to a **Z** group. Thus the product molecules are made to resemble the primary building blocks. Indeed, these product molecules, termed dendrons, are the new building blocks for the next reaction step. This next step involves repeating the first step by reacting two dendrons with the same trifunctional molecule as before, to produce new, larger dendrons. When the dendrons reach the desired size, a final assembly reaction is performed, where three dendrons are reacted with a trifunctional molecule with three **X** groups, to form a molecule of spherical symmetry.

The advantage to this methodology over the divergent synthesis is that reaction yields are much better, as each intermediate step involves reaction at only two sites (the

---

51. a) Miller, T.M.; Neenan, T.X., *Chem. Mater.* **1990**, *2*, 346. b) Kwock, E.W.; Neenan, T.X.; Miller, T.M., *Chem. Mater.* **1991**, *3*, 775. c) Miller, T.M; Neenan, T.X.; Zayas, R.; Bair, H.E., *J. Am. Chem. Soc.*, **1992**, *114*, 1018.
52. Hawker, C.J.; Frechet, J.M., *J. Chem. Soc., Chem. Commun.*, **1990**, 1010.

Z-X coupling). Furthermore, the final step, involving the reaction of three large dendrons, would give, by definition, only mono-, di-, and tri-substituted products which are easily separable by chromatography, due to their large molecular weight difference. Thus perfectly monodisperse samples may be obtained using the convergent route, a significant achievement in polymer chemistry, and particularly important for several applications.

Different dendrimers have been convergently synthesized, based on 1,3,5-triarylbenzenes [51], 1,3,5-triarylamides [51a] and 1,3,5-triarylesters [51b]. Second generation dendrimers for each of these starting materials are illustrated in Figure 7. The triarylbenzene dendrimers have also been fluorinated [51c]. These molecules are spherical, owing to the completeness of reaction at every step and the rigidity of the aromatic branches. The dendrimers have very high solubilities. With the exception of the fluorinated dendrimers, they all dissolve in such solvents as benzene, toluene, and chloroform. The solubilities are also high when compared to linear polymers of the same molecular weight. Furthermore, the solubilities of the dendrimers are observed to increase with increasing molecular weight. The aryl ester dendrimers and the lower molecular weight aryl benzene dendrimers are crystalline. The 46 ring aryl benzene dendrimer is amorphous. The dendrimers have high thermal stability (>350°C in air), and also some interesting vitrification properties [51c].

Although these molecules are not typical amphiphiles, it was thought that a comparison of their behaviour at the air/water interface to that of the fullerenes would be interesting. The two materials have some similarities, both being very hydrophobic and spherical. However, whereas the fullerenes are hard spheres, with no possibility of interpenetration, the dendrimers have more potential flexibility in their branched conformations. When compared to linear polymer chains, dendrimers are considered to be very rigid, with no evidence of interpenetration or aggregation in solution [51b]. Nevertheless, at the high two-dimensional concentrations that are imposed at the

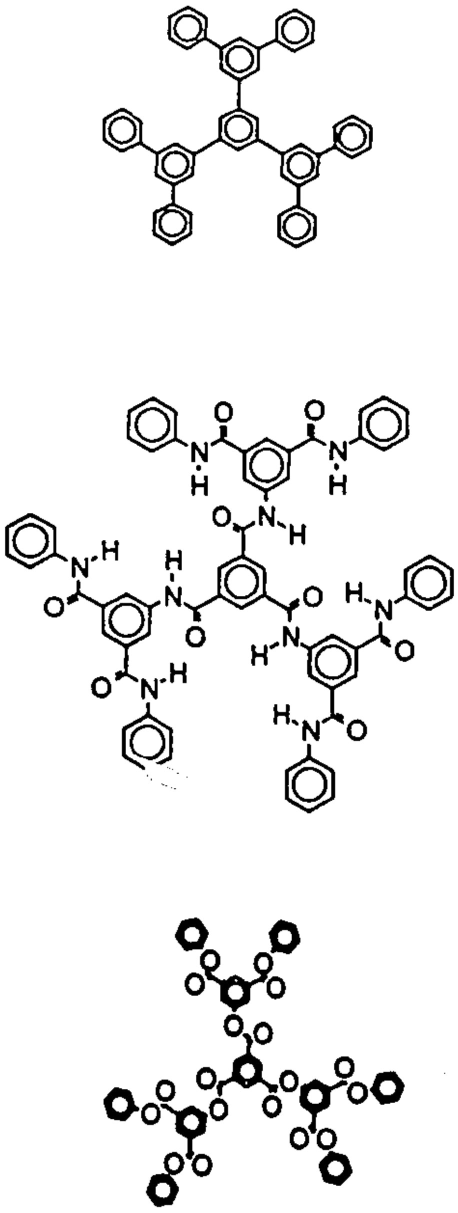

Figure 7. Three 22-ring, second generation dendrimers based on aryl benzene, aryl amide and aryl ester bulding blocks, respectively.

air/water interface, they may be able to adopt a range of conformations, perhaps under the influence of solvent effects. The study of these dendrimers at the air/water interface in conjunction with similar studies of C_{60} and C_{70} would allow for the comparison between the Langmuir films of these two families of molecules. Thus, the question regarding the nature of the surface film balance experiment, and how it is affected by the presence of hydrophobic molecules may be pursued.

I.1.5.3. Polyimides

As was mentioned in previous sections, there have been numerous studies of polymers at the air/water interface, working towards the formation of LB films of polymeric materials. Polymers are thought to be central to the future of LB film applications, as reported in Sections I.1.4.1 and I.1.4.2. Until quite recently, however, the formation of Langmuir and LB films of polymers was thought to require amphiphilicity in the polymer molecule, as for small molecules [53]. In particular, it was assumed that for a polymer to spread at the air/water interface, it must consist of polar groups regularly interspersed with lipophilic moieties, as discussed in Section I.1.3. Indeed, this type of polymer will spread at the air/water interface with varying degress of success, the balance between the polarity and frequency of the hydrophilic groups, and the extent of lipophilicity being crucial. However, studies of some unusual polymers at the air/water interface by Wegner and coworkers challenge this notion [3].

Wegner and coworkers have spread polymers such as phthalocyanine-polysiloxane derivatives [19a] and poly(alkoxy)silanes [19b] at the air/water interface that have no obvious hydrophilicity. Instead they are characterized by a rigid backbone, from which extend long lipophilic chains. Wegner has termed these "hairy-rod" polymers. These molecules spread at the air/water interface as rigid rods, much the same

---

53. a) Ringsdorf, H.; Schmidt, G.; Schneider, J., *Thin Solid Films*, **1987**, *152*, 207. b) Tredgold, R.H., *Thin Solid Films*, **1987**, *152*, 223.

as wooden matchsticks would do. Upon compression, their rigidity is maintained, and they are assembled in a two dimensional nematic type of liquid crystalline phase, again much the same as matchsticks would do. The rods do not collapse into a three-dimensional mass as this would involve the whole rod lifting off the water surface, a costly process in terms of energy. Thus the rigidity of these rods is the key to their spreadability. When in contact with one another at high compressions, their alkyl chains combine to form a fluid solvent layer which surrounds the rigid rod polymers. It is this film of rigid rod polymer molecules surrounded by a solvating network of lipophilic chains that, surprisingly, may be transferred as an LB film to a solid substrate. In fact, upon transfer, sheer forces cause the rods (or backbones) to line up in the direction of dipping, giving the films a high degree of anisotropy. Because of the rigidity of the polymer backbone and the fluidity of the solvating network, these films exhibit the mechanical properties of a solid, and the optical properties of a liquid. Wegner terms this a "molecular composite".

With the poly(alkoxy)silanes it was observed that the number and length of alkyl chains are important in forming LB films, presumably as they make up the integral solvating network. Furthermore, the alkoxy functionality is necessary to allow the polymer to spread; a simple alkyl chain does not have sufficient polarity to do this. Thus slight polarity is necessary for the spreading of these materials, although much less than is usually required for small molecules. To conclude, the key features that provide the integrity for this type of film are the rigidity of the rods (for spreading) and the abundance and polarity of the solvating network (for deposition).

It can then be stated that experience shows there are two possible types of polymer that may be spread at the air/water interface, and transferred as an LB film to a solid substrate. These are amphiphilic polymers and rigid "hairy-rod" polymers [54].

---

54. Embs, F.; Funhoff, D.; Laschewsky, A.; Licht, U.; Ohst, H.; Prass, W.; Ringsdorf, H.; Wegner, G.; Wehrmann, R. *Adv. Mater.* **1991**, *3*, 25.

One family of polymers that may find use for the latter category is the polyimides. Polyimides are very popular for use as engineering thermoplastics, one of the most important high performance materials used in industry today. They are materials that demonstrate extraordinary stability at high temperatures. Their applications are numerous, as they are designed to replace metals and even ceramics in the automotive and aeronautical industries. Their light weight in relation to their strength makes them very efficient materials for engine and body parts, particularly in aircraft and spacecraft, where weight is of critical importance.

The important physical properties of these polymers are quantified by their glass transition temperature (T_g) and their thermo-oxidative stability, as measured by thermogravimetric analysis (TGA). The former property is the temperature at which the material loses its glassy nature, and turns to a rubbery material. Obviously, if the material is being used in an application that depends upon its glassy properties, then this temperature delineates the limit of its usefulness. Thermogravimetric analysis involves heating the sample while monitoring a loss of mass. TGA data is usually quoted as a temperature at which a specified weight loss is observed. Successful materials will therefore combine a high T_g and TGA with good mechanical properties, specifically toughness and stiffness. In addition, their processability must be considered. If solvent resistance is desired, a crystalline polymer is best, but an amorphous material that will dissolve easily in standard organic solvents will be less expensive to process.

Much effort has gone into making LB films of these materials, as poor thermal stability is one of the problems facing attempts to use LB films for practical purposes. Despite the excellent thermal and mechanical properties of polyimides, however, the formation of LB films of these polymers has posed problems. Polyimides have often been deliberately made to be difficult to dissolve in common organic solvents, by making them highly crystalline. This hampers the spreading of these materials at the air/water interface, however. Furthermore, their crystallinity and high rigidity are not conducive to good film formation. The most successful efforts to make polyimide LB films have been by spreading polyimide precursors, most notably polyamic acid [55], and thermally converting this to polyimide after deposition onto a solid substrate. As noted earlier, this technique often produces films which exhibit cracking and crazing, or have substantial internal strain. Recently, LB films of several pyromellitimide polymers were formed from the appropriate polyamic acid derivatives, and examined by Scanning Tunnelling Microscopy (STM) [56]. They show a highly regular film, with periodicity that suggests a zigzag conformation with rotation about the aryl ether linkages. However, to date no polyimides which can be spread at the air/water interface have been reported.

Recently, a series of highly amorphous polyimides was synthesized [57]. The lack of crystallinity in these polymers makes them soluble in common organic solvents. It was felt that they would be good candidates for LB film formation, particularly in light of the propositions of Wegner and coworkers regarding the requirements of macromolecules for spreading. The polyimide molecules that are examined in this thesis were synthesized by Dr. Marko Strukelj, as part of his PhD work under Prof. A.S. Hay at McGill University, Chemistry. The molecular structure of the polymers is shown in Figure 8a. The synthesis involves the condensation polymerization of a dihalide containing the imide functionality and a biphenol containing the sulfone, ketone or bisketone group. The left half of the repeat unit is shown in an energy-minimized structure diagram [58] in Figure 8b, for R = phenyl. These materials exhibit unique properties in the bulk, which are listed in Table 1 [59]. Of primary importance are their high T_g values. Also important is their amorphous

---

55. Kakimoto, M.; Suzuki, M.; Konishi, T.; Imai, Y.; Iwamoto, M.; Hino, T., *Chem. Lett.*, **1986**, 823.
56. a) Sotobayashi, H.; Schilling, T.; Tesche, B., *Langmuir*, **1990**, *6*, 1246. b) Schedel-Niedrig, Th.; Keil, M.; Sotobayashi, H.; Schilling, T.; Tesche, B.; Bradshaw, A.M., *Ber. Bunsenges. Phys. Chem.* **1991**, *95*, 1385. c) Fujiwara, I.; Ishimoto, C.; Seto, J., *J. Vac. Sci. Technol. B.*, **1991**, *9*, 1148.
57. a) Struklelj, M.; Hay, A.S., *Macromolecules*, **1991**, *24*, 6870. b) Struklelj, M.; Hay, A.S., *Macromolecules*, **1992**, *25*, 4721.
58. The Molecular Modeling System, Cambridge Scientific Computing Inc., 875 Massachusetts Ave., Suite 61, Cambridge MA, US.
59. PhD thesis, Marko Strukelj, McGill University, Chemistry.

a)

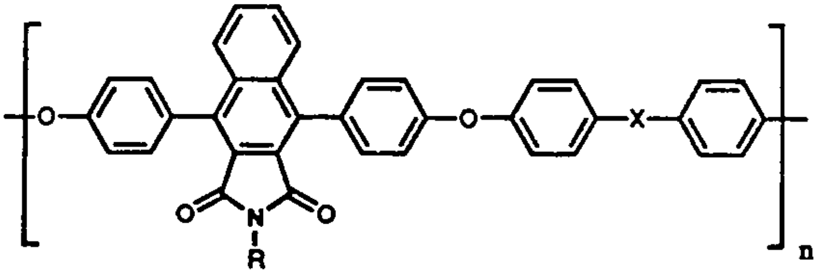

	R
a	methyl
b	dodecyl
c	phenyl

Polymer	X
1a-c	CO
2a-c	SO2
3a-c	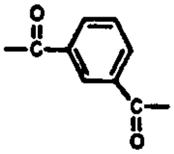

Figure 8a. General structure of polyimide series studied.

b)

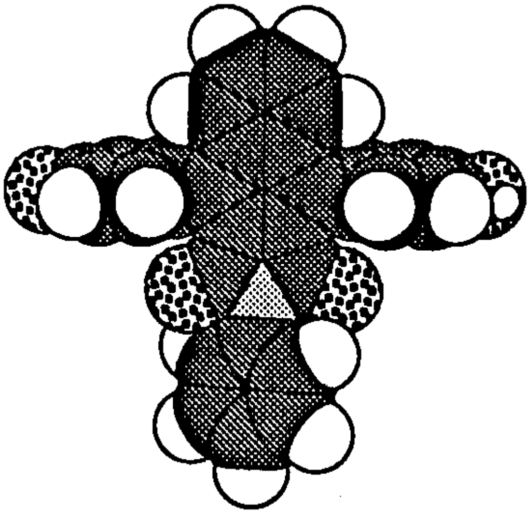

Figure 8b. Minimized structure for the imide-containing (left) half of the repeat unit shown in Figure 8a [58].

TABLE 1 Physical properties of polyimides [57]

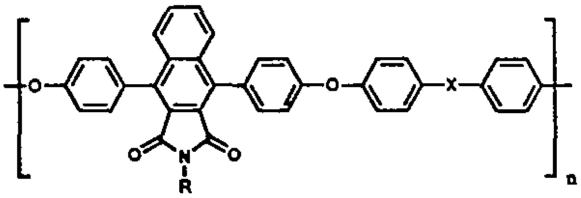

Polymer	X	R	T_g(°C)	Young's Modulus @25°C(GPa)	TGA(°C) in air(-10%)
1b	CO	dodecyl	147	2.6	482
2b	SO_2	dodecyl	167	2.6	471
2c	SO_2	phenyl	310	2.6	555
3a	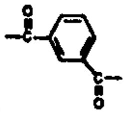	methyl	251	2.4	524
3b		dodecyl	140	2.7	489
3c		phenyl	245	2.0	568

state, which makes it possible to dissolve them in a spreading solvent for the surface film balance studies. This lack of crystallinity is due to the fact that the two phenyl rings directly adjacent to the imide functionality are coplanar, and in a plane perpendicular to the imide functionality, as shown in Figure 8b [59]. This also lends an appreciable rigidity to the polymer, leading to the high T_g values mentioned above. By the same token, the series of polymers for which $X = SO_2$ have the highest T_g values, due to the rigidity of the sulfone unit relative to the ketone and bisketone units. For a given X group, the polymers for which $R = C_{10}H_{21}$ have the lowest T_g values. This is because the dodecyl chain acts as an internal plasticizer by introducing flexibility into the polymer structure.

The Young's moduli of these polymers are listed in Table 1. It is important to note the Young's moduli of these polymers are much lower than those of "rigid rod" or "high modulus" polymers such as polyethylene (240GPa) and polypropylene (42GPa) [60]. Generally speaking, a high modulus polymer is one with a Young's modulus of >25GPa [60]. The polymers considered by Wegner and coworkers [3] are generally of the rigid rod, high modulus category. Young's modulus is as much a function of interchain interactions as it is of the rod-like character of the polymer backbone. Thus, high modulus polymers must not only have a rod-like character, but must also pack efficiently to introduce high crystallinity. The polyimides studied here are specifically designed not to pack well, preventing crystallinity. Nevertheless, their chains have a certain rigidity that could possibly lead to a spreading at the air/water interface of the type suggested by Wegner. Thus, these molecules will allow the novel ideas of Wegner and coworkers to be tested with a slightly different type of rigid polymer, and will possibly provide LB films with very unique thermal properties. Furthermore, they will provide yet another view of

---

60. Jaffe, M. in *Encyclopaedia of Polymer Science and Engineering, 2nd ed.* John Wiley & Sons, Inc., New York, **1985**, 7, 699.

the ways in which the change in surface tension of water, induced by the presence of non-traditional amphiphiles, may be measured by the surface film balance technique.

I.2. EXPERIMENTAL

I.2.1. Surface Film Balance Experiments

The surface film balance experiments were performed on two different troughs. The first was a LAUDA Model D trough, (600x200mm), with one moving barrier (speeds 0.1-200mm/min) and a Langmuir torsion balance (±0.01mN/m). The other trough was a KSV 3000, (600x150mm), with two moving barriers (speeds 0.01-400mm/min) and a Wilhelmy plate (±0.004mN/m), as well as a dipping device (speeds 1.0-85mm/min, ±0.1mm/min). The latter apparatus was used to make LB films. Substrates for these included mica (J.T. EM Services, Inc.), silicon wafers (Semiconductor Processing, Boston MA), evaporated gold (both bare and alkylated) on glass slides (Evaporated Metal Films, Inc. Ithaca, NY), and untreated and silanized glass. To prepare the alkylated gold, the gold substrates were soaked in hot $CHCl_3$ for at least 1 hour. They were then incubated in a 0.005M solution of octadecyl thiol (Aldrich, Milwaukee, WI.) in ethanol overnight. Finally they were rinsed copiously in ethanol to remove excess thiol. To make silanized glass, microscope slides (75x25mm) were suspended in 1M NaOH (ACP Chemicals Inc.)/ethanol solution for 1 hour, while the solution was stirred. They were then rinsed with water and transferred to a similar setup with a 3% aqueous HCl (Anachemia) solution, where they were suspended for 1 hour. Finally, 5-10ml of *n*-octyltriethoxysilane (Petrarch Systems Inc.) was applied slowly with a Pasteur pipette so that it ran down each side of the glass slide. These silanized glass slides were left in $CHCl_3$ overnight to remove all free *n*-octyltriethoxysilane. Both the alkylated gold and the silanized glass exhibited considerably larger contact angles with water than the bare substrates before treatment. No attempt was made to quantify these contact angles.

Sample solutions were manually applied with a μl Hamilton syringe, in 5-10μl drops. The temperature was kept constant at 25°C with a Haake water bath except in the temperature studies, where it was varied from 7°C to 38°C. Sample solutions were allowed at least 15 minutes evaporation time. This is the time elapsed between the application of the sample solution to the water surface and the beginning of the compression cycle.

I.2.2. Compound Preparation

I.2.2.1. Fullerenes

The fullerene samples were obtained from two sources, Research Materials (Boulder, Colorado) and Aldrich. The former sample consisted of C_{60}:C_{70} in a ratio of 85:15, the latter, 90:10. The former ratio was verified by Fast Atom Bombardment Mass Spectroscopy (FAB/ms, VG Inst., Model ZAB HF), using a *m*-nitrobenzyl alcohol matrix [61].

Separation of C_{60} and C_{70} was performed by chromatography, using alumina (Aldrich) as the stationary phase, which was activated by heating at 160°C overnight, and hexanes (American Chemical Ltd., Montreal, Que.) as the mobile phase. Details of this separation are described in references 62. It was conveniently monitored visually, as the C_{60} band, which emerged first, was violet, and the C_{70} band which followed was red. The purity of each fraction was verified by FAB/ms and UV-vis spectroscopy (Varian DMS 300 UV-vis spectrometer).

Surface film balance studies were performed on both the LAUDA and KSV film balances, described in section I.2.1. Sample solutions for the surface film balance studies were made up in a variety of solvents, benzene, chloroform, toluene, methylene chloride (American Chemical Ltd., spectrograde) and mixtures of these. Isotherms of neat solvents were run to ensure that any effects observed were due only to the fullerenes.

---

61. I wish to thank Dr. O. Mamer, McGill Biomedical Mass Spectrometry Unit for the FAB/ms results.
62. Ajie, H.; Alvarez, M.M.; Anz, S.J.; Beck, R.D.; Diedrich, F.; Fostiropoulos, K.; Huffman, D.R.; Krätschmer, W.; Rubin, Y.; Scriver, K.E.; Sensharma, D.; Whetten, R.L., *J. Phys. Chem.*, **1990**, *94*, 8630.

Concentrations ranged from 0.05-2.0mg/ml, or 2.7×10^{-3}-6.7×10^{-3}M. Sample solution volumes applied to the water surface ranged from 25-500µl.

When measuring isotherms, compression rates were varied from 2-30mm/min. Evaporation times varied from 15-900min (0.25-15hours). Finally, the temperature was varied from 13.7-34.6°C.

I.2.2.2. Dendrimers

The synthesis of the dendrimer compounds is described in reference 51. In this study, four compounds were examined. These are shown in Figure 9. The first three compounds (**22**, **22F** and **46** [63]) are dendrimers of 1,3,5-arylbenzenes, with **22F** being a fluorinated version of **22**. The fourth compound (**15-OH** [64]) is a precursor of a dendrimer of 1,3,5-arylesters, termed a dendron, as described in Section I.1.5.2. These compounds were kindly provided by Drs. Thomas X. Neenan and Timothy M. Miller from AT&T Bell Laboratories, and were used as received. All dendrimers and dendrons used appear as white powders.

All dendrimers and dendrimer precursors were dissolved in benzene or chloroform (American Chemicals Ltd.) for the film balance studies. **46** was dissolved in both solvents, **22** was dissolved in benzene only, and **15-OH** was dissolved in chloroform only. The latter compound is not sufficiently soluble in benzene. The fluorinated dendrimer, **22F**, is not sufficiently soluble in either solvent to allow for surface film balance studies. Concentrations of these dendrimer solutions ranged from 0.84-1.24mg/ml. Sample solution volumes ranged from 5-50µl.

All dendrimer studies were performed on the KSV surface film balance described in I.2.1. Besides examining the effects of concentration, solvent and volume, **46** was co-spread with two different amphiphiles, 1,2-dipalmitoyl-sn-glycero-3-phosphocholine

---

63. The numbers for all of these compounds refer to the number of phenyl rings in the molecule.
64. The "OH" refers to the functional group of the dendron.

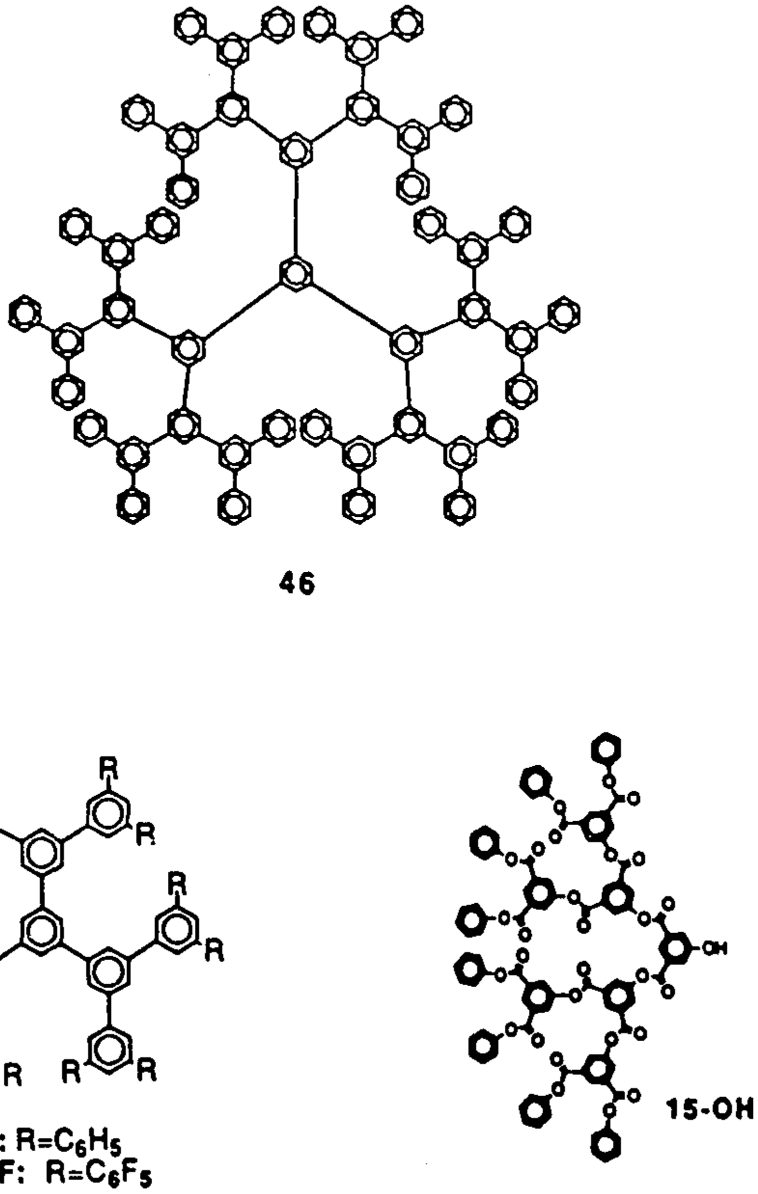

46

22: $R=C_6H_5$
22F: $R=C_6F_5$

15-OH

Figure 9. Dendrimer compounds examined at the air/water interface.

(DPPC, Avanti Polar Lipids Inc., Birmingham, AL.) and palmitic acid (PA, Sigma, St. Louis, MS.). The former was co-spread in mole ratios ranging from 0:100-35:65 **46**:DPPC. The latter was co-spread in mole ratios ranging from 0:100-27:73 **46**:PA.

An attempt was made to produce LB films of **46** co-spread with PA in mole ratios of 27:73, 1:10, 6:94 and 1:40 **46**:PA. Target pressures ranged from 10-30mN/m. Dipping rates of 2 and 5mm/min were used. Both mica and regular hydrophilic glass were employed as substrates. Deposition was attempted both upon immersion and upon withdrawal.

Atomic Force Microscopy (AFM) was used to characterize some of the resulting films. A Digital Nanoscope III was operated in height mode for this characterization. Both uncoated and carbon-coated samples were examined. Carbon-coating was achieved with a Phillips E600 vacuum coater.

I.2.2.3. Polyimides

The polyimides used in this work were synthesized as described in reference 57b. Six polyimides, of the general structure shown in Figure 8a, were examined at the air/water interface. They are listed in Table 1, along with their glass transition temperatures (T_g), their thermo-oxidative stabilities in air, as analysed by thermogravimetric analysis (TGA), and their mechanical properties, as defined by Young's modulus [57]. All six polymers were dissolved in chloroform (American Chemicals Ltd., spectrograde). Neither polymers **1a** (R=*N*-methyl, X=ketone), nor **1c** (R=*N*-phenyl, X=ketone), nor **2a** (R=*N*-methyl, X=sulfone) were sufficiently soluble in chloroform to warrent further examination. Solution concentrations ranged from 0.46-2.36mg/ml. Volumes applied to the water surface ranged from 20-150μl.

All surface film balance studies of polyimides were performed using the KSV film balance equipped with a Wilhelmy plate, as described earlier. The temperature was again controlled by a Haake water bath, and ranged from 7-25°C.

To study effects of molecular weight, **2c** samples of 50, 75 and 150 monomer units were spread at the water surface. A 75 unit sample endcapped with 3,5-di-*t*-butylphenol was also spread for comparison with the non-endcapped sample. In addition, a second solution of **2c** was made in a 9:1 solution of chloroform:*N*-methylpyrrolidinone (NMP, Aldrich), to test for solvent effects.

Deposition experiments were performed with **2b** and **2c** at 25, 9.5 and 8.5°C using the dipping apparatus of the KSV equipment. Dipping speeds of 1.0-5.0mm/min were used. Deposition was attempted at target pressures of 5, 10, 20 and 25mN/m. Hydrophobitized glass, alkylated gold, silicon wafers, and mica were used as substrates.

I.3. RESULTS

I.3.1. Fullerenes

I.3.1.1. UV-vis and Mass Spectrometry Data

Both commercial C_{60}:C_{70} mixtures are black powders. Benzene solutions of these samples yield reddish solutions. The UV-vis spectrum in hexanes at 25°C shows maxima at 258nm, 328nm, 403nm, and 469nm [65], in agreement with previously reported spectra [66], where maxima at 258nm, 328nm, and 403nm are due to C_{60}, and the maximum at 469nm is due to C_{70}.

The UV-vis spectra of C_{60} and C_{70} were used to determine the purity of the eluents from their chromatographic separation. Specifically, the peaks at 403nm and 469nm were monitored in each fraction to detect C_{60} and C_{70}, respectively. Figure 10 shows the spectra of purified C_{60} and C_{70}. Solutions of purified C_{60} in all solvents used are violet in appearance, while those of purified C_{70} are deep red. The purified solid materials are too dark to distinguish between the two fullerenes. However, when compressed to multilayer thicknesses on the water surface, the C_{60} appears yellow, whereas the C_{70} appears red. These colours, the yellow in particular, have been observed for pure fullerene crystals [66].

The mass spectral data show that the 85:15 C_{60}:C_{70} mixture has <1% of higher fullerenes. When analysing the eluents of the purification chromatography, small amounts of C_{60} were detected in the C_{70} fractions (<1%) by FAB/ms. Previous reports [62] suggest that the latter result arises because C_{60} is a decomposition product of C_{70} in the FAB process.

---

65. I wish to thank Antonnella Badia for the measurement of this spectrum.
66. a) Taylor, R.; Hare, J.P.; Abdul-Sada, A.K.; Kroto, H.W., *J. Chem. Soc. Chem. Commun.*, **1990**, 1423. b) Ajie, H.; Alvarez, M.M.; Anz, S.J.; Beck, R.D.; Diedrich, F.; Fostiropoulos, K.; Huffman, D.R.; Krätschmer, W.; Rubin, Y.; Scriver, K.E.; Sensharma, D.; Whetten, R.L., *J. Phys. Chem.*, **1990**, *94*, 8630 (reference 62).

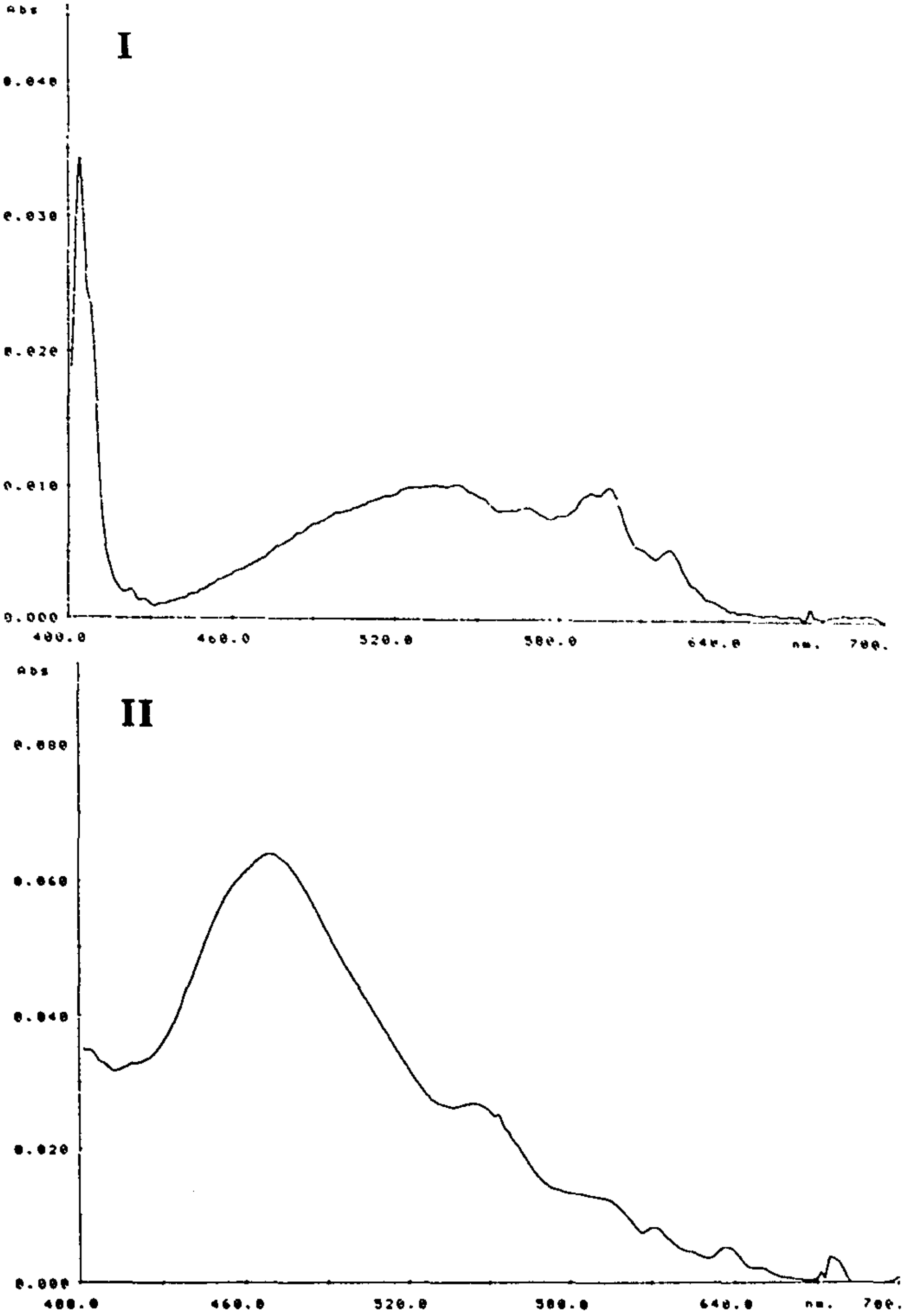

Figure 10. Visible spectra of purified I) C_{60} and II) C_{70} samples in hexanes. Scan rate 100nm/min.

I.3.1.2. Isotherms

One of the important experimental parameters when measuring isotherms is the initial surface density of the sample molecules. If the initial surface density is too high, sample molecules may be induced to form aggregates before compression is effected, with potential consequences that include prohibition of the formation of monolayers [67]. This is particularly true of fullerenes. Thus, in the initial conditions specified for all fullerene isotherms a "relative surface density", C_i/C_t, will be included. In this parameter, C_i is the initial surface concentration for the given experiment, and C_t is the theoretical surface concentration of a close-packed monolayer. The latter is taken to be 10^{12} molecules/mm^2 (from 100Å^2/molecule) for the fullerenes.

A typical compression isotherm for the C_{60}:C_{70} mixture measured at the air/water interface on the KSV film balance is shown in Figure 11a. A similar isotherm, measured on the LAUDA film balance, is shown in Figure 11b. The Langmuir torsion balance in the latter film balance gives consistently higher absolute values of π than the Wilhelmy plate, a feature noted before by Kumaki in his study of polystyrene Langmuir films [23]. The shapes of the isotherms from the two surface films balances, however, are identical, indicating that the critical areas are not dependent on the type of device used to measure the surface pressure isotherm. There is more experimental error in measurements made on the LAUDA film balance, due to difficulties in thoroughly cleaning the various parts of this film balance, especially the Langmuir torsion balance itself. The fullerenes are inclined to stick tenaciously to most surfaces, including Teflon. The design and construction of the KSV film balance, however, lends itself to more facile cleaning.

Since the maximum surface pressure achieved depends upon the amount of sample applied to the surface, there was some difficulty in measuring $A_{\lim}$. Specifically, if $A_{\lim}$ values are taken as the *x*-intercept of the tangent to the curve at high compressions, then $A_{\lim}$ varies with experimental conditions, decreasing as the maximum surface

---

67. This has been found, for example, with polystyrene by Kumaki (Reference 23).

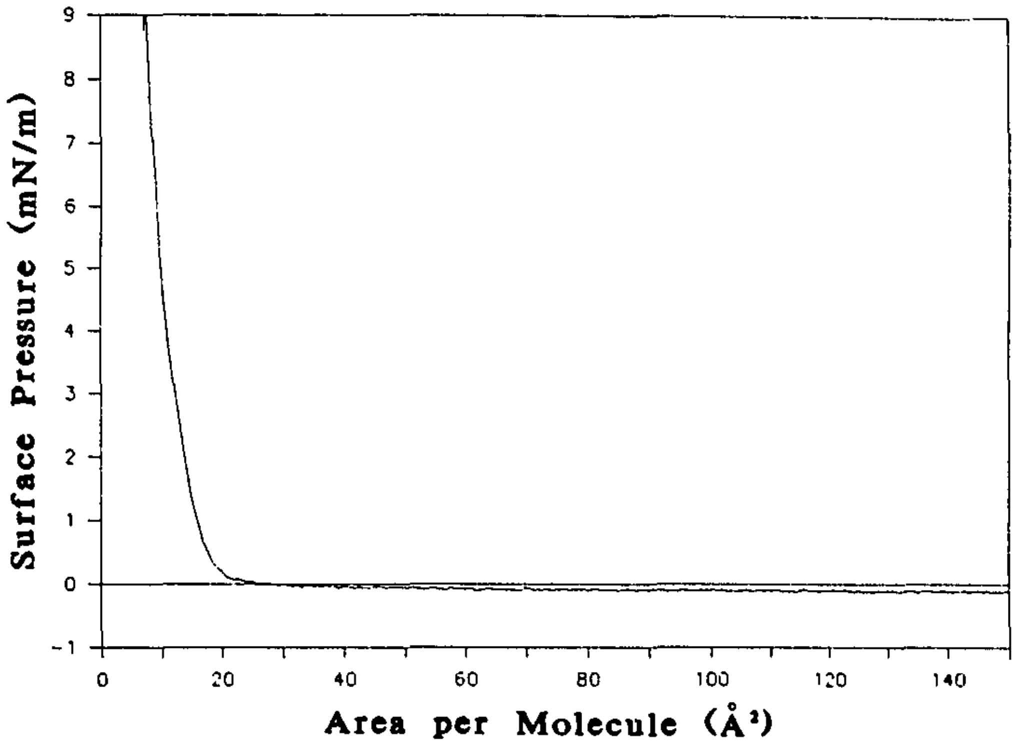

Figure 11a. Compression isotherm of C_{60}:C_{70} mixture at 25°C, measured on the KSV film balance. 25µl of a 1.92mg/ml stock solution (C/C = 0.514) in toluene was applied to the water surface, and 30min were allowed for the toluene to evaporate. Compression was effected at 20mm/min.

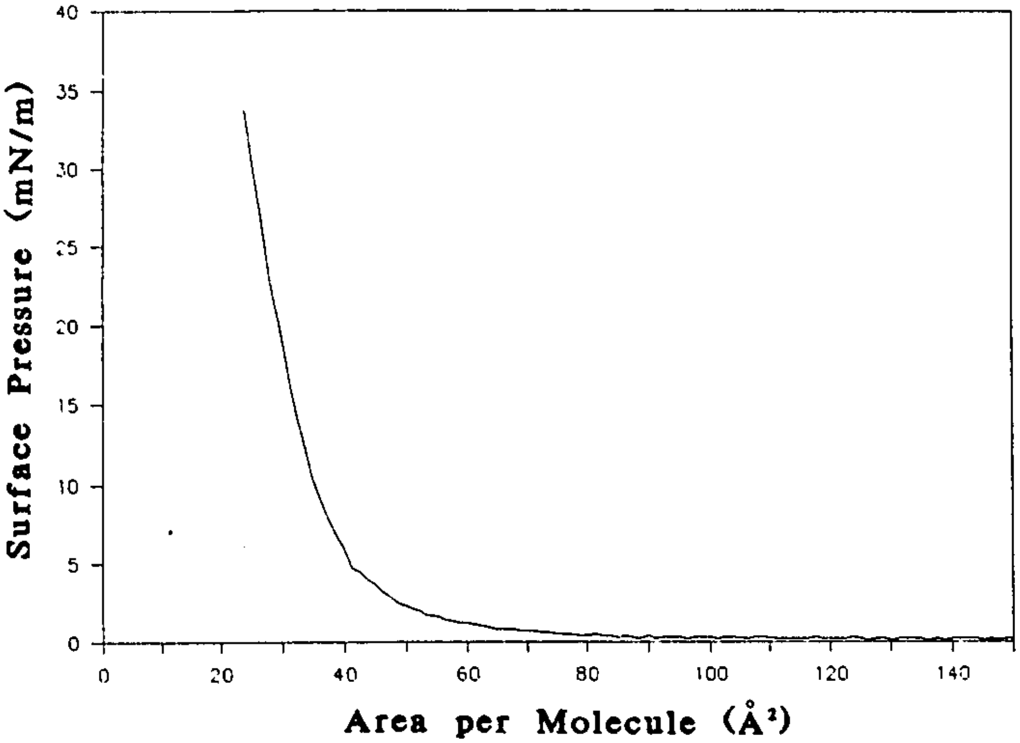

Figure 11b. Compression isotherm of C_{60}:C_{70} mixture at 25°C, measured on the LAUDA film balance. 200μl of a 0.05mg/ml stock solution (C_7/C_T = 0.090) in benzene was applied to the water surface, and 30min were allowed for the toulene to evaporate. Compression was effected at 15mm/min.

pressure increased. A_{lim} values are therefore not defined in this work.

Nonetheless, all the isotherms measured have the same shape, regardless of the conditions employed. This is invariant with solution concentration, solution volume, solvent composition, compression rate, evaporation time, and temperature. In particular, the relative surface density, C_i/C_t, was found to have a minimal effect on the isotherm in the range of C_i/C_t values investigated (0.1-0.8). Besides the question of cleanliness of the film balance apparatus, the degree of purity of the fullerene samples could contribute to slight variations in the isotherms, particularly those measured on the KSV film balance. Fresh solutions were made up periodically, however, with no discernable difference between the isotherms of a fresh solution and that of a solution that was several months old.

The isotherms of purified C_{60} and C_{70} are shown in Figure 12a and 12b. The features of these isotherms are also invariant under all the experimental conditions listed previously, with the exception of an observed temperature dependence of the C_{70} isotherm which will be presented in section I.3.1.4. The rise in surface pressure occurs at slightly smaller molecular areas than for the C_{60}:C_{70} mixture. The C_{70} isotherm has an additional feature, in the form of a kink in the isotherm, suggestive of a phase transition. The molecular area at which the kink appears is 19Å^2.

I.3.1.3. Calculation of Work of Compression

The area under the surface pressure - molecular area isotherm can be calculated to yield the work required to effect the compression in question. Specifically, (mN/m)x(Å^2/molecule) may be converted to J/mol. In the case of the fullerenes, the work required to compress the fullerene films (or the work done by the fullerene film on the barrier) is calculated in increments of molecular thickness. Specifically, for each

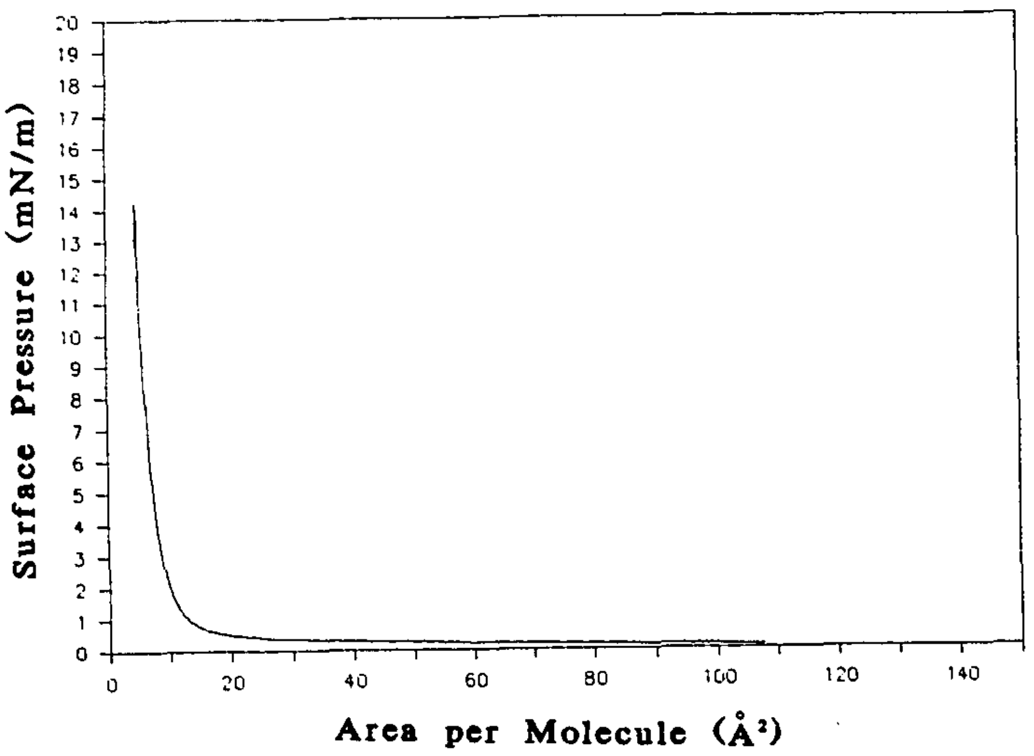

Figure 12a. Compression isotherm of purified C_{60} sample at 25°C, measured on the KSV film balance. 200µl of a 0.365mg/ml stock solution (C_i/C_t = 0.782) in benzene was applied to the water surface, and 15min were allowed for the benzene to evaporate. Compression was effected at 10mm/min.

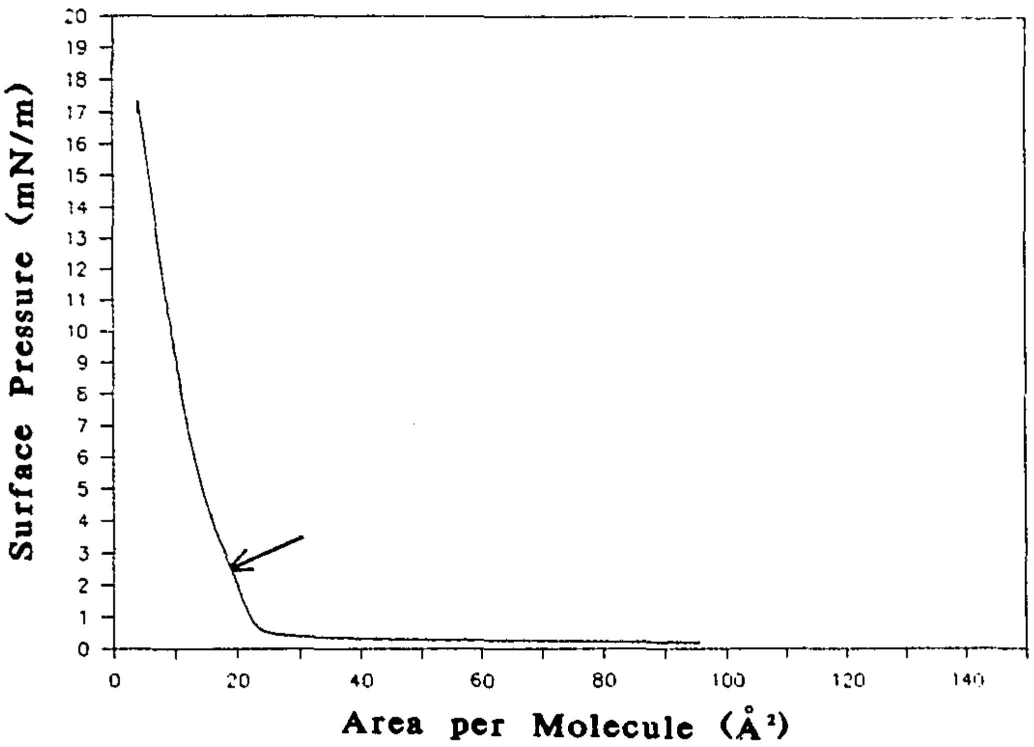

Figure 12b. Compression isotherm of purified C_{70} sample at 25°C, measured on the KSV film balance. 500μl of a 0.07mg/ml stock solution (C_7/C_t = 0.376) in benzene was applied to the water surface, and 30min were allowed for the benzene to evaporate. Compression was effected at 10mm/min.

isotherm (C_{60}:C_{70}, C_{60}, and C_{70}), the work required to compress the film from one monolayer equivalent thickness to two monolayer equivalents thickness was determined. The work required to compress the film further, from two monolayer equivalents thickness to three monolayer equivalents thickness, was then determined, and so on. This was accomplished by dividing the area under each curve into slices, the divisions for these slices being at 100Å^2, 50Å^2, 33Å^2, 25Å^2 and so on, corresponding to 1, 2, 3 and 4 monolayer equivalents thicknesses, respectively, assuming molecular areas of 100Å^2 for both fullerenes [68]. Thus the area of each slice represents the work required for that particular stage of the compression.

Using the data in the isotherms of Figures 11a, 12a and 12b, these calculations lead to the data plotted in Figure 13. Owing to the difficulty in zeroing the surface pressure measuring device in these experiments, and the problem with a slowly increasing baseline of the isotherms, (which occurs in the presence and absence of sample (or solvent) on the water surface), there appears to be a slightly <u>decreasing</u> amount of work required to compress the first few monolayer equivalents of all three films. Once this drift is accounted for, there is no increase in the surface pressure that can be attributed to C_{60} or C_{70} from >100Å^2 to about 25Å^2 for C_{60} and 30Å^2 for C_{70}. Therefore, the area under the curves up to these molecular areas can be taken to be zero and no work is required for the compression of the fullerenes up to these molecular areas. As a result, each work plot has been zeroed at its minimum value. In the C_{60} plot, the minimum is at the 3→4 monolayer equivalents transition and in the C_{70} plot the minimum lies at the 2→3 monolayer equivalents transition.

---

68. Obviously this is only an approximation, and the exact calculation would require consideration of the larger molecular area of C_{70} in its horizontal position, a much more complicated calculation, as it would have to take into account the phase transition of the C_{70} from the aforementioned horizontal position to the vertical position, which has the same molecular area as C_{60}.

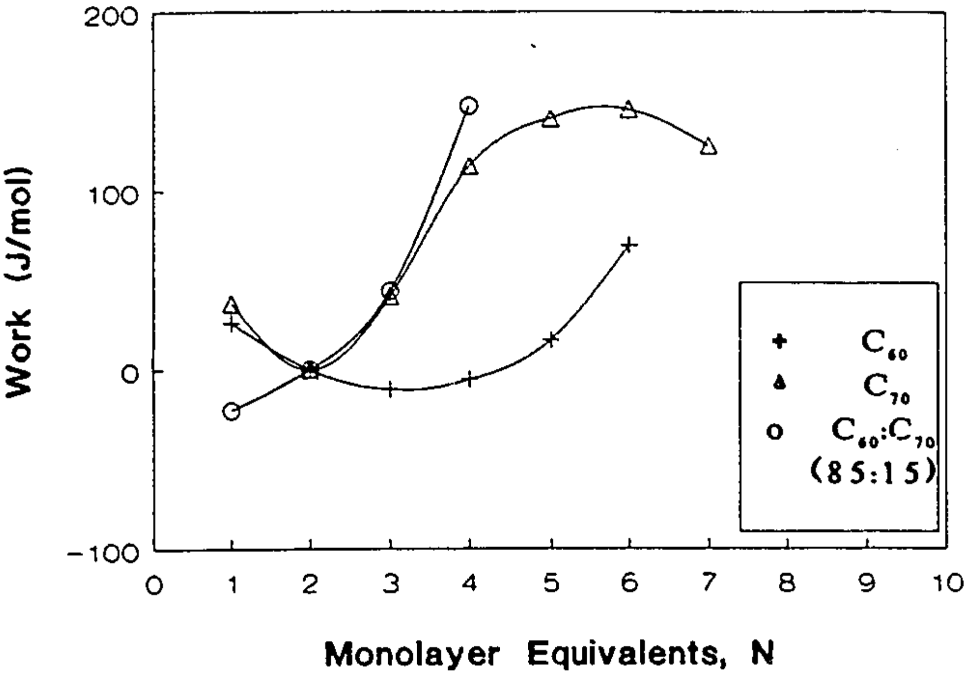

Figure 13. Work required to compress fullerene films (C_{60}, C_{70}, and C_{60}:C_{70} mixture) from N to N+1 monolayer equivalents. Data is taken from isotherms in Figures 12a, 12c, and 12d. One monolayer equivalent is assumed to be 100Å^2/molecule for both fullerenes.

I.3.1.4. Temperature Study of C_{70}

In order to verify that the inflection point in the C_{70} isotherm is indeed a phase transition, the curve was recorded over several temperatures. These are shown in Figure 14 for 8, 15, 28 and 38°C. As is expected for a phase transition, the curve shifts as a function of temperature. The phase transition is found to occur at higher surface pressures as the temperature is lowered. At temperatures higher than 28°C, however, no shift was detected.

I.3.2. Dendrimers

I.3.2.1. Isotherms

The results for the dendrimer studies at the air/water interface are summarized in Table 2. All measurements were made on the KSV film balance. A typical compression isotherm for **46** is shown in Figure 15. The principal feature in this isotherm is an A_{lim} value of 312Å^2 per molecule. Blank measurements were made by applying neat solvent to the water surface, to ensure that these isotherms were indeed a result of the presence of dendrimer. The diameter of **46** has been calculated from space-filling models [51c] to be 31Å. The cross sectional area calculated from this diameter is 755Å^2. Thus the Langmuir film of **46** is not a monolayer. The shape of the isotherm of **22** is identical to that of **46**. The A_{lim} value for **22** is smaller than that of **46**, (following the expected trend), and the Langmuir film of **22** is not a monolayer either. It is not profitable to compare the A_{lim} values for **15-OH** to the A_{lim} values for the two dendrimers, for reasons that will become apparent shortly.

When the volume of a given sample solution applied to the water surface is increased, the A_{lim} value decreases. This observation is very reproducible. The isotherms of dendrimers are strongly dependent on the amount of sample applied to the water surface. It is for this reason that the results for **15-OH** are not directly comparable to the results for the two dendrimers, as the volumes of **15-OH** solution applied to the water

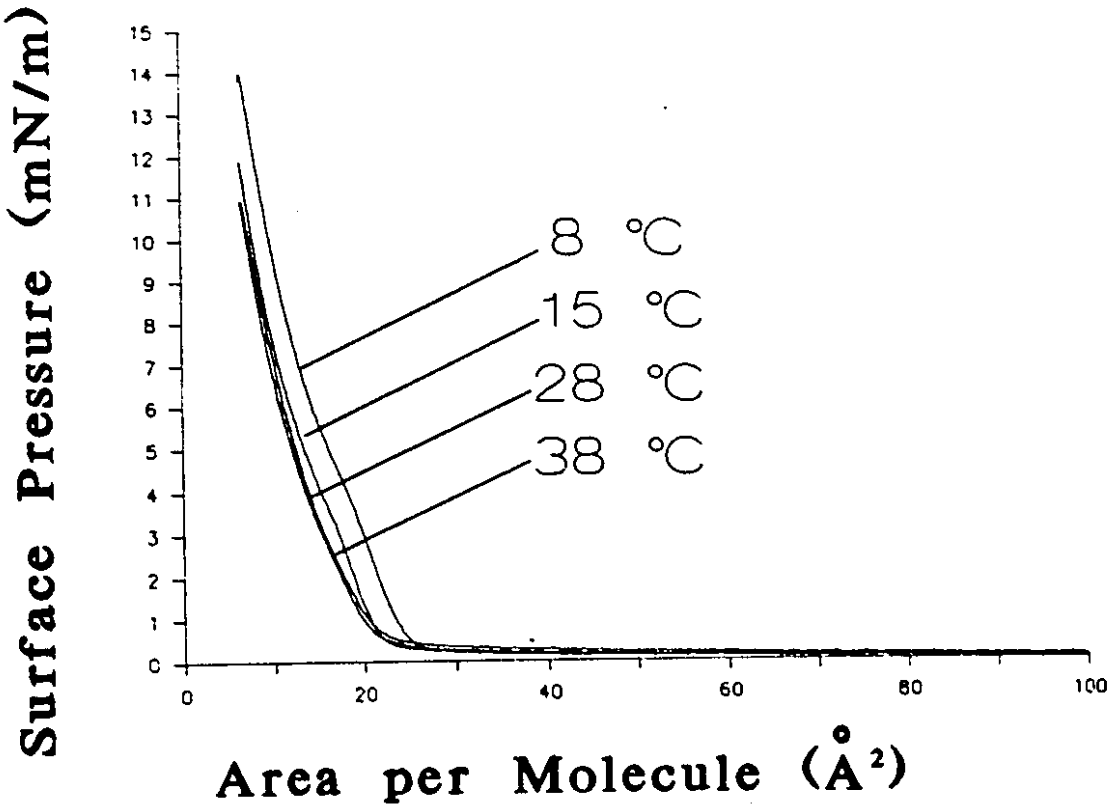

Figure 14. Temperature dependence of C_{70} compression isotherms. 300μl volumes of a 0.22mg/ml stock solution (C_i/C_t = 0.707) in benzene were applied to the water surface at temperatures of 8, 15, 28, and 38°C, and 30min were allowed for the benzene to evaporate. Compression was effected at 10mm/min.

TABLE 2 Data from compression isotherms of dendrimer and dendron compounds.

Dendrimer	Solvent	Volume (μl)	A_{lim} (Å^2)	A_{calc}* (Å^2)
46	benzene	25	310	755
46	benzene	50	140	755
46	chloroform	25	-	755
22	benzene	25	120	491
15-OH	chloroform	5	330	-
15-OH	chloroform	10	220	-

* These areas are calculated from diameters obtained from space-filling models [51]

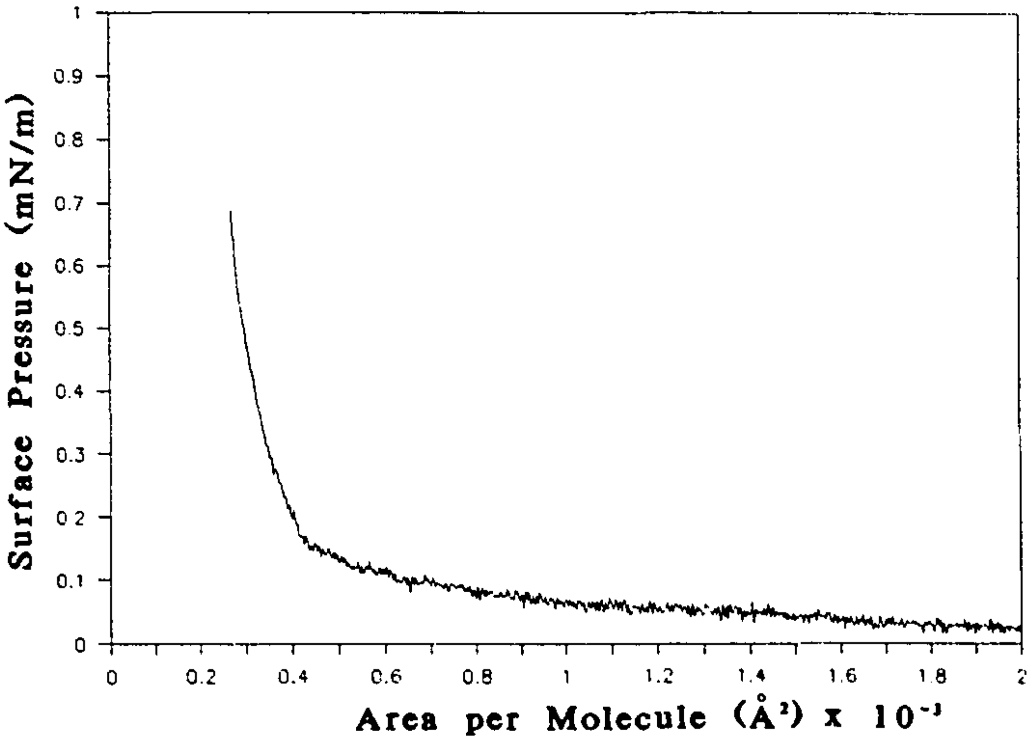

Figure 15. Compression isotherm of **46** at 25°C, measured on the KSV film balance. 25μl of a 0.84mg/ml stock solution in benzene was applied to the water surface, and 15min were allowed for the benzene to evaporate. Compression was effected at 10mm/min.

surface and the concentration of **15-OH** solution are different than the volumes and concentrations of the two dendrimer solutions applied to the water surface, and thus the surface densities are different. It is important to note, however, that the two A_{lim} values obtained for **15-OH** show the same trend with volume of sample solution applied.

The nature of the deposition solvent also affects the dendrimer isotherms. In the case of **46**, benzene solutions give A_{lim} values as reported in Table 2. If the deposition solvent is chloroform, however, there is virtually no rise in surface pressure even at very small areas, and thus there are no recordable A_{lim} values. This is another reason that the isotherms of **15-OH** cannot be directly compared to those of **46**, as **15-OH** is dissolved in chloroform only. Because the dendrimer shows a rise in surface pressure only at small water surface areas, regardless of the amount of dendrimer applied to the water surface, LB films of dendrimer cannot be deposited.

I.3.2.2. Co-spreading Studies

In order to induce a better spreading of the dendrimers, and possibly deposit LB films containing dendrimers, co-spreading studies were undertaken with **46**. The values of A_t, the molecular area at which a phase transition is observed, for the co-spreading experiments with DPPC and PA are listed in Table 3. The compression isotherms from which these values are obtained are shown in Figure 16. The molecular area in each set of isotherms is calculated as a weighted average molecular area, having taken into account the number of moles of each molecule that are spread on the water surface [69]. The A_t values in Table 3 are taken from these average molecular area axes

---

[69] To obtain the average molecular areas on the isotherm axis, the molecular weight of the sample molecules was calculated as $x_{mole}A_{MW} + y_{mole}B_{MW}$, where x_{mole} and y_{mole} are the mole fractions of the two cospread molecules, and A_{MW} and B_{MW} are their respective molecular weights. The concentration was calculated as $x_{vol}A_{conc} + y_{vol}B_{conc}$, where x_{vol} and y_{vol} are the volume fractions of the two cospread molecules, and A_{conc} and B_{conc} are the concentrations of their respective sample solutions. Finally, the volume is the total volume of sample solutions applied to the water surface.

TABLE 3 Data from compression isotherms of co-spread DPPC (1,2-dipalmitoyl-sn-glycero-3-phosphocholine) and **46**, and PA (palmitic acid) and **46** (Figure 16).

%**46**	%DPPC	%PA	A_t* ($Å^2$/molecule)**	A_{46}*** ($Å^2$)	Vol(μl)	
					46	total
0	100	0	68	0	0	10
14	86	0	74	111	25	35
21	79	0	88	163	25	31
35	65	0	100	159	25	28
0	0	100	22	0	0	15
2	0	98	25	150	10	25
6	0	94	27	105	25	40
8	0	92	33	160	25	35
16	0	84	36	110	50	60
27	0	73	44	103	50	55

* Molecular area at transition (for DPPC, π_t=17.6mN/m, for PA, π_t= 30.0mN/m)
** Scale is averaged to consider all molecules spread (DPPC and **46**, or PA and **46**)
*** Calculated with the following formula:

$$A_{46} = \{A_t - \%\text{surfactant}(A_{\text{surfactant}})\}/\%\mathbf{46}$$

where $A_{\text{surfactant}}$= 68$Å^2$ for DPPC and 22$Å^2$ for PA

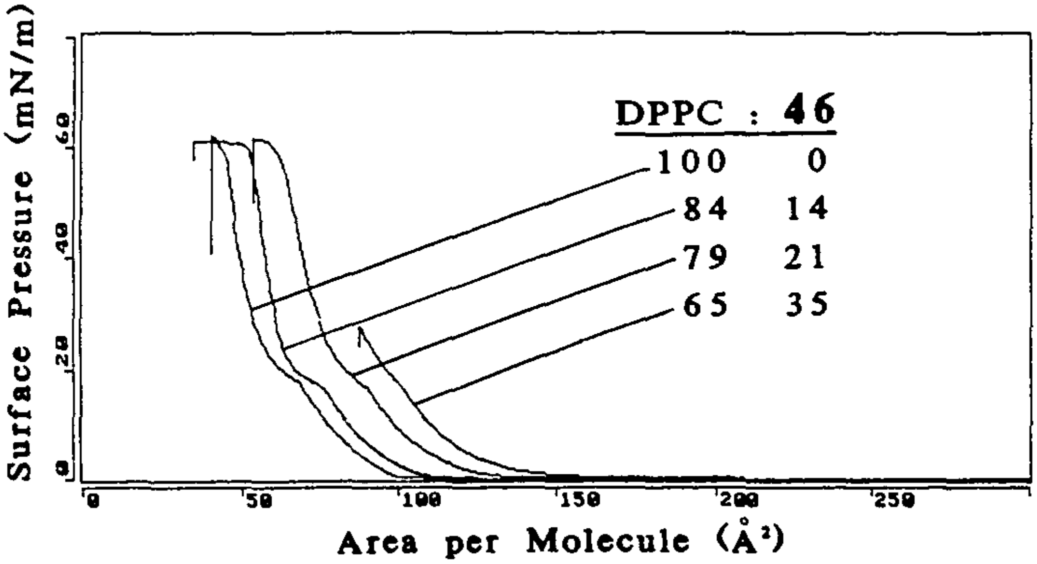

Figure 16a. Compression isotherms of various combinations of DPPC and **46**, at 25°C. 2.76mg/ml solutions of DPPC in $CHCl_3$ and 0.22mg/ml solutions of **46** in benzene were used, and 15min were allowed for the solvents to evaporate. Compression was effected at 10mm/min.

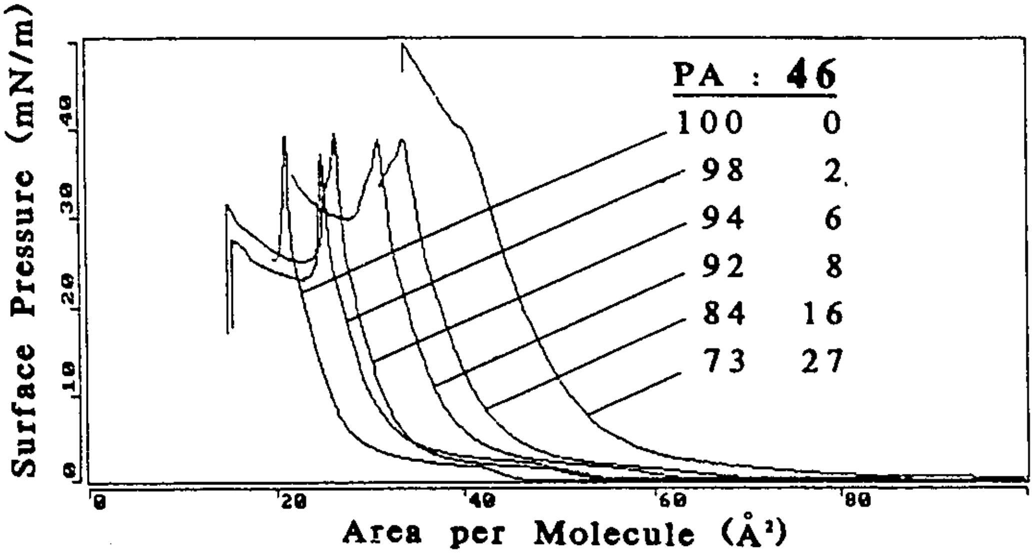

Figure 16b. Compression isotherms of various combinations of PA and **46**, at 25°C. 1.66mg/ml solutions of PA in $CHCl_3$ and 0.22mg/ml solutions of **46** in benzene were used, and 15min were allowed for the solvents to evaporate. Compression was effected at 10mm/min.

and are measured at one surface pressure for each amphiphile (17.6mN/m for DPPC and 30mN/m for PA). Also listed in Table 3 are the areas occupied per dendrimer molecule for each co-spreading experiment. These are calculated assuming that the amphiphilic molecules occupy the same molecular area in the presence and the absence of dendrimer, an assumption which will be discussed. Although the dendrimer molecules do not manifest themselves at 750Å^2, their projected area in the absence of external influences, they do cause the gradual loss of the phase transition feature observed in the isotherm of the pure amphiphile. It is for this reason that all the A_t values are taken at the same π, as the exact π_t becomes difficult to discern. It should be noted that co-spreading experiments were all performed with **46** in benzene. When **46** was spread in chloroform, very little change in the DPPC and PA isotherms was observed, in keeping with the observed effects of chloroform on the isotherms of pure **46** (I.3.2.1.).

Of the different mole ratios, the films of 1:10, 6:94 and 1:40 **46**:PA are successful at forming LB films. A target pressure of 30mN/m causes the films to collapse so that deposition is impossible. A target pressure of 25mN/m, on the other hand, does not cause this collapse. Lower target pressures (down to 5mN/m) give better transfer ratios. Deposition by withdrawal is more successful than deposition by immersion, and in many cases immersion causes the previously deposited film to be lost to the water surface. This phenomenon is indicated by negative transfer ratios. Mica is a good deposition substrate, and its molecular smoothness in the subsequent AFM experiments proved to be useful. The optimum rate of withdrawal is 5mm/min, with slower rates leading to poor transfer ratios, due to a gradual collapse of the film.

A carbon-coating treatment is helpful in performing the AFM experiment in the cases of the dendrimer/palmitic acid LB films. Without this pretreatment, the films are severely altered by the AFM probe, in such a way as to make them very difficult to characterize.

In Figure 17a, the AFM image of an uncoated LB film with 40:1 PA:**46** is shown. The damage incurred by the film from the probe made it neccessary to collect data on the first sweep over the surface, as subsequent sweeps revealed a damaged surface. Figure 17b shows the image of a carbon-coated LB film with 16:1 PA:**46**. The circular shape of the clumps is much more regular, and the clumps are larger than in Figure 17a. Another uncoated sample, with 10:1 PA:**46**, allowed for better characterization than the uncoated sample with 40:1 PA:**46**, as shown by its AFM image in Figure 17c. This sample also exhibits the largest clumps.

In these three samples, the diameters of the circular clumps range from 30-100nm, and the heights from 5-20nm. Thus these clumps are fairly disk-like. Although each sample contains a range of clump sizes, the clumps appear to be larger, on average, when the ratio of PA:**46** is smaller, that is when there are more dendrimer molecules piled on top of the PA film. Thus the clumps in Figure 17c, in which PA:**46** is 10:1, range in diameter from 50-100nm, whereas the clumps in Figure 17a, in which PA:**46** is 40:1, range in diameter from 30-60nm. The carbon-coated sample shows smaller clump sizes, but this may be due to the sharper image obtained from the carbon-coated sample because of its durability.

It should be noted that the AFM image of a film of PA shows no discernable features >10nm in diameter. This film is easily damaged by the AFM probe (more easily than the film containing dendrimer molecules), and so was not further characterized. Carbon-coating would not be useful, as it would tend to obscure the delicate features of this film. What appears to be certain is that the features in the images in Figure 17 are due to the presence of dendrimer molecules.

These palmitic acid:dendrimer films do not always show the regular, circular features in their AFM images, whether they are carbon-coated or not. Some co-spread films reveal only very blurred clump features. No particular pattern is apparent in the success or failure of a given film to exhibit the well-defined circular features.

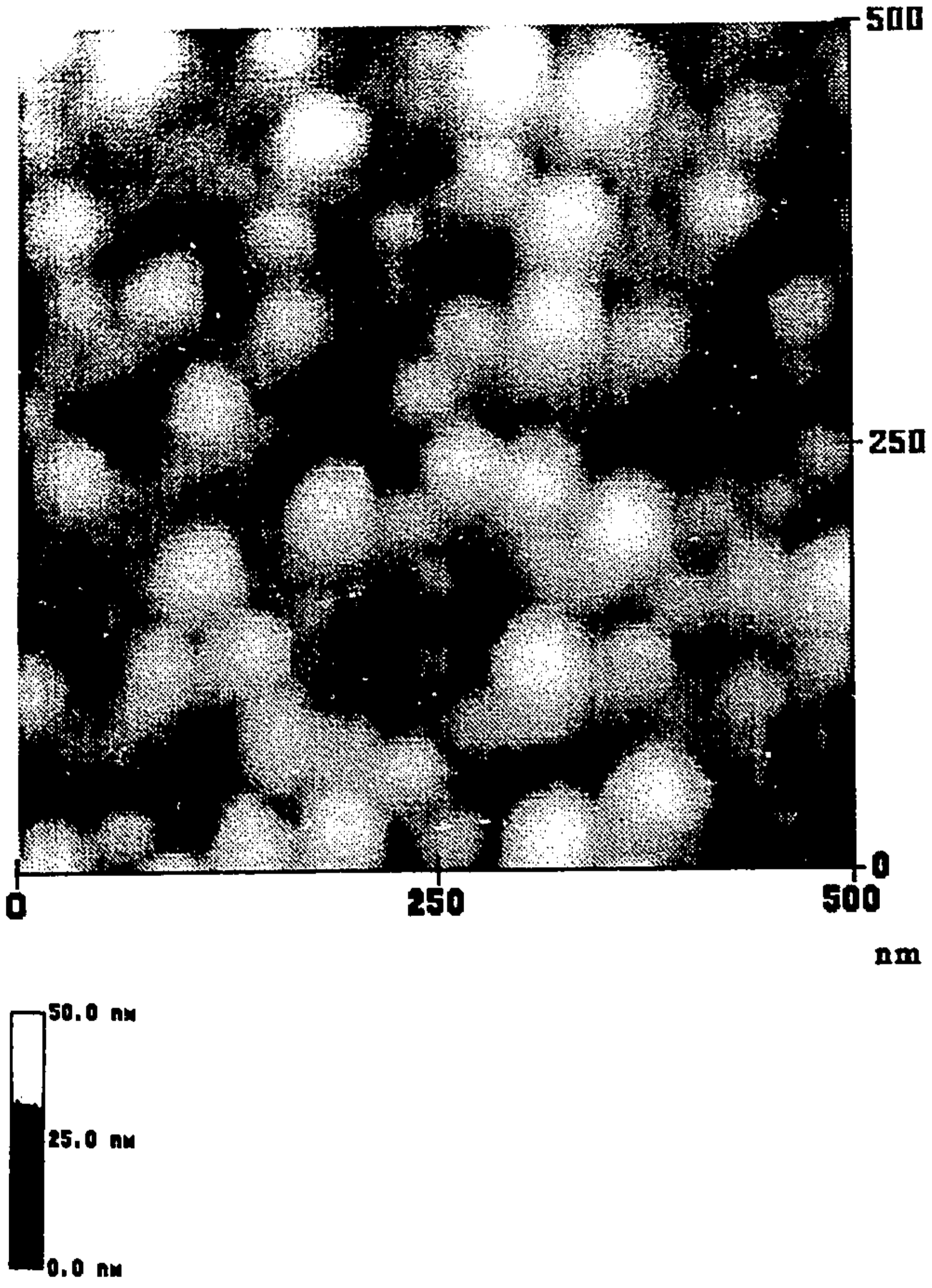

Figure 17a. AFM image, measured in height mode on a Digital Nanoscope III, of an uncoated LB film consisting of 40:1 PA:**46**, deposited at 10mN/m at a withdrawal rate of 5mm/min. Transfer ratio was 0.99. The height range is 50nm. The number of samples taken was 512, and the scan rate was 4.1Hz.

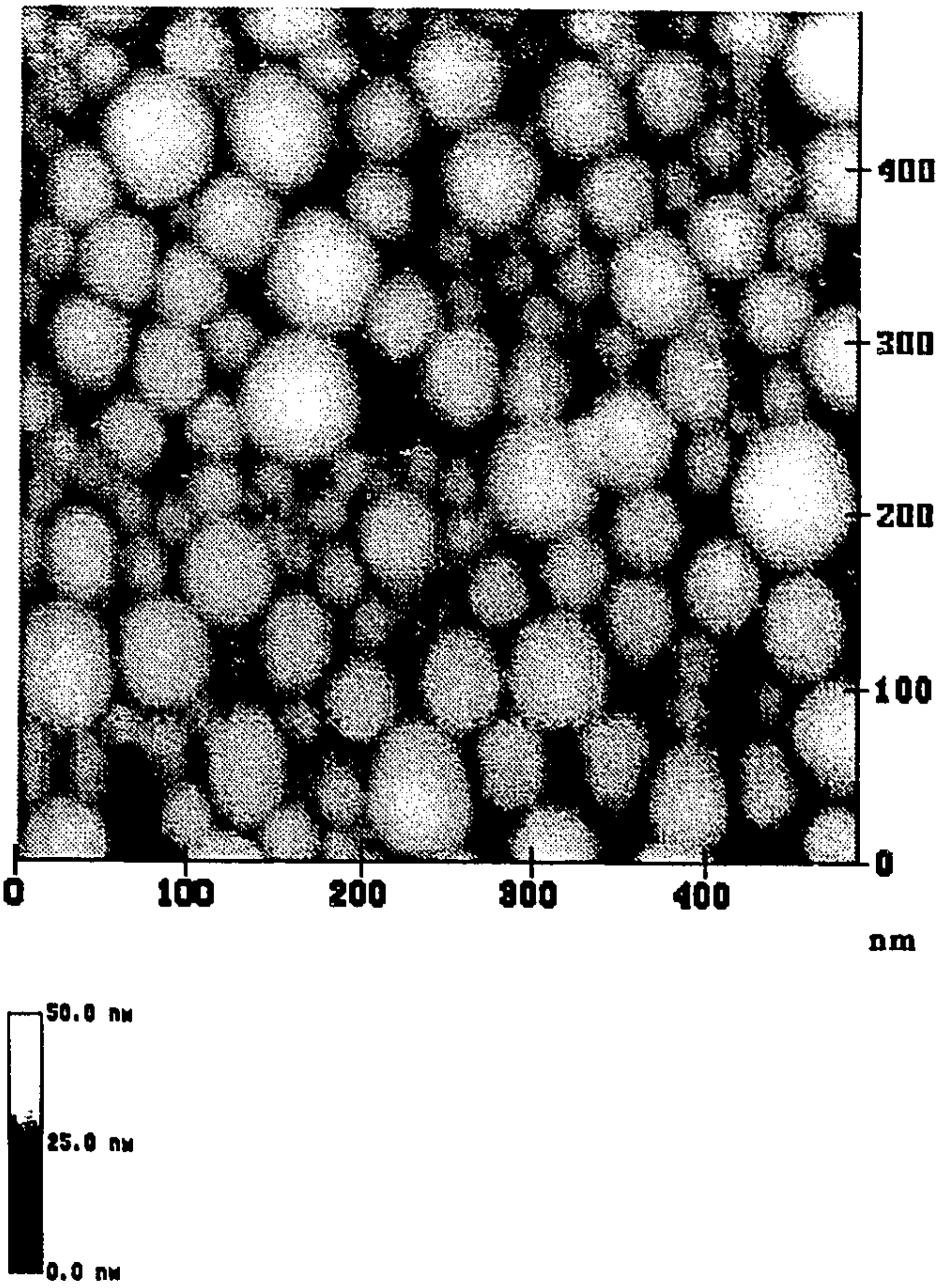

Figure 17b. AFM image, measured in height mode on a Digital Nanoscope III, of a carbon-coated LB film consisting of 16:1 PA:46, deposited at 25mN/m at a withdrawal rate of 2mm/min. Transfer ratio was 1.22. The height range is 50nm. The number of samples taken was 512, and the scan rate was 4.1Hz.

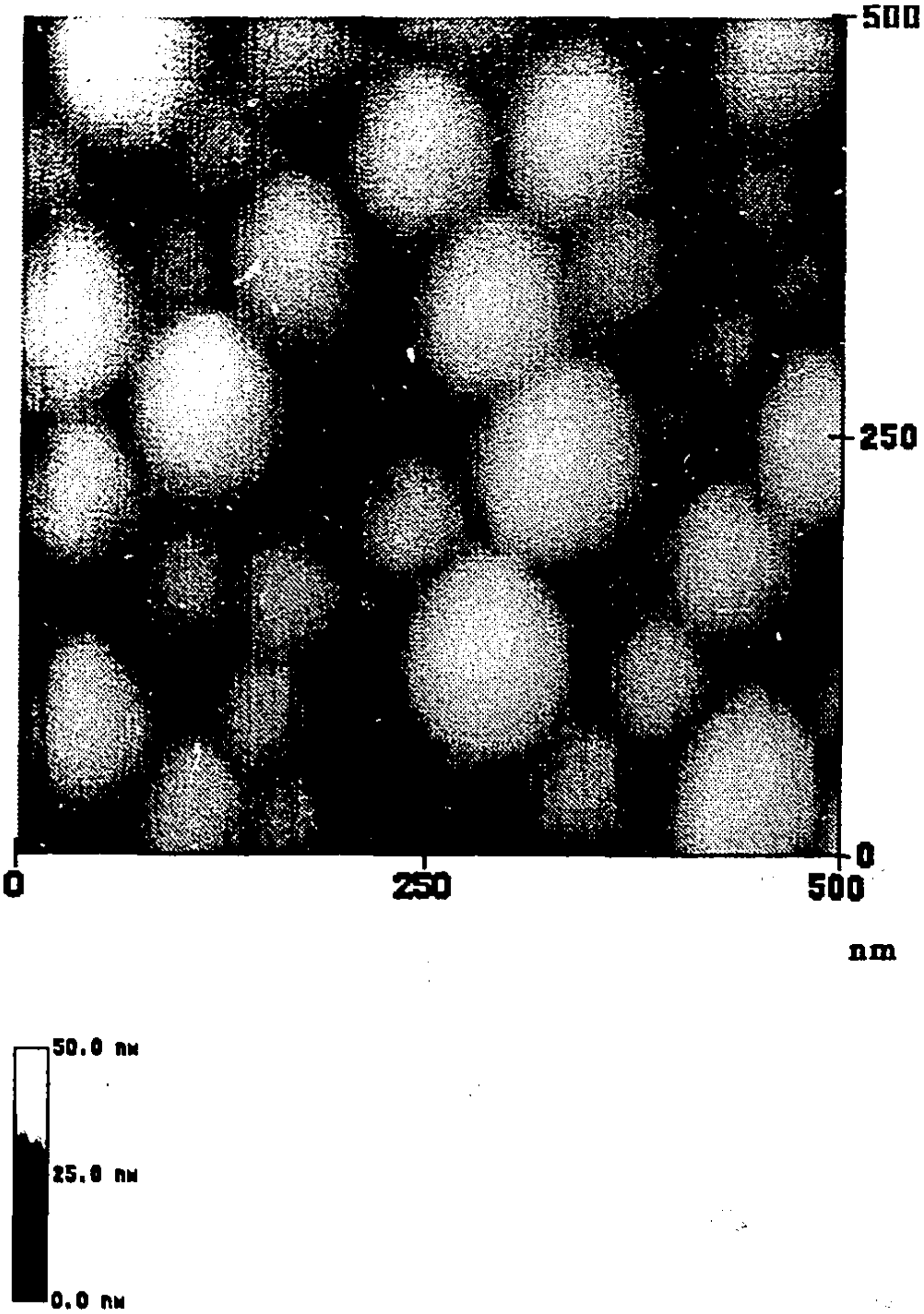

Figure 17c. AFM image, measured in height mode on a Digital Nanoscope III, of an uncoated LB film consisting of 10:1 PA:46, deposited at 25mN/m at a withdrawal rate of 5mm/min. Transfer ratio was 1.26. The height range is 50nm. The number of samples taken was 512, and the scan rate was 4.1Hz.

I.3.3. Polyimides

Figure 18 show the compression isotherms of the three bisketone polyimides, **3a**, **3b**, **3c**. The A_{lim} values are measured as shown for **3a**. All data from polyimide isotherms are provided in Table 4. Polymer **3a**, possessing the methyl group, gives the least compressible film, and polymer **3b**, possessing the dodecyl group, gives the most compressible film of the three polymers. The compression isotherms of the two sulfone polyimides, **2b** and **2c**, are shown in Figure 19. The film of **2b**, possessing the dodecyl chains, is by far the least compressible of the two, unlike the trend observed in the bisketone series. The compression isotherms of three polyimides containing dodecyl groups, **1b**, **2b** and **3b**, are shown in Figure 20. Again it can be seen that for this *N*-dodecyl series, the sulfone polyimide **2b** is by far the least compressible of the three. Note that of the two *N*-phenyl polymers examined here, (**2c** and **3c**), the bisketone polyimide, **3c**, gives a less compressible film than the sulfone polyimide, **2c**. For all polymer samples, long thread-like pieces of white material are visible on the water surface at high levels of compression, near or beyond the collapse points. At extremely high loading, irreproducible discontinuities were observed in the isotherm curves for all samples.

All samples of **2c** studied give the same compression isotherm, within experimental error. These samples include a range of molecular weights, end-capped and non-endcapped polymers, and experiments were performed for a range of concentrations and volumes. Experimental errors were calculated from these isotherms as the standard deviation of the A_{lim} and π_t values for all isotherms of **2c** to be $\pm 3Å^2$ and $\pm$3mN/m.

The solution of **2c** in 9:1 chloroform:NMP gives a much different isotherm than the other solutions. The Langmuir film formed from this solution is much more compressible, as indicated by the A_{lim} value listed in Table 4.

The effects of temperature on the polyimide isotherms are noted in Table 4. Polymers **2c**, **3b** and **1b** all show less compressibility (larger A_{lim} values) upon cooling.

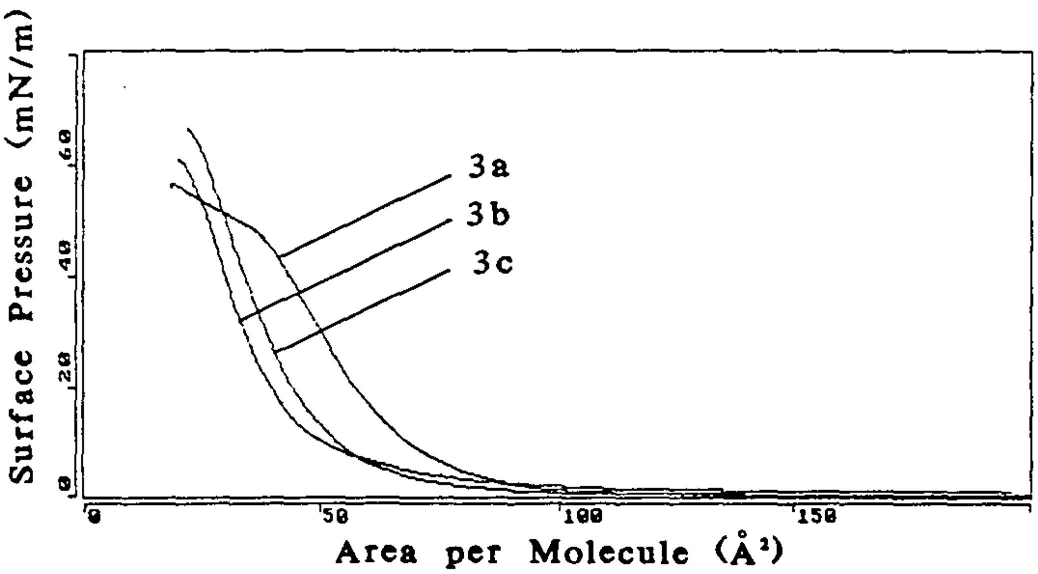

Figure 18. Compression isotherms of the three bisketone polyimides (**3a**, **3b**, **3c**) at 25°C, measured on the KSV film balance. 25µl volumes of stock solutions of 1.89, 2.17, and 1.73mg/ml, respectively, in $CHCl_3$ were applied to the water surface, and 30min were allowed for the $CHCl_3$ to evaporate. Compression was effected at 10mm/min.

TABLE 4 Data from compression isotherms of polyimides.

Polymer ($Å^2$)	A_{lim} (mN/m)	π_c	conc (mg/ml)	solvent	vol (µl)	T(°C)
3a	69	47	1.89	$CHCl_3$	25	25
3b	46	-	2.17	$CHCl_3$	25	25
3c	52	-	1.73	$CHCl_3$	25	25
2b	85	34	1.84	$CHCl_3$	25	25
2c	45	43	0.46-1.26	$CHCl_3$	50-150	25
1b	35	-	2.36	$CHCl_3$	20	25
2c	22	-	1.2	$CHCl_3$:NMP	50	25
1b	39	-	2.36	$CHCl_3$	20	7
2b	75	41	1.84	$CHCl_3$	25	7
3b	69	35	1.76	$CHCl_3$	25	7
2c	48	-	1.26	$CHCl_3$	50	7

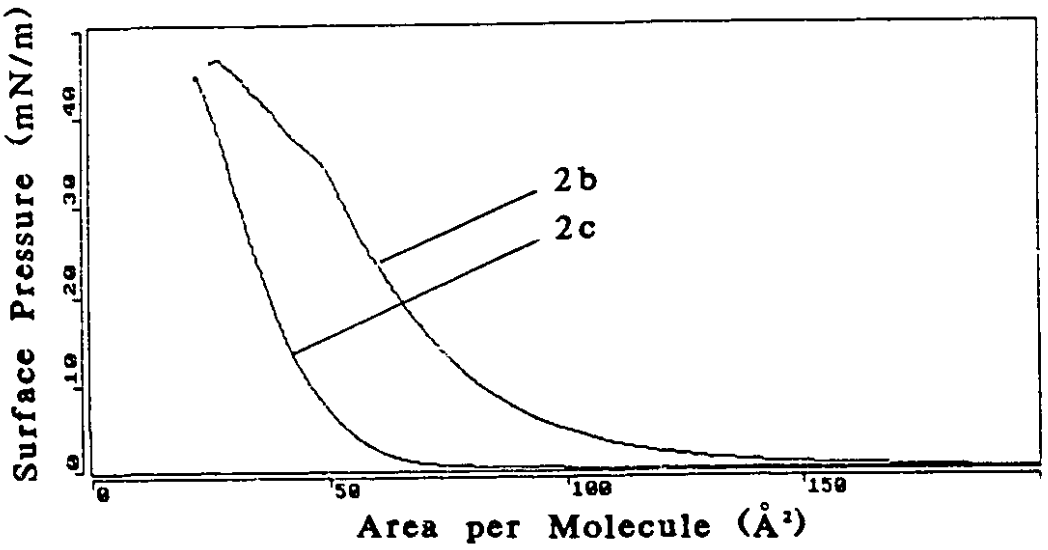

Figure 19. Compression isotherms of the two sulfone polyimides (**2b** and **2c**) at 25°C, measured on the KSV film balance. 25μl volumes of stock solutions of 1.84 and 0.46mg/ml, respectively, in $CHCl_3$ were applied to the water surface, and allowed 15min were allowed for the $CHCl_3$ to evaporate. Compression was effected at 10mm/min.

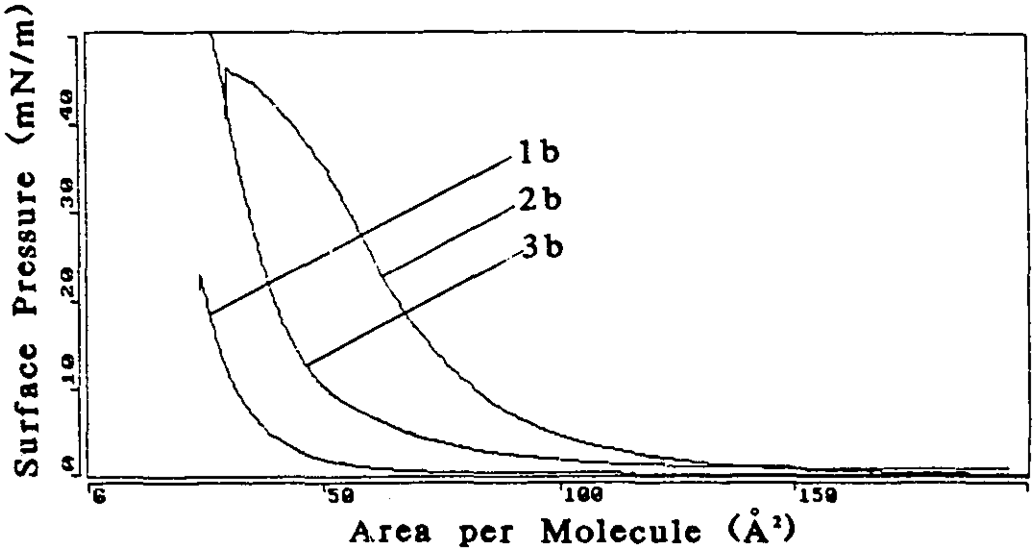

Figure 20. Compression isotherms of the three dodecyl polyimides (**1b**, **2b**, and **3b**) at 25°C, measured on the KSV film balance. A 20μl volume of stock solution of 2.36mg/ml **1b**, and 25μl volumes of stock solutions of 1.84 **2b**, and 2.17mg/ml **3b**, all in $CHCl_3$, were applied to the water surface, and 15min were allowed for the $CHCl_3$ to evaporate. Compression was effected at 10mm/min.

Polymer **2b**, on the other hand, shows a more compressed film (smaller A_{lim} value) at lower temperatures. It should be recalled that at room temperature, **2b** appears to be much less compressible than all of the others, exhibiting a very large A_{lim} value, contrary to the trend observed in the bisketone series for the three R substituents.

Attempts to deposit LB films of these polymers onto solid substrates were all unsuccessful except in the case of **2b**. For this polymer, the best transfer ratio was 0.3 upon immersion and subsequent withdrawal. Further immersion and withdrawal steps cause the transfer ratio to decrease. The lower target pressure (5mN/m) is most favourable for deposition, as is a slow dipping speed (1.0mm/min), and a moderate temperature (25°C). However, at these slow dipping speeds, it is difficult to discern whether the higher transfer ratio is due to true transfer, or to slow collapse of the Langmuir film on the water surface. In any case, deposition is approximately the same using immersion and withdrawal modes. Hydrophobitized glass gives better transfer results than mica. Alkylated gold is also a successful substrate, but silicon wafers are not. The films on alkylated gold appear (by AFM visualization) to have no integrity. On the contrary, they appear as clumps with, at best, long narrow (50-70nm broad, 10-20nm in height) ridges comprised of multiple chains.

I.4. DISCUSSION

I.4.1. Fullerenes

I.4.1.1. Multilayer Films

Two conclusions can be made from data presented in Figures 11a and 11b. Firstly, given the diameter of C_{60} (10.02Å, I.1.5.1.), (which would also be the end-on diameter of the C_{70} molecule), the area required per molecule at a close-packed monolayer coverage of the C_{60}:C_{70} mixture on the surface film balance would be roughly 100Å^2. Since no surface pressure is observed in the isotherm of the C_{60}:C_{70} mixture at the close-packed molecular area, it may be concluded that no monolayer is formed from the fullerene mixture.

The second conclusion concerns the rise in surface pressure observed in the same isotherm at areas between 20 and 25Å^2/molecule. This phenomenon is observed under a variety of conditions, in particular for a range of concentrations and quantities, precluding a simple "piling-up" of the molecules as they are swept together by the moving barriers. This suggests that the molecular area of 20-25Å^2/molecule, which would correspond to a film with an average thickness of 4-5 fullerene molecules, is significant.

These observations are in agreement with three other very recent reports of Langmuir films of C_{60} [28b,c,e] but in contradiction to another recent report [70]. In the latter, Obeng and Bard claim to have formed highly incompressible monolayers of C_{60} at the air/water interface. Their evidence for a C_{60} monolayer is an isotherm of C_{60} with a remarkably sharp increase in π at 96Å^2/molecule. A strong dependence of the ability to observe monolayers on concentration and volume of sample solution applied to the water surface was reported [28a]. In particular, it was stated that only very dilute solutions may be used, and of these a maximum volume exists, above which no monolayer formation is

---

70. a) Reference 28a. b) Bard, A.J. private communication.

observed. In other words, a maximum number of C_{60} molecules may be used to observe the formation of monolayers. A serious difficulty arises, however, if one recalculates the total number of molecules used in these monolayer-forming experiments, where it is apparent that the area per molecule at maximum compression is much greater than the reported 96Å^2. The critical molecular area quoted in reference 28a is therefore inachievable using the stated experimental conditions.

These results are thus difficult to understand and interpret, although the discrepancy between them and the results reported in this thesis is not easy to ignore entirely. The possibility of impure fullerene samples discussed earlier may partially explain the observations of Obeng and Bard, although insufficient details are presently known to warrant further speculation.

In order to further investigate the multilayer films, the C_{60}:C_{70} mixture was separated into C_{60} and C_{70} fractions. The isotherm of pure C_{60}, shown in Figure 12a, indicates that the multilayering is not simply a manifestation of an impure sample, but rather is a consequence of the fullerenes themselves. In this isotherm, the surface pressure rises at smaller molecular areas than in the isotherm of the C_{60}:C_{70} mixture, as a side-on orientation of the C_{70} molecules would occupy approximately 15% more area than C_{60}. The isotherm of pure C_{70}, (Figure 12b) exhibits a phase transition (as indicated by the arrow at 19Å^2/molecule) that may correspond to an orientational phase transition, in which the C_{70} molecules pass from a horizontal orientation to a vertical orientation. The lift-off area for the C_{70} molecules is therefore larger than the lift-off area for the C_{60} molecules, owing to the larger area occupied by the horizontally oriented C_{70} molecules. The two films are both compressed to the same extent, however, since vertically oriented C_{70} occupies the same area as C_{60}. The observation of this phase transition in the C_{70} sample indicates that all the C_{70} molecules must be in more or less the same environment. If they were in vastly different environments, specifically in patches of different thicknesses, then the surface pressure at which this reorientational transition occured would be different for each of the different environments or thicknesses, and would average out to give a smooth curve with no kink. This is further support for the idea of a fairly uniform multilayered film of fullerenes at the air/water interface, as opposed to a mechanical "piling up" of the molecules. This phase transition is observed to begin when the C_{70} film is approximately 5 molecules thick, and to finish when the C_{70} film is approximately 6 molecules thick, as depicted in Figure 21.

The following is proposed to account for the formation of a multilayered film of fullerenes. At large molecular areas, the fullerene molecules are believed to exist in aggregates of a fairly uniform thickness, and these aggregates are non-interacting, as illustrated in Figure 22. As the aggregates are brought closer together by the reduction of the total surface area, a critical molecular area is reached when they coalesce to form a continuous film. When this film is of the critical thickness of 4-5 molecules, the surface pressure begins to rise, leading to the observed isotherms. The nature of this critical thickness will be discussed shortly.

There are other possible mechanisms of the multilayering process of the fullerenes. It is possible that, prior to compression, the molecules are not in fact in aggregates, but are evenly distributed on the water surface as individual molecules. Although the extreme hydrophobicity of the fullerenes would not suggest that this would be likely, a calculation may be performed to rule out this possibility. If the molecules were indeed non-interacting prior to compression, they should exist in a gas-analogous phase. In this case, the surface pressures anticipated from two-dimensional ideal gas law calculations would satisfy equation (2),

$$\pi A = nkT \qquad (2)$$

where π is the surface pressure, A is the surface area occupied by the molecules in question, n is the number of molecules in question, k is the Boltzmann constant, and T is the temperature.

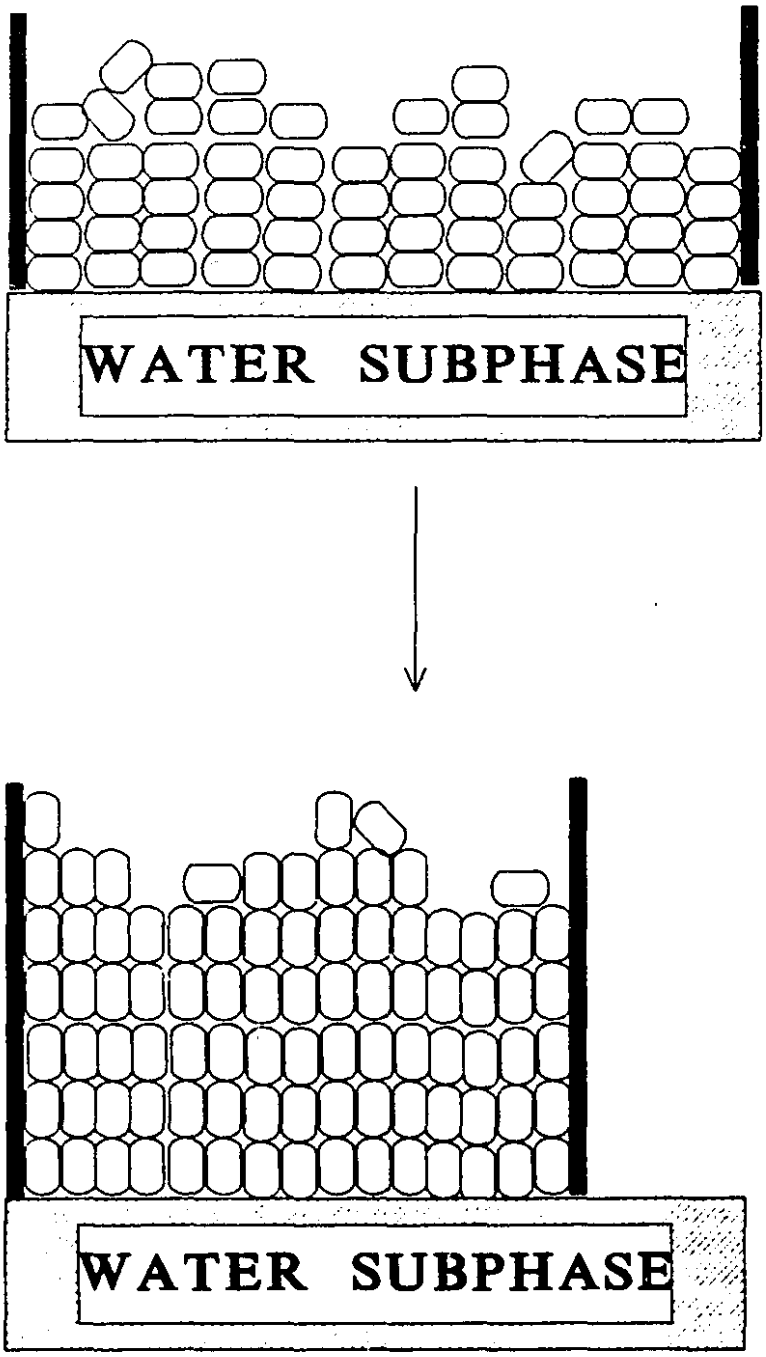

Figure 21. Proposed description of the phase transition observed in the C_{70} compression isotherm (Figure 12b).

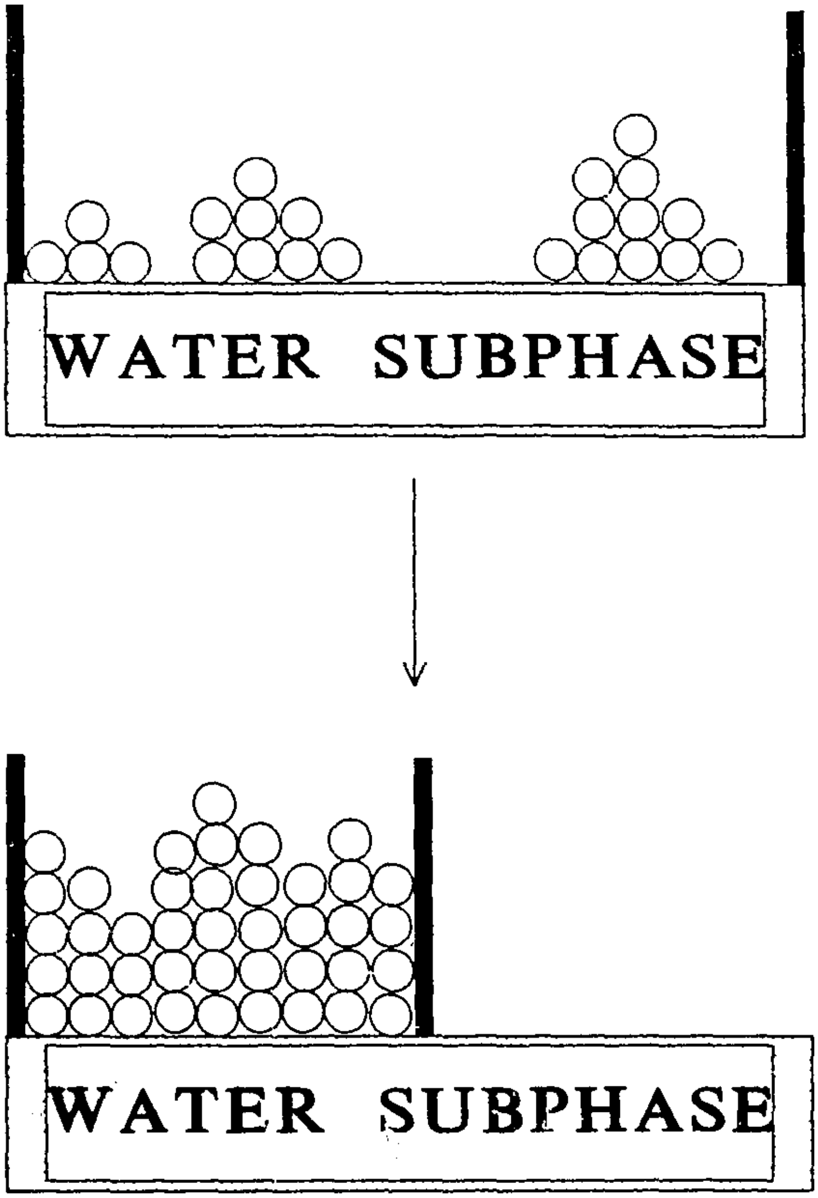

Figure 22. Proposed description of the formation of multilayer fullerene films.

This relationship is plotted in Figure 23, along with an isotherm of the C_{60}:C_{70} mixture. The poor correspondance is consistent with attractive interactions between the C_{60} and C_{70} molecules being significant, reducing the surface pressure from the ideal two-dimensional gas prediction, and leading to fullerene aggregates. Thus it can be stated that the fullerene molecules do not exist as isolated species at the air/water interface under the experimental conditions described here. Since the similarity of all the fullerene isotherms, regardless of experimental conditions, shows that the fullerene molecules all experience a similar environment, it is concluded that they exist in uniformly sized aggregates prior to compression.

Aggregates have recently been detected for phthalocyanine derivatives at the air/water interface prior to the formation of a continuous film [71]. The authors attribute the formation of these aggregates to high intermolecular attractive forces between phthalocyanine molecules, and relatively low hydrophilicity of the same phthalocyanine molecules. This and the aggregation of the fullerenes are consistent with the expected behaviour of hydrophobic molecules at the air/water interface, where they will prefer the interactions with one another to the interactions with water molecules. Thus, the report of a monolayer of C_{60} at the air/water interface by Obeng and Bard [28a] is difficult to reconcile with the hydrophobicity of these molecules.

The question remains as to the significance of the critical molecular area (20-25Å^2). If the surface pressure rises exactly at the point of coalescence of the aggregates to form a continuous film, then it is the aggregate size that determines the critical molecular area, and the critical film thickness of 4-5 molecules is a reflection of the average thickness of the aggregates. If, on the other hand, the coalescence of the aggregates does not cause the surface pressure to rise, but instead the film is further compressed until it reaches the aforementioned critical thickness, then it is this film thickness which must determine the point at which the surface pressure rises.

---

71. Burack, J.J.; LeGrange, J.D.; Markham, J.L.; Rockward, W., *Langmuir*, **1992**, *8*, 613.

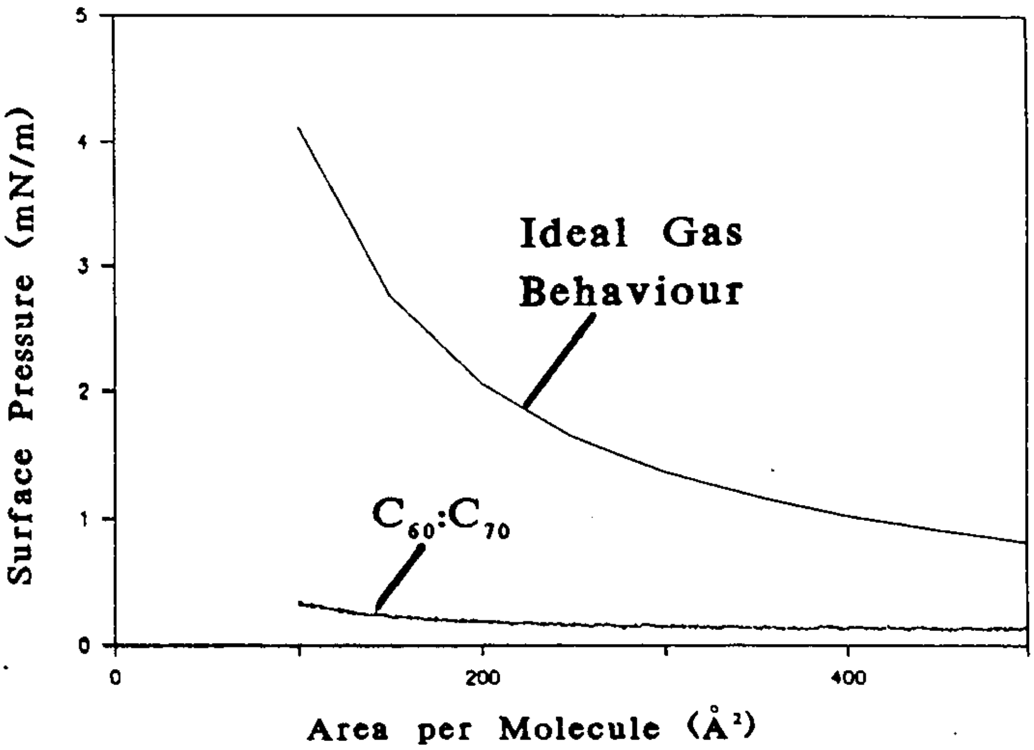

Figure 23. Ideal gas behaviour for a two-dimensional film, plotted with the compression isotherm of C_{60}:C_{70} (Figure 11a). k=1.3807 x 10^{-23}J/K and T=298K.

In either case, the surface pressure is believed to rise when a film of 4-5 molecules thick covers the water surface. This observation is not readily explained by classical perceptions of the surface film balance experiment. It is generally assumed in surface film balance studies that surfactants with polar head groups cause the surface tension of the water to drop when their polar head groups orient themselves at the water surface, disrupting the order amongst the surface water molecules. The question that arises is how the hydrophobic fullerenes succeed in changing the water surface tension. To understand this, one must consider the concept of an interface being determined by both media that define it. In this context, classical surface film balance studies are primarily concerned with the <u>air/water</u> interface. When this interface is clean it has a defined surface tension, which is used either to zero the Wilhelmy plate measuring device, or serves as the "clean" side of the Langmuir film balance measuring device. However, the surface tension of water at the <u>benzene/water</u> interface, for example, is different from that at the <u>air/water</u> interface. Therefore, when enough benzene is deposited on the water surface to form a coherent film of benzene, and hence create a new interface, the surface tension changes even though benzene has no polar head group. Thus, the surface tension of the water could conceivably be changed by the fullerene molecules if they actually created a new interface, namely a <u>fullerene/water</u> interface.

If this is the origin of the change in surface tension observed in the fullerene isotherms, then the rise in surface pressure must signify the formation of a complete film of a critical thickness of fullerenes on the water surface, with properties more bulk-like than thin film-like. The idea that the surface film balance can be used to monitor this transition from an aggregate state to a bulk state at an interface is intriguing. Such transitions in three dimensions, with metal atoms or rare gas atoms are the subject of many ongoing studies [72].

---

72. *Physics and Chemistry of Finite Systems: from Clusters to Crystals*, NATO Series, Series C, no. 374, eds. Jena, P.; Khanna, S.N.; Rao. B.K., Dordrecht, Boston, Kluwer Academic Publishers, **1992**.

I.4.1.2. Work of Compression

The plots of work vs number of monolayer equivalents (Figure 13) yield some interesting information. Taking into account that the apparent decrease in work required to compress the C_{60} and C_{70} films up to 4 and 3 monolayer equivalents, respectively, is an artifact of the calculation method, as described in Section I.3.1.3., data in Figure 13 shows that the energy costs to compress the film of pure C_{60} increase, from about 4 monolayer equivalents and beyond. This observation supports the proposal of a critical C_{60} film thickness of 4-5 monolayer equivalents, after which the film takes on bulk-like properties which are different from the properties of thinner films. In particular, the compressibility of this bulk film is very different from that of the thinner film. The film of pure C_{70}, however, is quite different. A steady increase in the work is required to continue the compression beyond 3 monolayers, until about 6 monolayer equivalents are reached. At that point, the increase becomes less pronounced, levelling off to a slight maximum at 7 monolayer equivalents. This behaviour is consistent with the proposed compression mechanism of C_{70}, in which at large areas the C_{70} molecules are predominantly in a horizontal position, and become vertically oriented when the film is 5-6 monolayer equivalents in thickness. The work plot suggests that the horizontally oriented C_{70} molecules are in fact more difficult to compress than are the vertically oriented molecules at these film thicknesses. The work plot for the C_{60}:C_{70} mixture appears to be a simple combination of the plot for the two pure samples, as is the corresponding isotherm.

I.4.1.3. Thermodynamics of C_{70} Films

Gaines [14] derives the following relation between the Helmholtz free energy of an interfacial system, F, and the surface tension, γ, at constant temperature, T, volume, V, and number of moles of surfactant, n, to be

$$\gamma = \left.\frac{\partial F}{\partial s}\right|_{T,V,n} \qquad (3)$$

where s is the surface area. An equivalent relation is defined for the Gibbs free energy, G, for constant temperature, T, pressure, P, and number of moles of surfactant, n, to be

$$\gamma = \left.\frac{\partial G}{\partial s}\right|_{T,P,n} \qquad (4)$$

Integrating this expression yields,

$$\Delta G = \int \gamma ds \qquad (5)$$

Thus the area under the π-A isotherm represents the free energy of the system. This is the reasoning that leads to the correlation of work with the area under the same isotherm presented in the previous section.

In relation to the previous section, the C_{70} film requires more work to compress at lower temperatures. In light of the temperature studies, it can be stated that the free energy associated with the compression of C_{70} films is higher at lower temperatures.

Recalling the thermodynamic relationship between the Gibbs free energy and enthalpy as a function of temperature,

$$\frac{\partial(\Delta G/T)}{\partial T} = \frac{-\Delta H}{T^2} \qquad (6)$$

and observing that, for the isotherm of C_{70}, the term on the left of equation (6) is negative up to 28°C, it can be concluded that the compression of C_{70} is endothermic up to 28°C. At 28°C, however, ΔG becomes invariant with temperature. This could be simply a minimum value for ΔG. Experimental limitations prevented testing this at temperatures higher than 37°C. In any case, at that point the ΔH is necessarily zero. To satisfy the equation

$$\Delta G = \Delta H - T\Delta S \qquad (7)$$

the entropy for this process must then be negative. A negative ΔS implies a phase transition from a less ordered state to a more ordered state. This is consistent with the vertically oriented C_{70} molecules being more ordered than the horizontally oriented molecules.

I.4.2. Dendrimers

I.4.2.1. Dendrimer Films

The isotherms of the dendrimers indicate that their Langmuir films are not simple monolayers. The A_{lim} values (Table 3) are too small for this to be the case. One possible arrangement of the dendrimers in these Langmuir films is a multilayered network held together by slight interpenetration of the dendrimers on the water surface. Although no interpenetration is observed in solutions of dendrimers [51b], the surface results may be explained by the high two-dimensional concentration achieved during compression of the molecules at the interface. These two-dimensional concentrations are much higher than the solubilities of these molecules will permit in three dimensions. This high surface concentration may lead to the proposed interpenetration. This is supported by the observation that increasing the number of molecules spread on the water surface (and hence the ultimate surface concentration achievable on the water surface) decreases the A_{lim} value for a given dendrimer, consistent with further interpenetration occurring.

The isotherm of **22**, whose A_{lim} value is smaller than that for **46**, also supports this proposal. If indeed a well defined dendrimer network is formed and held together by a degree of interpenetration that is dependent on concentration but independent of dendrimer size, then the network density would be the same for **22** and **46**. This is reasonable if the origins of interpenetration are considered. These include solvent affinities, hydrophobicity, and intermolecular attractive forces between dendrimer molecules, which would all be virtually the same for dendrimers **22** and **46**. Thus if the surface concentrations of **22** and **46** films are the same and hence the network densities are the same, then the A_{lim} value of **22** would be expected to be smaller than that of **46**, since the size of the molecule would still manifest itself in the isotherm. For the isotherm of **15-OH**, the data are not so straightforward, since they may not be directly compared to the data for **22** and **46**. Firstly, the volumes of the **15-OH** solution applied to the water surface, and hence the surface concentrations, are different than the volumes of the dendrimer solutions applied to the water surface. This has already been shown to be a critical experimental parameter. Secondly, **15-OH** has both ester groups and the alcohol group which may change the molecule's affinity for the water surface. In fact, linear polymers such as the polymethacrylates actually have enough polarity in their ester group to spread by the conventional amphiphilic mechanism to give coherent films [18b]. Therefore, it is difficult to speculate as to what configuration the **15-OH** molecules actually assume within their Langmuir film. In any case, the Langmuir film of **15-OH** is not a monolayer, as the A_{lim} value for a monolayer does not change with the volume applied, as it does in the **15-OH** experiments. An interpenetrated network, perhaps with a stronger affinity for the water than the hydrophobic dendrimer Langmuir films, is the most likely description for the **15-OH** Langmuir film.

In the studies involving solvent variation, the solution of **46** in chloroform showed an even smaller A_{lim} value for **46** than isotherms measured with solutions of **46** in benzene. To explain this solvent effect, it is proposed that in benzene, the dendrimer molecules are swollen, and thus at sufficiently high surface concentrations interpenetration occurs to form the dendrimer network discussed earlier. The dendrimer molecules do not swell in chlorofrom, and thus do not interpenetrate. Upon compression, the interpenetrated network spread from benzene forms a film with long range integrity afforded by the intermolecular interpenetration. This film exhibits a rise in surface pressure when the surface concentration reaches a critical value, (A_{lim}), perhaps related to the film thickness and the degree of interpenetration achieved. The individual dendrimer molecules spread from chloroform cannot form a film with the same integrity, as there is not the cohesiveness between molecules that is achieved through interpenetration, and as a result they simply pile up on the water surface, with no rise in surface presssure.

This rise in surface pressure, caused by a multilayered film, can be compared to that observed for fullerenes in a multilayered configuration at the air/water interface. Although it is not the conventional decrease in surface tension caused by the presence of amphiphilic molecules, it may be that a new interface is being established, that of a dendrimer/water interface, with a different surface tension than the air/water interface. In the case of the fullerenes, interpenetration is not possible and multilayered films are of constant density. Thus the transition from the air/water interface to the fullerene/water interface always occurs at the same area per molecule (20-25Å^2 for C_{60}) or the same film thickness. In the case of the dendrimers, however, interpenetration can change the density of the resulting multilayered film, and thus the transition from the air/water interface to the dendrimer/water interface does not always occur at the same area per molecule, or the same film thickness or density. Although the case of the dendrimers is one of many more variables, the proposal of a new interface with a different surface tension, first suggested for the fullerenes in Section I.4.1.1., is believed to apply with equal validity to the behaviour of the dendrimers.

Thus, the film of interpenetrated dendrimer, at the point of the rise in surface pressure, has assumed bulk properties that create the new interface. If the observed solvent effects are re-examined in this light, it seems probable that the dendrimer film relies upon the existence of an interpenetrated network to achieve these bulk properties.

I.4.2.2. Dendrimer Films Co-spread with Surface-Active Molecules

Since the deposition of LB films must be performed at substantial surface pressures (usually >2mN/m), LB films can not be made of the dendrimers by themselves, because their Langmuir films did not cause sufficient rise in surface pressure. Indeed, upon addition of more material to the Langmuir film of pure dendrimer, the surface pressure at a given molecular area decreased, as discussed above. In co-spreading **46** with DPPC and PA, it was hoped to make a Langmuir film that would produce sufficiently high surface pressures to deposit LB films of these materials.

The isotherms in Figure 16 indicate that the presence of dendrimer does have an effect on the Langmuir films of DPPC and PA. In both cases, the phase transition in the isotherm of pure amphiphilic molecules is observed to become less sharp with the addition of dendrimer. This is probably analogous to the broadening of the melting point range in three dimensional melting caused by impurities in the bulk. The average molecular area also increases with increasing amount of dendrimer, suggesting that the dendrimers are expressing themselves through some interaction with the amphiphiles. However, when the molecular areas in which the dendrimer molecules manifest themselves in the Langmuir films are calculated (see Table 3), they are found to be small relative to the projected area of an isolated dendrimer molecule (755Å^2). This suggests that they are not incorporated into the film at the air/water interface, and are probably being squeezed out from the water surface. This process is probably aided by their low affinity for the water. In this configuration, resting on top of the Langmuir film of amphiphilic molecules in an array of oriented hydrocarbon chains, the dendrimers cause the increase in the average molecular area by slightly disrupting the packing order of the amphiphilic molecules.

It should be noted that the co-spreading results with DPPC indicate, not surprisingly, that the dendrimers are not compatible with the phospholipid film. This is an example of how preliminary information regarding possible biocompatibility can be obtained from such co-spreading experiments. Compatibility of the two species would be indicated by isotherms reflecting the presence of both species at the air/water interface. Furthermore, a miscibility of the two species would be confirmed by a change in the transition surface pressure for different ratios of the two species, much as a three-dimensional solution containing two liquids will show a gradual change in the boiling point as the ratio of the two components is varied.

Only dendrimers dissolved in benzene may effect this disturbance of the hydrocarbon chains. Dendrimers dissolved in chloroform cause only minimal disturbance to the Langmuir films of DPPC and PA. This is probably due to the lack of swelling of the dendrimers in chloroform, which also prevents them from forming a network of interpenetrated dendrimer molecules (Section I.4.2.1.). Only the swollen dendrimers may interact with the hydrocarbon chains of DPPC and PA, as the hydrocarbon chains are not able to penetrate the dendrimers spread in chloroform, which are not swollen.

AFM was employed to further characterize the Langmuir and LB films of PA with **46**. Since the co-spreading isotherms indicate that the dendrimers are for the most part not in contact with the water surface, but are localized on the hydrocarbon tails of the amphiphilic molecules, the co-spreading ratios chosen for these experiments are 1:10, 6:94 and 1:40 **46**:PA. The latter ratio is that for which the area occupied by all of the PA molecules in a vertical orientation would be approximately equal to the area required for all of the **46** molecules. That is, 40 x 22Å^2 is approximately equal to 1 x 755Å^2. The assumption that the PA molecules will each occupy 22Å^2 is not entirely valid, as is shown in the isotherms previously discussed. Nevertheless, it is a good approximation for the purpose of chosing the right size of "fatty acid carpet" on which the given number of dendrimer molecules may reside.

The AFM images (Figure 17) show that dendrimer molecules are spread on top of the fatty acid array, although not in any particular order. Furthermore, judging by the diameter of the features observed by AFM, the dendrimer molecules are not spread individually, but are arranged in clumps consisting of several molecules each. It is interesting to observe that the thickness of the clumps is much less than their diameter, usually by a factor of approximately 5. A range of 5-20nm in height corresponds to the clumps being 3 dendrimer molecules thick, on average. Furthermore, at ratios less than the 40:1 PA:**46** that is calculated to give monolayers of PA and **46** of equivalent areas, the clumps of dendrimers are noticeably larger. In Figure 17c, the ratio of 10:1 PA:**46** shows larger clumps, both in diameter and height, than the ratio of 40:1 PA:**46** (Figure 17a). It must be acknowledged that the LB film in Figure 17c was also deposited at a higher surface pressure, and hence a slightly higher surface density than the film in Figure 17a. This is not believed, however, to be the full cause of the differences between the two films.

Thus by co-spreading the dendrimers with a surfactant such as PA, LB films that consist of one layer of ordered surfactant and a second, less ordered "monolayer" or ultrathin film of small dendrimer clumps may be realized. This offers a unique way to make LB films of unconventional film-forming molecules. Although the idea of co-spreading a non-surfactant species with a surfactant is not new, previous attempts at this strategy utilized equal amounts of non-surfactant and surfactant molecules to make a homogeneous film. Here, the projected areas of the given molecules have been considered, and maintaining equimolar quantities in the film is accorded less importance than an "equi-area" condition. The result is essentially a bilayer film, deposited in one step.

I.4.3. Polyimides

The A_{lim} values for all the polyimides, (Table 4), indicate that these polymers do not lie flat on the water surface. A projected area of 271Å^2 can be estimated with space-fillng models for the monomer of polymer **3a**. This value is much larger than the A_{lim} value of 69Å^2 per repeat unit derived from the isotherm for the same polymer. Further evidence of this discrepancy is found in the bisketone series, in which the *N*-methyl polymer (**3a**) has the largest A_{lim} value, and the *N*-dodecyl polymer (**3b**) has the smallest A_{lim} value. If the polymer were extended flat on the water surface the situation would be expected to be reversed, with the dodecyl group being larger than the methyl group.

Thus, a "secondary" conformation, such as is observed for some polypeptides on a water surface [21], is proposed [73]. The aryl ether linkages have been shown to lend a kink to a polyimide backbone chain [56], and this could be the basis for this secondary conformation in the present polymers.

The polyimide isotherms are affected by neither molecular weight nor the presence of end caps, as is the case in the interfacial behaviour of most macromolecules [18a]. The fact that neither solution concentration nor spreading volume affects the isotherm indicates that the secondary conformation is most likely intramolecular in origin, (such as a helix), and not intermolecular (such as that which could arise through interpenetration of polymer chains).

This secondary conformation might also explain the spreadability of these relatively hydrophobic polymers. Recalling the rigid "hairy-rod" molecules of Wegner, it is possible that the secondary conformation of the present polymers might render the polymer molecules more rigid, and it may be through this rigidity that these polymers, like the rigid "hairy-rod" molecules, are able to spread at the air/water interface. In the recent polysilane studies by Wegner and coworkers [19b], a certain degree of polarity was needed to spread the rigid rods. In the present polyimides, the imide functional group may impart the required degree of polarity to allow the polyimides to spread as rigid rods. This is despite the fact that the imide group has less polarity than is usually required of small molecules to be spread at the air/water interface. There are certainly insufficient alkyl or alkoxy chains in the polyimides to form the "solvent skin" believed necessary for rigid rods to form LB film [3], especially in the *N*-methyl and *N*-phenyl polyimides (**2c**, **3a** and **3c**). This may in part explain the poor deposition results discussed below.

If it <u>is</u> the rigidity of the backbone which allows the polymer to spread, then the A_{lim} trends in the bisketone series may be rationalized by considering the T_g values of

---

[73] "Secondary" conformation simply implies a structure that is not the primary structure observed in the bulk material.

these polymers, (Table 1), since the T_g reflects the relative rigidity of the polymer backbone. Indeed, the *N*-methyl bisketone, **2a**, has the highest T_g of the three materials and is the least compressible on the water surface. Since it appears that the A_{lim} values vary in the same way as the T_g values, it may be concluded that indeed the rigidity of the polymer backbone correlates with the spreading ability of the polyimides at the air/water interface.

It is important to recall that these polyimides are not "high modulus" or "rigid rod" polymers, given the relatively low values of their bulk Young's moduli (Section I.1.5.3.). They do exhibit high T_g values indicative of a certain rigidity for individual chains, as mentioned previously, but their enforced inability to crystallize precludes strong interchain forces and hence high Young's moduli. Thus, if it is simply the rigidity of these individual chains that leads to spreading at the air/water interface, then the requirements of a "rigid rod" type of molecule, as described by Wegner [3], must be reconsidered. On the other hand, if it is the rigidity of the secondary conformation that allows these polymers to spread at the air/water interface, then the Young's modulus in three dimensions is not relevant. A secondary structure may create a whole new "backbone", with rigidity different than chains without the secondary conformation. Only a measure of Young's modulus on an assembly of polymer molecules with such secondary conformations could give further information about the relationship between spreadability and high modulus.

Temperature studies may be considered in light of a surface compression-induced secondary conformation. The Langmuir films of all the polyimides (except for the *N*-dodecyl sulfone polymer, **2b**), are more compressible at higher temperatures. This could be explained if the secondary conformation was destroyed at elevated temeratures. If this phenomenon occurred with the polyimides, however, larger A_{lim} values might also be anticipated at higher temperatures. This would be assuming that the polyimides, released from their secondary conformation, could spread themselves by the usual amphiphilic mechanism, through the interaction of polar groups with the water surface. However, if the extent of polarity was insufficient in the polyimides to allow this to occur even when the secondary conformation was destroyed, then smaller A_{lim} values would be expected. A_{lim} in this case would arise from a multilayered build-up of polymer, with no proper spreading. Smaller A_{lim} values are in fact observed. This may explain the variation of the isotherms of all the polyimides except **2b** with temperature, in a way that is consistent with the proposed secondary conformation of the polymers on the water surface.

The interesting result with the 9:1 chloroform:NMP solution of **2c** can be discussed in the context of polymer behaviour in solution. A standard procedure used to purify a polymer involves precipitating the polymer into a non-solvent, such as water or methanol. First the polymer is dissolved in a good solvent that is miscible with the precipitating solvent, such as NMP or dimethylsulfoxide (DMSO). The resulting polymer solution, which must be fairly concentrated (at least 10% by volume), is added dropwise to the precipitating solvent, whereupon the polymer precipitates out of the mixed solution and may be recovered by filtration. However, no precipitation will be observed if the polymer solution is not concentrated enough. In that case, the quantity of polymer solvent will be adequate to dissolve the polymer in the mixed solution. It is this condition that may affect the surface film balance results. It was thought that adding a small amount of NMP to the spreading solution would allow the polymers that were insoluble in pure chloroform to be dissolved and spread in this mixed solvent. The resulting isotherm, however, showed that for a given polymer, the mixed spreading solvent gave much smaller A_{lim} values. Thus it is concluded that the small amount of NMP, although successful at dissolving the polymer before spreading, actually caused some of the polymer molecules to be dissolved into the water subphase, while some remained at the air/water interface, resulting in smaller A_{lim} values for the total number of molecules.

As noted above, the one polyimide that did not fit the aforementioned patterns was the N-dodecyl sulfone polymer (**2b**). This material was much less compressible than the other dodecyl polymers (**1b**, **3b**). Furthermore, unlike the bisketone polymers (**3a**, **3b** and **3c**) out of which the *N*-dodecyl bisketone (**3b**) was the most compressible, the *N*-dodecyl sulfone (**2b**) is much less compressible than the *N*-phenyl sulfone (**2c**). Finally, the *N*-dodecyl sulfone polymer (**2b**) shows behaviour opposite to all the other polyimides when the temperature is raised. Specifically, the film becomes less compressible as the temperature is increased. One explanation for this is that the *N*-dodecyl sulfone (**2b**) has a different secondary conformation. Another explanation is that this polymer truly fits the category of rigid "hairy-rod" polymer, whereas the other polyimides do not. Specifically, the sulfone moiety might add the required rigidity, and the dodecyl chains might lend the required solubility to the molecules to allow them to behave as the other rigid "hairy-rods". It is believed that all of these polyimides are able to spread at the air/water interface because of their rigidity, as mentioned above. However, the *N*-dodecyl sulfone (**2b**) polymer may have just the right balance of rigidity and solubilizing alkyl chains to cause it to behave differently than the other materials. Certainly, the behaviour of the rigid "hairy-rods" relies upon a highly solubilizing network of covalently bound alkyl chains.

It is important to consider the results of the deposition experiments. The only polymer that could be deposited was the anomolous *N*-dodecyl sulfone, **2b**. This supports the idea that the unusual behaviour of this polymer is due to its strong resemblance to rigid "hairy-rod" polymers. While the behaviour of the other polyimides suggests rigidity of the backbone, the *N*-dodecyl sulfone polymer (**2b**) has, in addition to rigidity, alkyl chains emanating from its backbone. These may allow **2b** to be deposited onto a solid substrate.

Lastly, it should be noted that the transfer ratios are poor, much less than 1.0. This could be indicative of an "unravelling" of the secondary conformation upon deposition.

Since no ordered secondary conformations are observed for these materials in the bulk (no T_m could be detected by DSC), it seems the presence of the water surface is necessary for the adoption of the secondary conformations proposed here. Thus it is not surprising that the removal of the polymers from the water surface by deposition leads to the destruction of the secondary conformation, as indicated by the lack of structure observed by AFM in the LB films of **2b**. The low transfer ratio could also be a reflection of an inadequate number of alkyl chains. The molecules successfully deposited as rigid "hairy-rods" have, in general, a higher ratio of alkyl chains per repeat unit (6-8) and thus the single dodecyl chain per repeat unit for **2b** may be insufficient to fully solvate the polyimide backbone.

These polyimides are able to spread at the air/water interface, despite relatively hydrophobic repeat units. This may be due to a rigidity of the polymer molecules, coupled with the polarity of the imide groups. The A_{lim} values for these polymers suggest that some secondary conformation is adopted at the air/water interface, but this secondary conformation appears to depend heavily on the interaction between the polymers and the water surface. Thus deposition of these materials in ordered LB films is not possible. The *N*-dodecyl sulfone polymer (**2b**) behaves slightly differently, possibly due to its solvating alkyl chains coupled with its highly rigid backbone. These materials, unlike the fullerenes and dendrimers, may change the surface tension by the presence of their slightly polar groups, but the formation of a polyimide/water interface with new interfacial properties may not be discounted.

SECTION II
Thiophene/Ferrocene Compounds

II.1. INTRODUCTION

II.1.1. Approach

The research outlined in this Section provides a complementary approach to the study of ultrathin films presented in Section I of this thesis. Whereas Section I dealt principally with the use of the surface film balance technique to elucidate information regarding the formation and properties of ultrathin films for a variety of molecules, the following section describes the use of two series of closely related molecules which have been designed and synthesized, and then studied as ultrathin films. In contrast to the first approach, a number of different routes are taken to achieve ultrathin films. These routes are based upon two techniques. The first, electrochemistry, is a useful technique for studying ultrathin films, given that these films may be produced electrochemically, and then studied by the same electrochemical techniques as they are formed. This will be discussed in detail in Section II.3.1. The second technique employs the surface film balance, which has been thoroughly discussed in Sections I.1.1.-I.1.4. Both Langmuir films and LB films may be studied by this technique. Furthermore, compounds may be subjected to reactivity conditions while in these forms to produce new films. Information about these films is gathered in two ways. Firstly, by comparing the structure/property trends within the two series of molecules for a given type of film, deductions can be made regarding the molecular architecture of the film. Secondly, by making films from the same material by several methods, the different mechanisms of film formation may be studied. Whereas Section I of this thesis describes the formation of ultrathin films from a wide range of compounds using the surface film balance technique, the work described in the following section uses many techniques to make ultrathin films from one family of compounds.

The compounds shown in Figure 24 were selected on the basis of their postulated properties. They were synthesized by attaching a ferrocene group to a thiophene moiety through an alkyl ester linkage to form two series of compounds, a ω-ferrocenylcarbonyloxyalkyl 2-(3-thienyl)methyl ether series (TM-C_n-Fc), and a ω-ferrocenylcarbonyloxyalkyl 2-(3-thienyl)ethyl ether series (TE-C_n-Fc). The thiophene moiety of the molecules has many interesting features. Most importantly, it can be polymerized, through an oxidative mechanism, at the 2- and 5-positions. Polythiophenes exhibit some intriguing properties [1], most notable being a conductivity verging on the metallic for certain polythiophene derivatives. Furthermore, it has been found that in ultrathin films, some of the features of polythiophenes are actually enhanced, and hence it was felt that thiophene would be an interesting molecule for the ultrathin film studies. The ferrocene group was added through readily accessible syntheses, and serves to functionalize the resulting films for various potential applications, and acts as a probe of the system itself, being covalently bound to the film. This strategy, of covalently attaching some functionality to the backbone of polythiophene, has been described in a general sense by Roncali *et al* [2]. The thiophene and ferrocene functionalities will be discussed in more detail in the following sections. Four model compounds, shown in Figure 25, were also synthesized. It was thought that by studying the behaviour of these model compounds in relation to that of the thiophene/ferrocene compounds, it would be possible to attribute particular properties of these molecules to specific molecular functionalities. The electrochemical and surface film balance studies of these compounds have been published [3], or submitted for publication [4].

---

1. Roncali, J., *Chem. Rev.* **1992**, *92*, 711.
2. Roncali, J.; Garreau, R.; Delabouglise, D.; Garnier, F.; Lemaire, M., *Synth, Met.*, **1989**, *28*, C341.
3. Back, R.; Lennox, R.B., *Langmuir*, **1992**, *8*, 959.
4. Back, R.; Lennox, R.B., *Langmuir*, submitted for publication.

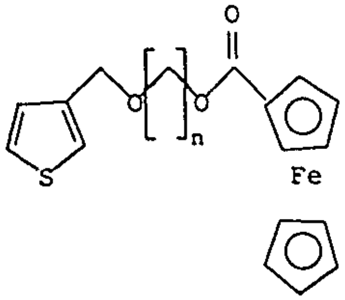

n=6,8,10

TM - C_n - Fc

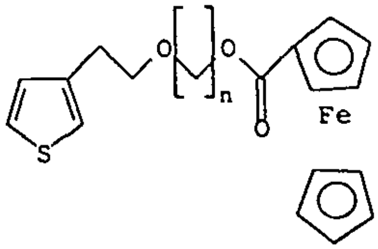

n=6,8,10,12,16

TE - C_n - Fc

Figure 24. The two series of polymerizable thiophene/ferrocene compounds studied as ultrathin films, TM-C_n-Fc and TE-C_n-Fc.

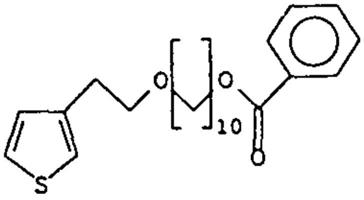

I

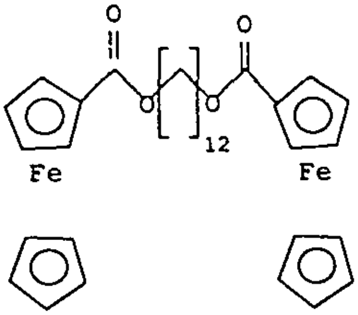

II

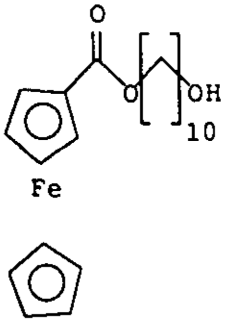

III

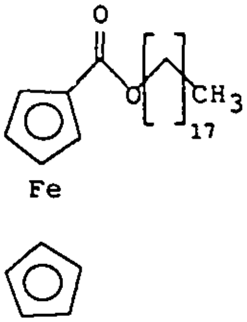

IV

Figure 25. Model compounds used in the study of ultrathin films of thiophene/ferrocene compounds (Figure 24).

II.1.2. Thiophene

II.1.2.1. Polymerization of Thiophene

The oxidative polymerization of thiophene can be achieved both chemically and electrochemically. To polymerize thiophene chemically, an oxidizing agent such as $FeCl_3$ is used with high concentrations of thiophene [5]. To polymerize thiophene electrochemically, unsubstituted thiophene is oxidized at applied potentials of +1.8V vs Ag/AgCl [6]. Substituents that alter the electron density of the thiophene ring will change this oxidation potential.

The mechanisms of these oxidative polymerizations are the subject of some debate [1]. Very little is known regarding the chemical polymerization mechanism [1]. The electrochemical polymerization is generally believed to proceed through a one-electron oxidation of thiophene to a radical cation, (Figure 26) [7]. Since this electron transfer is much faster than diffusion of the thiophene monomers to the electrode, there is always a high concentration of thiophene radical cations at the electrode surface. Thus, in the next step the radical cations combine to form a dication, which then undergoes deprotonation to give a neutral dimer. The driving force of this reaction is the rearomatization of the dimer, and thus the rate-determining step is the radical recombination. In support of this conclusion, the radical cation species have recently been detected using ultrafast cyclic voltammetry [8].

The dimer has more extensive delocalization, and is easier to oxidize than the monomer unit. In fact, as the oligomers become longer, their oxidation potential drops. Hence, under the conditions required to oxidize the monomer, the dimer (and subsequent

---

5. a) Sugimoto, R.; Takeda, S.; Gu, H.B.; Yoshino, K., *Chem. Express*, **1986**, *1*, 635. b) Hota, S.; Soga, M.; Sonoda, N., *Synth. Met.* **1988**, *26*, 267. c) Inoue, M.B.; Velasquez, E.F.; Inoue, M., *Synth. Met.* **1988**, *24*, 223.
6. Ag/AgCl represents the silver, silver chloride reference electrode, to which all potentials herein will be referred.
7. Genies, E.M.; Bidan, G.; Diaz, A.F., *J. Electroanal. Chem.* **1983**, *149*, 101.
8. Andrieux, C.P.; Audebert, P.; Hapiot, P.; Savéant, J.M., *J. Am. Chem. Soc.*, **1990**, *112*, 2439.

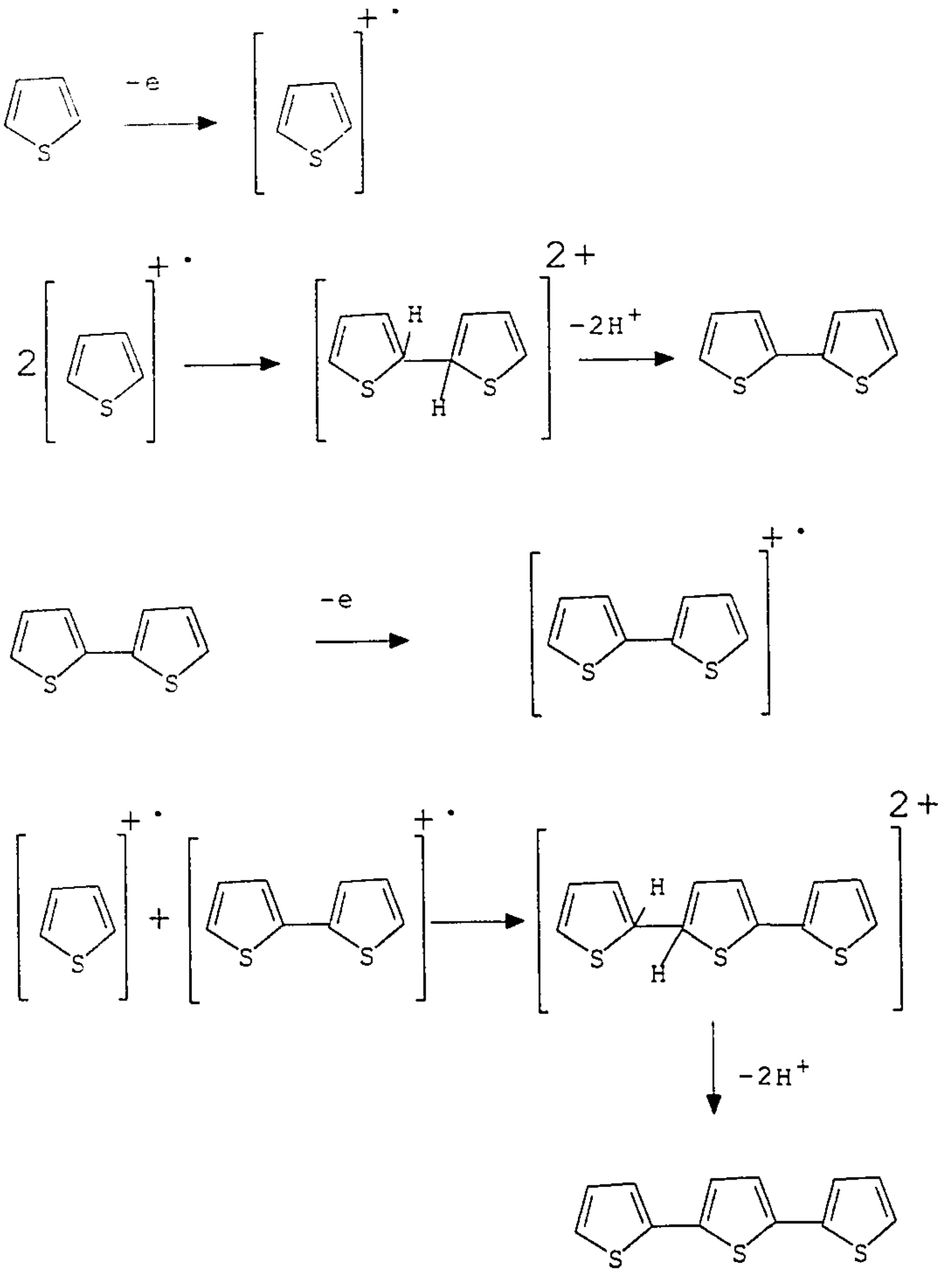

Figure 26. One-electron oxidation of thiophene to a radical cation, believed to be the first step in the electrochemical oxidative polymerization of thiophene.

oligomers) will readily be oxidized to its radical cation, as shown in Figure 26. Thus, further radical recombination reactions will involve not only monomer radical cations, but also higher molecular weight oligomer radical cations. In this manner, polymer chains are produced. When the chain reaches a length at which the solubility limit is exceeded, it is deposited onto the electrode surface. The overall process as described involves two electrons per repeat unit.

It is only possible to depict the first stages of the complex oxidative polymerization mechanism, as there are an infinite number of steps that could follow the oxidation of the thiophene monomer. Experimental conditions could clearly exert considerable influence over the final reaction path. The reaction path in turn could greatly affect the state of the resulting polymer. To begin, it should be understood that there are two competing processes in this polymerization [1]. The first process is the formation of insoluble polymer on the electrode surface, and the second is the formation of soluble oligomers. Although these two processes may seem to be complementary, in fact they are not. At the begining of polymerization, there is a high concentration of monomer radical cations at the electrode surface. These are highly reactive and combine as discussed above to form oligomers. These oligomers, although more easily oxidized to their radical cations, are also less reactive in this form, owing to the stabilization of the radical cation along the extensive conjugated system. Therefore, if there are no reactive radical cations (monomers, possibly dimers) in their vicinity, they may diffuse away from the electrode before they have time to react, thus precluding a build-up of polymer. Of course, once they become insoluble and are deposited onto the electrode surface, this cannot occur, and this is the basis for the competition between the formation of insoluble polymers and soluble oligomers.

Another complication in the electrochemical polymerization of thiophene is the so-called "polythiophene paradox" [9]. This refers to the fact that polythiophene is

---

9. Kritsche, B.; Zagorska, M., *Synth. Met.* **1989**, *28*, C263.

unstable at the potential required to oxidize the thiophene monomer (+1.8V vs Ag/AgCl), and is thus prone to decomposition. From this, one might conclude that polythiophene should not be able to form at all. Gratzl *et al* [10] suggest that in the competition between destruction of the polymer film and polymerization, the latter is kinetically favoured, and hence polymerization is possible. Furthermore, these authors examined the ohmic (iR) drop that develops as the polymer film grows. They found that polymerization was most effective when the applied potential was adjusted to take the iR drop into account. The iR drop constantly increases as the film grows, and thus the iR compensation has to be continuously adjusted. The changing resistivity of the film was cited by these authors as a possible cause for the apparent "polythiophene paradox".

Despite these mechanistic complexities, the electrochemical polymerization of thiophenes has many attractive features. No oxidizing agent or catalyst is required; the monomer is simply dissolved in an electrolytic solution and the required potential is applied to the electrode. The adsorption of resulting polymer film to the electrode surface makes the study of its electrochemical properties convenient. The thickness of the polymer films may be precisely controlled to within nanometers by controlling the amount of current (or electrons) passed through the cell. The chemical polymerization is more useful when a large quantity of bulk polymer is desired. However, translating the results of electrochemical studies to a chemical polymerization must be approached with caution. Whereas the electrochemical polymerization is initiated and propagated by the electrode, and hence localized to a certain degree, the oxidizing agent in the chemical polymerization is distributed throughout the reaction vessel, and thus the two reaction mechanisms could be quite different. There are certain similarities, nonetheless, and through studies like the ones described in this thesis, in which chemically and electrochemically prepared polymers of the same monomer are examined, further insights can be gained.

---

10. Gratzl, M.; Hsu, D.-F.; Riley, A.M.; Janata, J., *J. Phys. Chem.*, **1990**, *94*, 5973.

II.1.2.2. Properties of Polythiophene

Polythiophene is a redox-active polymer. Its backbone may be reversibly oxidized electrochemically by removal of approximately one electron from every four repeat units to give a doped, conducting material [11]. The doping involves migration of the anions of the electrolyte into the polymer to compensate for the positive charge generated by the oxidation. In the reduction of this material back to its neutral form, the anions are expelled and the material is undoped. In its neutral form, most polythiophene derivatives have conductivities typical of a semiconductor, whereas doping leads, in some cases, to metallic levels of conductivity. For example, a conductivity of 500S/cm for poly(3-methylthiophene) has been reported [12]. The electrochemistry of a typical polythiophene shows broad oxidation and reduction peaks, indicating a range of oxidation sites in the polymer network. The oxidation potential of poly(3-methylthiophene) is approximately +0.5V vs Ag/AgCl in 0.1M tetrabutylammonium hexafluorophosphate in acetonitrile (Figure 42a).

Although derivatization of the thiophene unit and different polymerization conditions will alter the precise characteristics of the polymer, the essential feature of these materials is the extended conjugated π system along the backbone of the polymer, which allows for delocalization of charge and hence conduction along the backbone. The conductivity is observed to be highly anisotropic, largely following the course of the backbone. The mean conjugation length can be defined as the average distance over which conjugation extends along the backbone. It is important to recognize that although the polymer chain may be several hundred repeat units in length, the conjugation along

---

11. Tourillon, G.; Garnier, F., *J. Electroanal. Chem.*, **1982**, *135*, 173.
12. Roncali, J.; Garnier, F.; Garreau, R.; Lemaire, M., *J. Chem. Soc., Chem. Commun.*, **1987**, 1500.

this backbone will persist for no longer than six to twelve repeat units [13] before it is disrupted by some irregularity in the chain. In any case, the mean conjugation length is the critical parameter in determining the conductivity of the material [14], as it will determine the band gap. If all the energy levels in a given material are classified as either filled or unfilled, and thus belonging to the valence band or the conduction band, then the band gap is the energy difference between the highest filled energy level (belonging to the valence band) and the lowest unfilled energy level (belonging to the conduction band). The band gap thus defines the excitation energy required for an electron to be excited to an unfilled level in the conduction band. The smaller this gap, the more conducting a material will be.

Another feature determined by the mean conjugation length is the redox activity. The longer the conjugation length, the more readily the backbone is oxidized, because the resonance delocalization stabilizes the resulting radical cation. This is best demonstrated by the decrease in the oxidation potential from the monomer to the dimer to the trimer, and so on. Although the oxidation potential of a polymer is closely related to its conductivity, it alone cannot be used to determine the absolute conductivity of a polythiophene film, as macroscopic factors such as film thickness, the nature of the electrode and electrolyte, and the morphology of the polymer are crucial in determining the conductivity of a polymer. It is important to realize that the conductivity of a polymer film is as much a function of bulk properties as it is of molecular structure.

Another aspect of the polymer material affected by the mean conjugation length is the electronic spectrum. As the energy required to excite an electron in the backbone decreases, not only is the conductivity affected, but the electronic spectrum undergoes a shift to lower energy (longer wavelength). Although this would seem again to provide a

---

13. a) Cao, Y.; Guo, D.; Pang, M.; Qian, R., *Synth. Met.* **1987**, *18*, 189. b) Sauvajol, J.L.; Chenouni, D.; Père-Porte, J.P.; Chorro, C.; Moukala, B.; Petrissans, J., *Synth. Met.* **1990**, *38*, 1.
14. Roncali, J.; Garnier, F.; Lemaire, M.; Garreau, R., *Synth. Met.* **1986**, *15*, 323.

means to indirectly determine the conductivity of a polymer, this can only be achieved in a qualitative way, as is the case for the oxidation potential, for many of the same reasons.

The two most important features in determining the mean conjugation length are the planarity and the stereoregularity of the backbone. Planarity will be disrupted largely by substituents on the thiophene ring. Although there are many advantages to be gained from adding substituents to the thiophene ring, as will be discussed shortly, care must be taken when choosing the substituents to ensure that the planarity of the consecutive thiophene rings is preserved when the derivatized thiophene is polymerized. 3-cyclohexylthiophene was chemically polymerized by Goedel *et al* [15], and the resulting material was compared to poly(3-hexylthiophene). It was found that the band gap of the former polymer was larger than that of the latter, giving a lower conductivity for poly(3-cyclohexylthiophene). This was attributed solely to the increased steric requirements of the cyclic substituent, which forced adjacent thiophene rings to be twisted out of a coplanar configuration.

The stereoregularity of the backbone refers to the extent of α–α' couplings, which lend regularity, and α–β' couplings, which induce irregularity. These are both illustrated in Figure 27. One strategy used to enhance the stereoregularity was surprisingly unsuccessful [14]; this involved chemically synthesizing an oligomer with only α–α' couplings, and electropolymerizing these to form polymer. It was proposed that this would reduce the total number of α–β' couplings. However, this proposal assumed that the probability of an α–α' coupling versus an α–β' coupling was the same for monomers and oligomers. In fact, the relative reactivity of the monomer α and β positions is 95:5 [1], thus ensuring substantial α–α' coupling between monomer radical cations. However, as the oligomer gets longer, this relative reactivity drops, resulting in a higher probability of α–β' coupling at longer oligomer chain lengths. This causes a drop

---

15. Goedel, W.A.; Somanathan, N.S.; Enkelmann, V.; Wegner, G., *Makromol. Chem.*, **1992**, *193*, 1195.

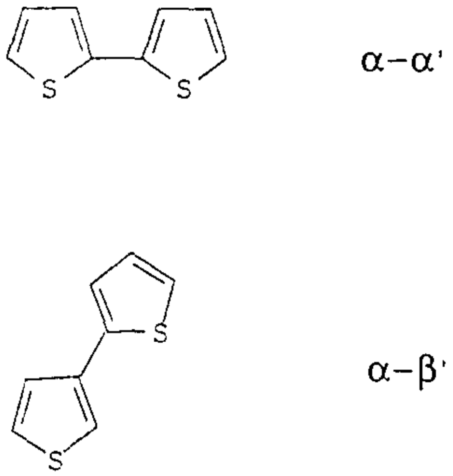

Figure 27. α–α′ and α–β′ coupling of thiophene monomers.

in stereoregularity for the product of these electropolymerized oligomers, and hence lower conductivity. Obviously a balance must be achieved between the increased number of α–α′ couplings that are synthetically created and the increased number of α–β′ couplings that result from the enhanced reactivity of the β position on the oligomer. To date, the monomer unit seems to be the best polymer precursor [1].

Another strategy used to improve the stereoregularity of polythiophene was to derivatize the thiophene monomer with alkyl groups at the 3- and 4-positions prior to polymerization, to preclude any α–β′ coupling [16]. It was found that although the polymer was limited to α–α′ linkages, the alkyl substituents were bulky enough to cause the thiophene rings to be twisted out of plane with respect to one another, substantially reducing the conductivity. Other groups reported that if one substituent was a methyl group and the other an alkoxy group, conductivities of the resulting polymers were five orders of magnitude larger than for dialkyl or dialkoxy thiophenes, although still two orders of magnitude lower than that of poly(3-methylthiophene) [17]. This improvement is thought to be due to reduced steric requirements of the asymmetrically substituted thiophene.

The strategy of disubstituting the thiophene ring was also adopted by Roncali *et al* [12], but they employed a fused ring (3,4-cyclopentathiophene), with the idea of reducing the steric requirements of the substituents. These monomers, when polymerized, had UV-vis spectra similar to poly(3-methylthiophene), but conductivities only equal to those of the poly(3-methyl-4-alkoxythiophene). This discrepancy between the spectral features and the conductivity is attributed to poor interchain conductivity, which is presumably due to the inability of the fused rings to pack as well as the single thiophene

---

16. Tourillon, G.; Garnier, F., *J. Electroanal. Chem.*, **1984**, *161*, 51.
17. a) Leclerc, M.; Daoust, G., *J. Chem. Soc., Chem. Commun.*, **1990**, 273. b) Feldhues, M.; Kampf, G.; Litterer, H.; Mecklenburg, T.; Wegener, P., *Synth. Met.*, **1989**, *28*, C487.

ring. From these sets of experiments, it is concluded that both the stereoregularity and the planarity must be optimized to observe good conductivities.

Another factor that will decrease the quality of the planarity and stereoregularity of electropolymerized material is simply the molecular weight. Under a given set of conditions, the longer the chain becomes, the greater the chance of defects, both in the planarity and the stereoregularity. This is the explanation given for the observations of Yassar *et al* [18] that the conductivity of a film of poly(3-methylthiophene) was related to its thickness. A 200nm thick film had a remarkable conductivity of 2000S/cm. As the films were grown thicker, the conductivity was found to decrease considerably. Spectral and electrochemical data suggested to the authors that films thinner than 200nm would exhibit even higher conductivities, but their standard four-probe technique for conductivity measurements was not effective at these film thicknesses. It must be noted here that, in light of the polythiophene paradox, it is difficult to rule out film destruction as polymer growth proceeds, which could also cause the decrease in conductivity as film thickness increases.

II.1.2.3. Derivatized Polythiophenes

Thiophene has the great advantage of easily achievable derivatization to form new, polymerizable molecules. Many thiophenes with substituents at the β (or 3)-position are commercially available. These may be used as purchased, or they can be further reacted to give a custom-designed monomer. It is observed that changing the substituent often has a considerable effect on the properties of the polymer, allowing for precise control over many polymer features. In this section, the scope of that control will be discussed.

The two features of particular interest with polythiophenes are their electronic properties and their processibility. Other less heralded features include their nonlinear

---

18. Yassar, A.; Roncali, J.; Garnier, F., *Macromolecules*, **1989**, *22*, 804.

optical properties. Derivatization of thiophene to produce new polymers is usually geared towards the improvement and enhancement of these features. When considering the polymerization of a substituted thiophene monomer, it is important to consider the resulting materials on many levels, as described by Roncali [1]. On the molecular level, the derivatized monomer must be viewed in light of its ability to polymerize relative to unsubstituted thiophene. Recalling the proposed competition between the formation of soluble oligomer and insoluble polymer, this will be determined primarily by the reactivity of the derivatized monomer, which can be greatly affected sterically and/or electronically by the substituent. On the macromolecular level, the material resulting from this polymerization must be examined. In particular, the planarity and stereoregularity of the polymer, and the inter-chain conductivity as discussed earlier, will affect properties such as the bulk conductivity. Of course, the electrochemical and optical properties of the derivatized polythiophene will also be of interest. Finally, on the macroscopic level, bulk properties, including the mechanical properties and processability of the material, will be important in determining the feasibility of any practical applications of a new material.

The reactivity of the monomer is of primary concern, as there is a finite window of reactivity that will result in high molecular weight polymer, as mentioned earlier. The reactivity of the monomer is determined by the stability of its radical cation, which is related to the electron density in the thiophene ring. An electron-withdrawing substituent will destabilize the radical cation, making it more reactive. An electron-donating substituent, on the other hand, will stabilize the radical cation, reducing its reactivity. (These changes are reflected in the oxidation potentials of the derivatized thiophene, as an electron-withdrawing substituent increases the oxidation potential, and an electron-donating substituent decreases the oxidation potential.) If the reactivity of the derivatized thiophene is too great, there is a risk of reaction with the solvent, thus precluding the establishment of a high concentration of radical cations at the electrode surface that is necessary for polymer formation. On the other hand, if the reactivity is too low, the radical cations will diffuse from the electrode before reaction can occur.

Simple alkyl chains were one of the first substituents to be used to derivatize thiophene at the 3-position [19]. An increase in solubility, and thus an improved processibility, of the resulting polymer relative to polythiophene are the most noticeable features of these materials. The effect of the alkyl chains is basically that of an internal plasticizer, and has been used to render many other polymers more processible. (See, for example, the dodecyl-substituted polyimides, Section I.1.5.3.). The alkyl chains are thought to disrupt crystallization and order in the polymers, and to lend more flexibility to the backbone, allowing the individual chains to be dissolved more readily. Unfortunately, the order within the polymers that makes dissolution difficult is necessary for the materials to be conducting. Thus, the longer the alkyl chain substituent, the more soluble and less conducting the resulting polymer. Furthermore, there is only a certain range of alkyl chain lengths that are successful in improving processibility. If the number of carbons in the alkyl chain, n, is 3 or less, the plasticizing effect is simply not observed [19a]. On the other hand, if n is greater than 10, the side chains are believed to crystallize, thus reducing the processibility of the polymer [19c].

Other substituents which have been used to modify polythiophene include branched alkyl chains [19c] and fluorinated alkyl chains [20]. The former act more or less as *n*-alkyl chains, unless the branch occurs too close to the thiophene ring, in which case the resulting polymer has both reduced reactivity and conductivity. The fluorinated polymers exhibit better mechanical properties than other derivatized polythiophenes, and

---

19. a) Elsenbaumer, R.L.; Jen, K.Y.; Oboodi, R., *Synth. Met.*, **1986**, *15*, 169. b) Chang, A.-C.; Blankespoor, R.L.; Miller, L.L., *J. Electroanal. Chem.* **1987**, *236*, 239. c) Roncali, J.; Garreau, R.; Yassar, A.; Marque, P.; Garnier, F.; Lemaire, M., *J. Phys. Chem.*, **1987**, *91*, 6706.
20. Büchner, W.; Garreau, R.; Lemaire, M.; Roncali, J., *J. Electroanal. Chem., 1990, 277, 355.*

have the high resistance to organic solvents that is typical of fluorinated materials. This can however lead to difficulties in processing.

Aryl groups have also been attached to the 3-position of thiophene [21]. As with the branched alkyl chains, the properties of the polymer are adversely affected if the aryl ring is too close to the polymer backbone. This appears to be true for bulky groups in general. The advantage to these materials is the possibility of reaction at the aryl ring after polymerization has been effected, so as to further functionalize the polymer.

Chains with one or more ether linkages have also been attached to thiophene through alkyl groups [22]. The ether linkages add solubility and a degree of hydrophilicity to the resulting polymer. Furthermore, they exhibit an affinity for cations such as Li^+, given their similarity to a crown ether structure. This aspect of the polyether substituents has yet to be explored fully. Although attaching the ether linkage directly to the thiophene ring would lower the oxidation potential below that for unsubstituted thiophene, the reactivity of the resulting radical cations has been shown to be too low for good polymerization conditions [19b].

From the various applications of doped polythiophenes arises the concept of self-doped polythiophenes [23]. These materials contain anions, usually sulfonates, covalently bound to the polythiophene backbone. In its reduced, non-conducting form, this polymer carries a negative charge, and charge-compensating cations migrate into the polymer matrix from the electrolyte. When the polymer is oxidized, its backbone becomes positively charged, and the mobile cations from the electrolyte leave the polymer matrix

---

21. a) Roncali, J.; Youssoufi, H.K.; Garreau, R.; Garnier, F.; Lemaire, M., *J. Chem. Soc., Chem. Commun.*, **1990**, 414. b) Lemaire, M.; Garreau, R.; Delabouglise, D.; Roncali, J., Youssoufi, H.K.; Garnier, F., *New J. Chem.*, **1990**, *14*, 359.
22. a) Blankespoor, R.L.; Miller, L.L., *J. Chem. Soc., Chem. Commun.*, **1985**, 90. b) Bryce, M.R.; Chissel, A.; Kathigamanathan, P.; Parker, D.; Smith, N.R.M., *J. Chem. Soc., Chem. Commun.*, **1987**, 466. c) Roncali, J.; Garreau, R.; Delabouglise, D.; Garnier, F.; Lemaire, M., *J. Chem. Soc., Chem. Commun.*, **1989**, 679. d) Feldhues, M.; Kämpf, G.; Litterer, H.; Mecklenburg, T.; Wegener, P., *Synth. Met.*, **1989**, *28*, C487 (reference 17b). e) Roncali, J.; Shi, L.H.; Garreau, R.; Garnier, F.; Lemaire, M., *Synth. Met.*, **1990**, *36*, 267.
23. Patil, A.O.; Ikenoue, Y.; Wudl, F.; Heeger, A.J., *J. Am. Chem. Soc.*, **1987**, *109*, 1858.

to maintain an overall neutral charge of the material. Thus, although the electrolyte ions are still involved in the doping process, it is the <u>oxidation</u> of these self-doped polymers to their conducting form that causes the flow of ions out of the polymer, a process that accompanies the <u>reduction</u> of the regular polythiophenes. Of added interest is the water-soluble nature of these materials.

Redox groups such as bipyridyl [24], viologen [25], anthracene [26], benzoquinone [27], tetrathiafulvalene [28] and recently ferrocene [3,29] have been attached to thiophene at the 3-position. The resulting polymer has, in addition to its own redox activity, a well defined redox couple bound to the electrode surface by the polymer backbone. From such a supramolecular structure, sensors, electrochromic devices and rechargeable batteries may be fashioned. Chiral substituents have also been introduced onto thiophene, with potential sensing applications indicated [30].

II.1.3. Ferrocene

Ferrocene is a transition metal complex comprised of two cyclopentadienyl anion ligands attached to Fe(II). Ferrocene may be reversibly oxidized to a ferricenium ion at +0.34V (vs Ag/AgCl). Although this redox couple is sometimes used as a standard in electrochemistry [31], the instability of the ferricenium ion in the presence of nucleophiles has been reported [32]. The presence of dissolved oxygen has also been

---

24. Mirazaei, R.; Parker, D.; Munro, H.S., *Synth. Met.*, **1989**, *30*, 265.
25. a) Shu, C.-F.; Wrighton, M.S., in *Electrochemical Surface Science: Molecular Phenomena at Electrode Surfaces*, Ed. Soriaga, M.P., **1988**, ACS Series *378*, p. 408. b) Bäuerle, P.; Gaudl, K.-U., *Adv. Mater.* **1990**, 2, 185.
26. Basak, S.; Nayak, K.; Marynick, D.S.; Rajeshwar, K., *Chem. Mater.*, **1989**, *1*, 611.
27. Grimshaw, J.; Perera, S.D., *J. Electroanal. Chem.*, **1990**, *278*, 287.
28. Bryce, M.R.; Chissel, A.D.; Gopal, J.; Kathigamanathan, P.; Parker, D., *Synth. Met.*, **1991**, *39*, 397.
29. a) Bäuerle, P.; Gaudl, K.-U., *Synth. Met.* **1991**, *41-43*, 3037. b) Reference 3.
30. Kotkar, D.; Joshi, V.; Ghosh, P.K., *J. Chem. Soc., Chem. Commun.*, **1988**, 917.
31. Peover, M.E. in *Electroanalytical Chemistry*, ed. Bard, A.J., Marcel Dekker, New York, **1967**, 2, 12.
32. Prins, R.; Korswagen, A.R.; Kortbeek, A.G.T.G., *J. Organometal. Chem.*, **1972**, *39*, 335.

reported to affect the stability of the ferrocene [33]. Furthermore, a study of the stability of the ferrocene redox couple under potential cycling conditions from -1.0V to +1.0V vs Ag/AgCl in acetonitrile at a platinum electrode showed a passivation of the electrode surface, and a decrease of the redox currents [34]. The authors concluded that a new species was being formed, as indicated by an irreversible reduction peak at potentials less than 0.0V, that was passivating the electrode surface.

Many synthetic routes are available for derivatization of ferrocene, primarily through a Friedel-Crafts reaction or a metallated ferrocene. Simple derivatives are also commercially available, which may be further reacted to give the desired product. When performing electrophilic aromatic substitution reactions at the cyclopentadienyl rings, care must be taken to avoid oxidizing conditions. Often, the ferrocene moiety is stabilized relative to its oxidized ferricenium form by derivatization. For example, ferrocene carboxylic acid has an oxidation potential of +0.62V vs Ag/AgCl, and is less prone to undesired oxidation.

Ferrocene has been employed in many applications. It is primarily useful as an electron shuttle or mediator. It acts as a mediator for many oxidase enzymes, particularly glucose oxidase (GOD) [35]. The electrochemical oxidation of ferrocene in the presence of glucose and GOD is characterized by an irreversible and catalytic oxidation wave, the ferricenium being reduced by reduced GOD. This has led to many glucose sensor designs, the first which simply incorporated the ferrocene and GOD into the electrode mechanically [36]. Later designs concentrated on improving the longevity of the electrodes by immobilizing one or both components on the electrode surface. In some, a

---

33. Sato, M.; Yamada, T.; Nishimura, A.; *Chem. Lett.*, **1980**, 925.
34. Daschbach, J.; Blackwood, D.; Pons, J.W.; Pons, S.; *J. Electroanal. Chem.*, **1987**, *237*, 269.
35. Cass, A.E.G.; Davis, G.; Green, M.J.; Hill, H.A.O., *J. Electroanal. Chem.* **1985**, *190*, 117.
36. Cass, A.E.G.; Davis, G.; Francis, G.D.; Hill, H.A.O.; Aston, W.J.; Higgins, I.J.; Plotkin, E.V.; Scott, L.D.L.; Turner, A.P.F., *Anal. Chem.* **1984**, *56*, 667.

ferrocene derivatized with functionalities such as anthracene [37] or an alkyl thiol [38] was bound to an electrode through the well known adsorption of these functionalities to glassy carbon and gold electrodes, respectively. One system relied upon the physical incorporation of ferrocene, along with the enzyme, GOD, into a polyacrylamide gel [39]. Ferrocene has also been covalently bound to the enzyme, which may then be physisorbed to a glassy carbon electrode [40]. In another system, ferrocene was covalently bound to polysiloxane [41]. This type of polymer-based system perhaps holds the most promise for practical devices, as several other ferrocene-derivatized polymers have since been reported, including polysilane, [42], polyaniline, [43], poly(L-lysine), [44], polypyrrole, [45] and poly(vinylferrocene), [46].

Another, less common use for ferrocene exploits the dependence of its electrochemical response on its relative mobility and accessibility. For example, ferrocene may be incorporated as a guest of the host molecule cyclodextrin, but becomes inactive as a mediator for the glucose-GOD catalysis under these conditions [47]. This may be used to detect, for example, antigen-antibody binding. If antigen is labelled with ferrocene, this ferrocene will be catalytically inactive when the derivatized antigen binds

---

37. Jönsson, G.; Gorton, L.; Pettersson, L. *Electroanalysis*, **1989**, 49.
38. a) Chidsey, C.E.D.; Bertozzi, C.R.; Putrinski, T.M.; Mujsce, A.M., *J. Am. Chem. Soc.*, **1990**, *112*, 4301. b) Uosaki, K.; Sato, Y.; Kita, H., *Langmuir*, **1991**, *7*, 1510.
39. Lange, M.A.; Chambers, J.Q., *Analytica Chimica Acta*, **1985**, *175*, 89.
40. a) Bartlett, P.N.; Whitaker, R.G.; Green, M.J., Frew, J., *J. Chem. Soc., Chem. Commun.*, **1987**, 1603. b) Degani, Y.; Heller, A., *J. Phys. Chem.*, **1987**, *91*, 1285.
41. Hale, P.D.; Inagaki, T.; Karan, H.I.; Okamoto, Y.; Skotheim, T.A., J. *Am. Chem. Soc.*, **1989**, *111*, 3482.
42. Diaz, A.; Seymour, M.; Pannell, K.H.; Rozell, J.M., *J. Electroanal. Chem.*, **1990**, *137*, 503.
43. Horowitz, C.P.; Dailey, G.C., *Chem. Mater.* **1990**, 2, 343.
44. Abeysekera, A.M.; Grimshaw, J.; Perera, S.D., *J. Chem. Soc. Perkin Trans. 2*, **1990**, 1797.
45. a) Inagaki, T.; Hunter, M.; Yang, X.Q.; Skotheim, T.A.; Okamoto, Y., J. *Chem. Soc., Chem. Commun.*, **1988**, 126. b) Eaves, J.G.; Mirrazaei, R.; Parker, D.; Munro, H.S., *J. Chem. Soc., Perkin Trans. II*, **1989**, 373.
46. a) Willman, K.W.; Rocklin, R.D.; Nowak, R.; Kuo, K.N.; Schultz, F.A.; Murray, R.W., *J. Am. Chem. Soc.*, **1980**, *102*, 7629. b) Peerce, P.J.; Bard, A.J., *J. Electroanal. Chem.*, **1980**, *114*, 89. c) Peerce, P.J.; Bard, A.J., *J. Electroanal. Chem.*, **1980**, *112*, 97.
47. Ryabov, A.D., *Angew. Chem. Int. Ed. Engl.* **1991**, *30*, 931, and references cited.

to the antibody. However, if further, underivatized antigen is introduced to the system, this will free some of the ferrocene-derivatized antigen, and this ferrocene will regain its catalytic activity. Thus, the presence of antigen may be monitored through the catalytic activity of the ferrocene label [47]. This dependence of the catalytic abilities of ferrocene on its relative mobility may also be relevent in designing the aforementioned glucose sensors. Indeed, it is not yet clear whether ferrocene bound to polymers and enzymes is always capable of mediating the catalytic oxidation of glucose, and in some studies it is possible that intermolecular catalysis or catalysis by some residual free ferrocene is responsible for the observed catalysis, when the mobility of the bound ferrocene is not sufficient [47]. In the work described in this thesis, a method is presented which definitively affixes ferrocene to an electrode surface with a range of tether lengths. This system could be useful in determining the effect of such anchoring on the catalytic activity of the ferrocene group.

II.2. SYNTHESIS

II.2.1. Experimental

The TM-C_n-Fc compounds (Figure 24) are prepared using the route shown in Figure 28. In a typical synthesis, 25mmol (2.5ml) of 3-methylthiophene was added to 25ml of dry benzene (American Chemicals Ltd.), followed by 50mg benzoyl peroxide (Aldrich). This solution was brought to reflux. Through a water-cooled funnel 22mmol (4.1g) N-bromosuccinimide (Aldrich) and a further 50mg benzoyl peroxide were added. The mixture was allowed to come to room temperature as the colour changed from orange to yellow. The succinimide was then removed by filter and the benzene was removed by rotary evaporation, leaving a highly lachrymatory orange oil [48].

The resulting oil was then dissolved in 125ml freshly distilled dimethylformamide (American Chemicals Ltd.) with 30mmol of diol (Aldrich) and 30mmol NaH (Aldrich). This mixture was stirred for up to 4 days, with the reaction time dependent on the specific diol. Following work up with water and chloroform (American Chemicals Ltd.), the mixture was separated using flash column chromatography (hexanes: ethyl acetate, with the specific ratio dependent upon the diol used, American Chemicals Ltd., silica gel Merck grade 60, Aldrich) to obtain the monoalcohol. ^{1}H NMR data (200MHz, Varian XL200) are given in Appendix I.

Ferrocene acid chloride was typically produced from 15mmol (2.3g) of ferrocene carboxylic acid (Aldrich) and a sixfold excess of oxalyl chloride (Aldrich, 2.0M solution in CH_2Cl_2). The former was dissolved in 80ml of dry CH_2Cl_2. The oxalyl chloride solution was then added to the reaction vessel, followed by four drops of dry pyridine (American Chemicals Ltd.). A white precipitate sublimed from the mixture at this point. This mixture was stirred in the dark for 14 hours at room temperature, whereupon refluxing was initiated and maintained for an additional 6 hours. The reaction mixture,

---

48. a) Campaigne, E.; LeSuer, W.M., *J. Am. Chem. Soc.*, **1948**, *70*, 1555. b) Campaigne, E.; Tullar, B.F., *Organic Synthesis Collective Vol. IV*, Ed. N. Rabjohn, **1963**, 921, John Wiley & Sons, Inc., New York.

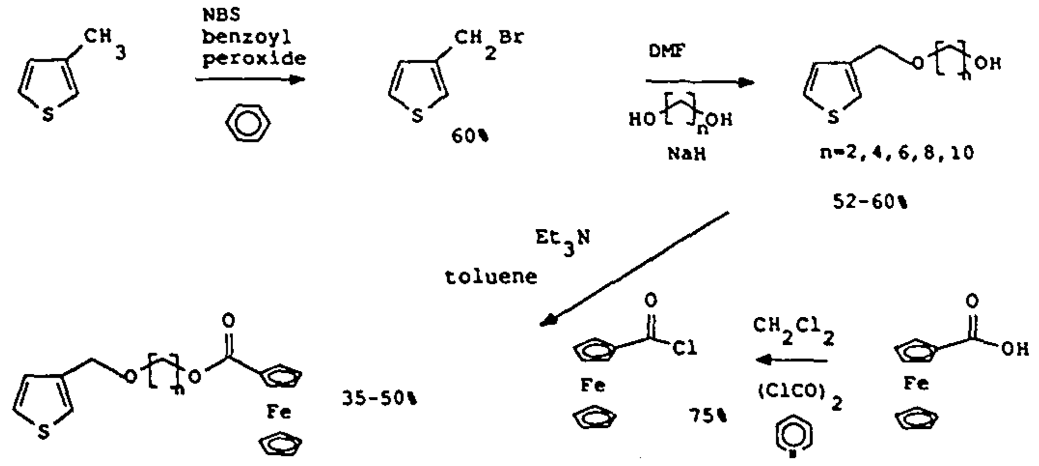

Figure 28. Synthesis of TM-C$_n$-Fc compounds.

which contained a dark insoluble precipitate, was then extracted with hot petroleum ether (American Chemicals Ltd.) to give a dark red solution, from which ferrocene acid chloride was recrystallized, to yield dark red crystals [49]. This acid chloride was then added to 125ml dry toluene (American Chemicals Ltd.), followed by the monoalcohol from the preceeding step, and a three-fold excess of triethylamine (Aldrich). The flask was stirred under N_2 for 3 days. The product was purified by flash chromatography (95:5 hexanes: ethyl acetate). ^{1}H NMR data and mass spectrometry data (KRATOS MS25 RFA Mass Spectrometer with DS90 data system) are given in Appendix II.

The synthesis scheme for the TE-C_n-Fc series is shown in Figure 29. In a typical synthesis, 10mmol (2.65g) ferrocene acid chloride, generated as described above, was dissolved in 30ml dry CH_2Cl_2 and added dropwise to a solution of 30mmol diol (Aldrich) in 200ml dry pyridine (Aldrich), with a catalytic amount of dimethylaminopyridine (DMAP) (Aldrich). This mixture was then allowed to stir at room temperature under N_2 for up to 30 hours, to give a ferrocene-substituted alcohol. This ferrocene-substituted alcohol was purified by flash liquid chromatography (60:40 petroleum ether: ether, Aldrich, silica gel Merck grade 60, Aldrich). ^{1}H NMR data are given in Appendix III. The purified ferrocene-substituted alcohol and di-*t*-butylpyridine (Aldrich) were added in a 0.8:1.05 ratio [50] to 30ml dry CH_2Cl_2 and cooled to 0°C. In an addition funnel trifluoromethanesulfonic anhydride (Aldrich) (ratio to base of 1.0:1.05 [50]) was dissolved in 15ml CH_2Cl_2. This was added dropwise to the ferrocene solution. After addition was completed, the mixture was allowed to come to room temperature over 1.5 hours. Without isolating the triflate, a further amount of base (fourfold excess) was added to the flask, followed by a twofold excess of 2-(3-thienylethanol) (Aldrich), [51]. Product was isolated after up to 64 hours by flash liquid chromatography (90:10 petroleum ether:ether). ^{1}H NMR data and mass spectrometry data are given in Appendix IV.

---

49. Knobloch, F.W.; Rauscher, W.H.; *J. Polym. Sci.*, **1961**, *54*, 655.
50. Vedejs, E.; Engler, D.A.; Mullins, M.J., *J. Org Chem.*, **1977**, *42*, 3109.
51. Evans, P.A.; Sheppard, G.S., *J. Org. Chem.*, **1990**, *55*, 5192.

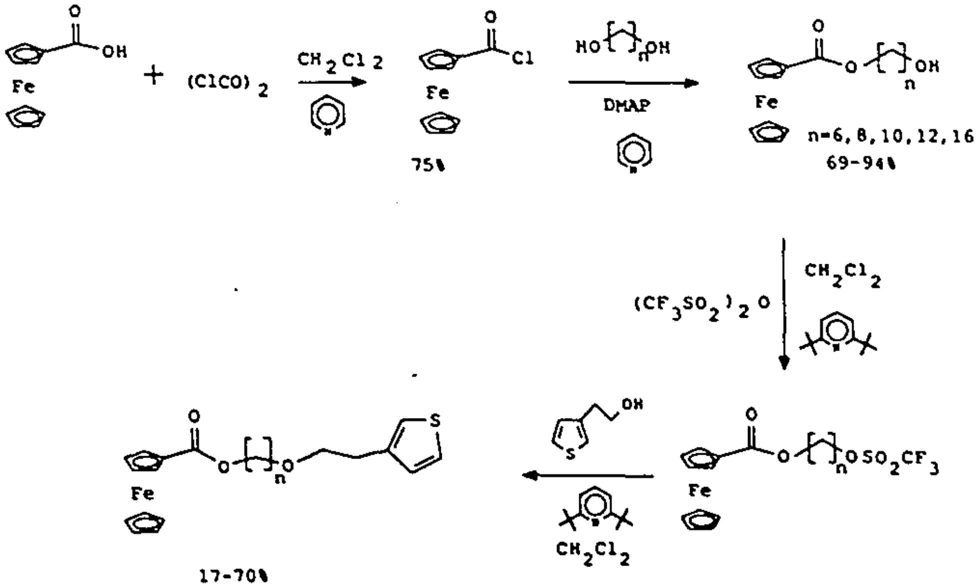

Figure 29. Synthesis of TE-C_n-Fc compounds.

Compound I was synthesized following the procedure for the TE-C_n-Fc series, replacing ferrocene acid chloride with benzoyl chloride (Aldrich). Compounds II, III and IV can all be derived as shown in Figure 30 from ferrocene acid chloride, which is obtained from ferrocene carboxylic acid, as for the thiophene/ferrocene compounds. The methodology is similar to the second step in the TE-C_n-Fc series synthesis, and the ferrocene alcohol, III, is an actual intermediate in the synthesis of the TE-C_n-Fc series. It is obtained by reacting a large excess (5:1) of diol with ferrocene acid chloride in dry pyridine (American Chemicals, Ltd.), in the presence of a catalytic amount of dimethylaminopyridine (DMAP, Aldrich), as described above. When a stoichiometric amount of diol is used (1:2), however, the bis-ferrocene compound, II, is formed. The alkyl ferrocene, IV, is synthesized from ferrocene acid chloride using the same conditions as for II and III, with the appropriate monoalcohol replacing the diol. ^{1}H NMR data are given in Appendix V.

II.2.2. Results and Discussion

Synthesis of the TM-C_n-Fc series presented no major obstacles. Yields for steps 1,2 and 3 were 60, 60 and 40% respectively. Some difficulties were encountered in the synthesis of the TE-C_n-Fc series which will be described below. Initially, the reaction of ferrocene carboxylic acid and diol to produce a ferrocene alcohol was performed with trimethylsilyl chloride (TMS-Cl) as it was hoped that the TMS group would attach itself to the ferrocene carboxylic acid by displacement of the proton, and then in turn be displaced by one end of the diol, as illustrated in Figure 31 [52]. This reaction, however, did not go to sufficient conversion, and much ferrocene carboxylic acid remained after several days.

The next strategy used was to attach the diol to the thiophene end. To achieve this, the mesylate of 2-(3-thienyl)ethanol was synthesized, as shown in Figure 32. The

---

52. Brook, M.A.; Chan, T.H., *Synthesis - Stuttgart*, **1982**, 201.

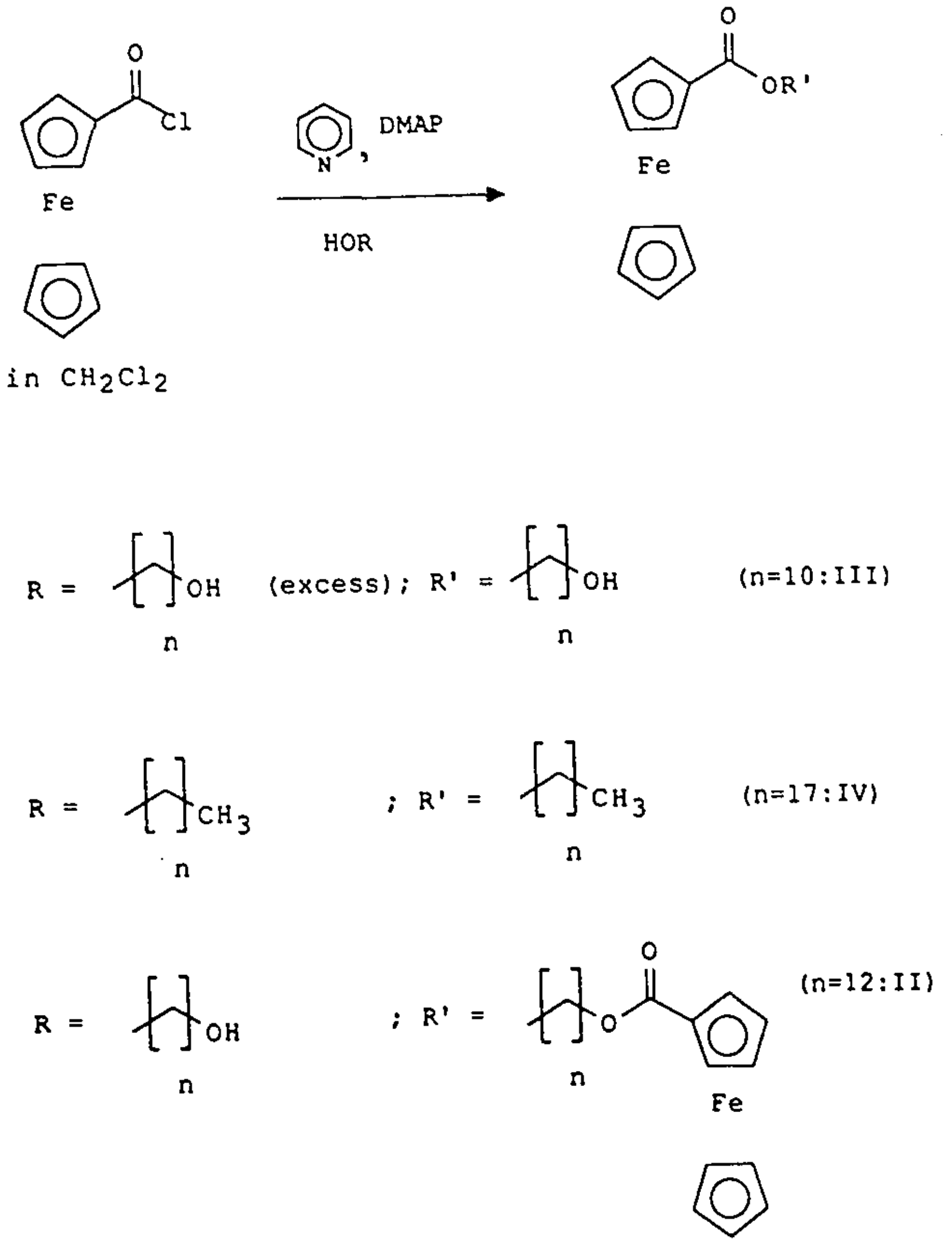

Figure 30. Synthesis of model compounds II, III, and IV from ferrocene acid chloride.

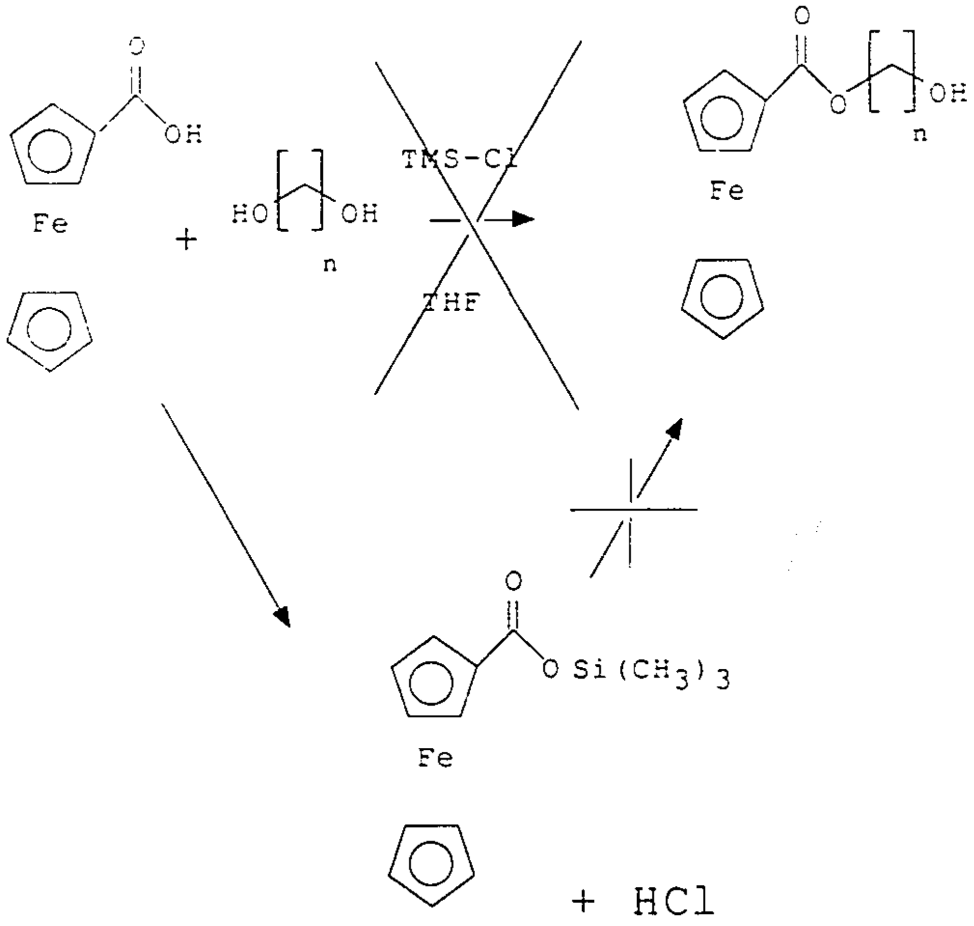

Figure 31. Attempted condensation of ferrocene acid chloride and diol, using TMS-Cl.

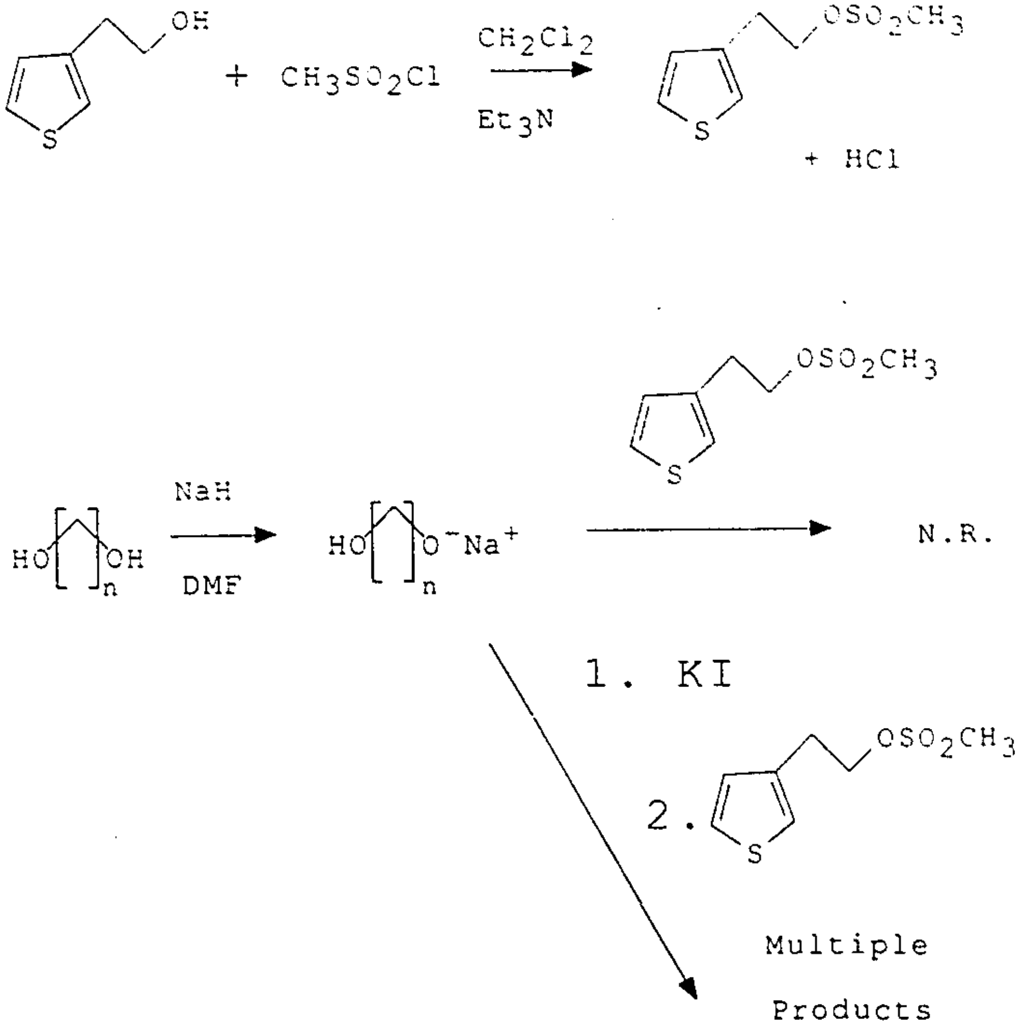

Figure 32. Synthesis of 2-(3-thienyl) ethanol mesylate, and attempted displacement of the mesyl group.

displacement of the mesyl group, however, proved to be unattainable under a host of different conditions, including the deprotonation of the diol with sodium hydride in dimethylformamide. The latter conditions did give some elimination product, but a large quantity of starting material still remained. Addition of potassium iodide to the reaction lead to multiple products, one of them again being the elimination product (Figure 32).

The next approach was to attempt again to attach the diol to the ferrocene group, this time through the ferrocene acid chloride, as synthesis of the acid chloride was a reliable procedure, with 75% yields after recrystallization. This acid chloride was reacted with a straight chain diol to give a ferrocene alcohol compound, as described in Section II.2.1. Pyridine proved to be an excellent solvent, and acted as the required base at the same time, to give good yields (69-94%) when conditions were optimized. This included working with a threefold excess of diol with respect to ferrocene acid chloride, and adding the latter, dissolved in dichloromethane, dropwise to the solution of diol in pyridine, to create a condition of high dilution. This minimized the formation of the main side-product of this reaction, the bis-ferrocene compound (II). A catalytic amount of dimethylaminopyridine was also required.

The first attempt to attach the desired thiophene group to the ferrocene alcohol was through mesylation of the ferrocene alcohol (Figure 33). Without deprotonating the 2-(3-thienyl)ethanol, it proved to be impossible to displace the mesyl group. However, upon deprotonation of the 2-(3-thienyl)ethanol, the ferrocene alcohol was cleaved at the ester position (Figure 33).

Next, synthesis of the ferrocene triflate was attempted. It was hoped that the more labile triflate group could be displaced under conditions that would not cleave the ester group. This turned out to be facile, with deprotonation of the 2-(3-thienyl)ethanol being unnecessary. The displacement step required the use of a sterically hindered base, 2,6-di-*t*-butylpyridine, in order that the base should not itself displace the triflate.

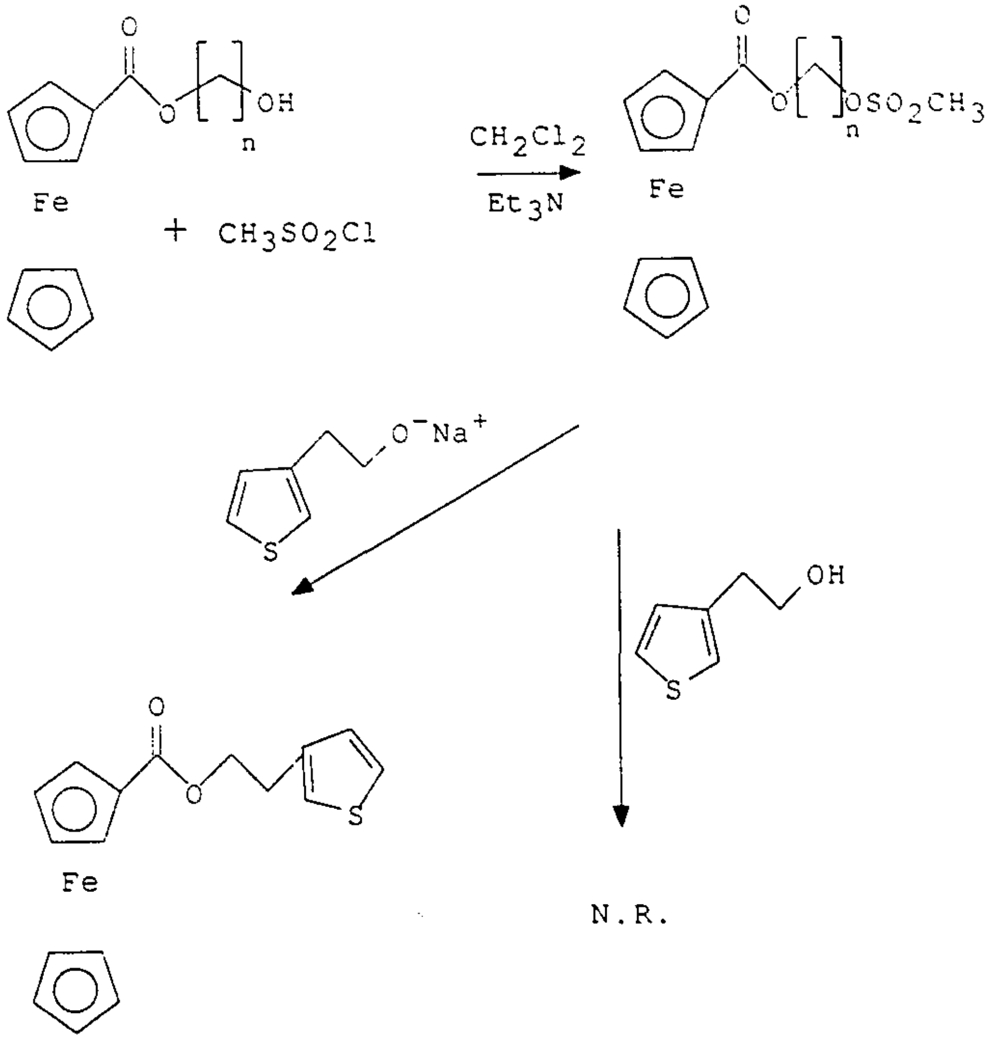

Figure 33. Synthesis of ferrocene alcohol mesylate, and attempted displacement of the mesyl group.

The yield was more than tripled over the last two steps (triflate formation and displacement) by the final modification of the procedure (from <20% to 70%). Instead of isolating the triflate, or performing a workup after the first step, the two steps were performed in one pot. It is important to use the sterically hindered base employed in the triflate displacement in the triflate formation step as well, adding 1.05 equivalents initially, (for the triflate formation), and then an additional threefold excess (plus the 2-(3-thienyl)ethanol) when the triflate formation is deemed to be complete.

II.3. ELECTROCHEMICAL STUDIES

II.3.1. Introduction

Electrochemistry is one of the tools that was employed to explore the properties of thin films of the thiophene/ferrocene compounds. In order to establish a good understanding of the experiments that will be described herein, some basic concepts of electrochemistry will be outlined in this section. For further information, the reader is referred to several good texts [53].

The electrochemical experiment is performed in an electrochemical cell. A typical cell is shown in Figure 34. It consists of three electrodes, the working electrode (W), the reference electrode (R), and the auxilliary electrode (A). These electrodes are connected to a potentiostat, which can apply the desired voltage or current to the cell. While the current runs between the working and auxilliary electrodes, the potential at the working electrode is controlled with respect to the reference electrode. This is accomplished by the use of operational amplifiers, and the reader is referred to other references for more details [54]. The goal of this configuration is the minimization of the current, i, between the working and reference electrodes, and hence the minimization of the ohmic drop, iR, between them. There will be a drift in the signal if the resistance, R, is not minimized, as R will vary with the applied potential. In the cell shown in Figure 34, the three electrodes are immersed in an electrolyte solution. This consists of an ionized salt dissolved in a solvent. The solvent generally must have a high dielectric constant (>20), such as that for water (78.5), methanol (32.6), nitrobenzene (34.8) or acetonitrile (35.8), and exhibit no electrochemistry over the potential range of interest. The salt must be soluble in the solvent at the desired concentration, and of course not interfere with the electrochemistry

---

53. Bard, A.J., Faulkner, L.R., *Electrochemical Methods*, John Wiley and Sons, Toronto, **1980**.
54. a) Kissinger, P.T.; Heineman, W.R., *Laboratory Techniques in Electroanalytical Chemistry*, Marcel Dekker, Inc., New York, **1984**. b) Southampton Electrochemistry Group, *Instrumental Methods in Electrochemistry*, Ellis Horwood Limited, Toronto, **1985**.

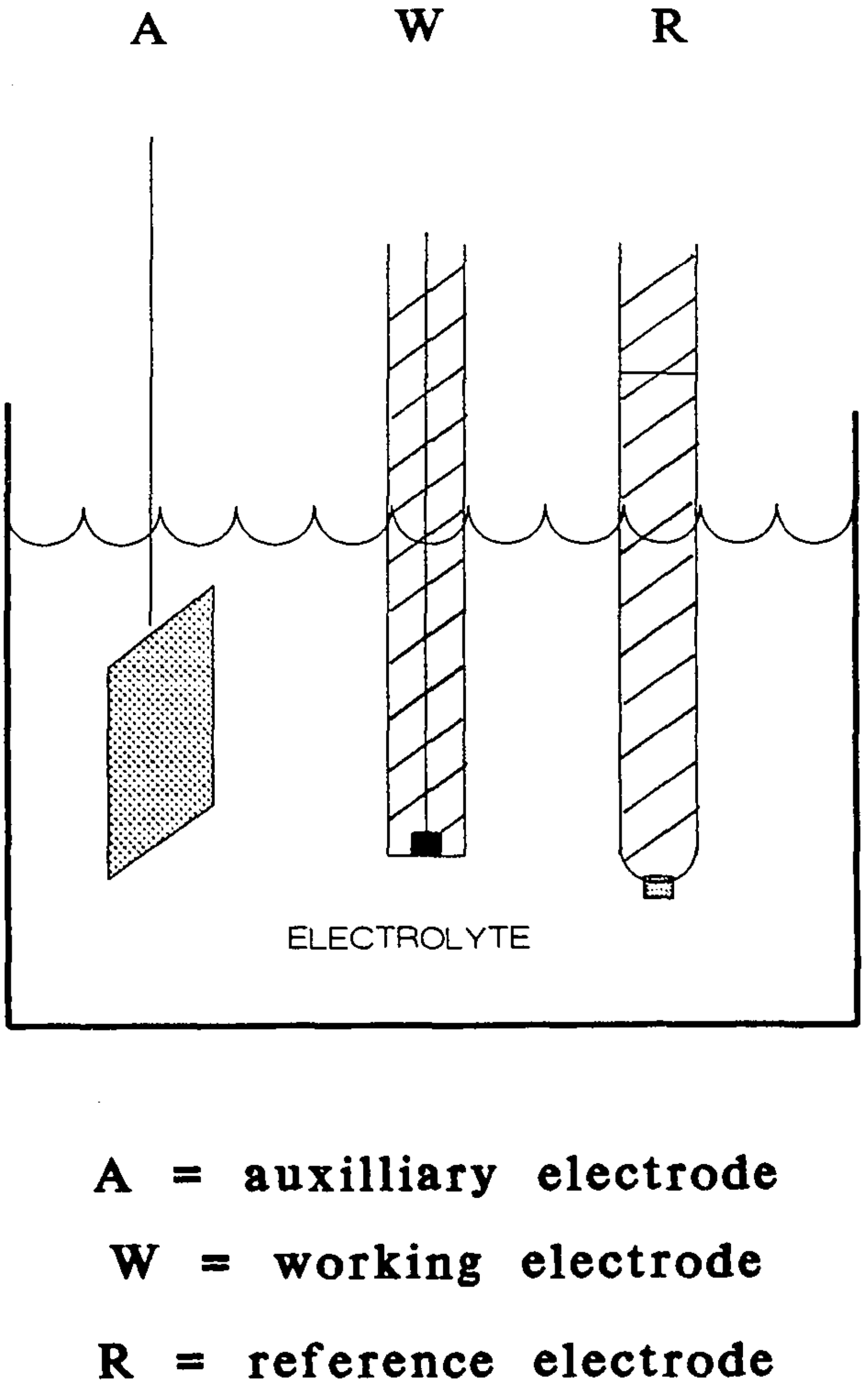

Figure 34. A typical electrochemical cell, with the working electrode (W), the reference electrode (R), and the auxilliary electrode (A) immersed in an electrolyte solution.

of the analyte. The purpose of the salt is to minimize the resistance of the electrolyte solution and to prevent the migration of the analyte molecules, as will be discussed shortly. The electrolyte solution is characterized by a potential "window". This is the potential range over which only capacitive current can be detected. In this potential "window", any redox activity can then be attributed to the analyte.

For the electrochemical polymerization of thiophene, there are some additional restrictions on the electrochemical cell. The solvent, for one, must be anhydrous, as water is reported to have a deleterious effect on the polymerization [55]. Nucleophilic solvents are also undesirable. The best salts are small anions of strong acids with Li^+ or a tetraalkylammonium cation. The working electrode, onto which the polymer is deposited, may be chosen to enhance the adhesion of the polymer to its surface. Pt and Au are often good electrodes in terms of adhesion [56].

Once the proper electrolyte is chosen, the analyte is added to the solution and studied in the electrochemical cell. There are three means by which the analyte may reach the electrode surface. The first is diffusion, which is random, and is the slowest way to supply analyte to the electrode surface. The second is convection, which may be deliberately implemented by stirring the electrolyte or by rotating the electrode, and is sometimes accidentally effected by uneven temperature control or careless deaeration of the electrolyte. The third is ionic migration. This occurs when analyte ions experience a strong potential gradient across the electrochemical cell, and can be minimized by the use of sufficient salt concentrations in the electrochemical cell to transport the current exclusively through the electrolyte.

Normally, the latter two means of mass transport are minimized, and diffusion is assumed to be the primary means of supplying analyte to the electrode surface. If this is

---

[55] Downward, A.J.; Pletcher, D., *J. Electroanal. Chem.*, **1986**, *206*, 147.

[56] a) Porter, M.D.; Bright, T.B.; Allara, D.L.; Chidsey, C.E.D., *J. Am. Chem. Soc.*, **1987**, *109*, 3559. b) Troughton, E.B.; Bain, C.D.; Whitesides, G.M.; Nuzzo, R.G.; Allara, D.L.; Porter, M.D., *Langmuir*, **1988**, *4*, 365.

the case, then theoretical predictions may be made concerning various parameters of the cell. The most important is the potential of the cell. If an electrochemical cell contains a redox couple, O and R, in equilibrium at bulk concentrations C_O^∞ and C_R^∞ respectively, and no current is allowed to pass through the cell, the potential of the cell is described by the Nernst equation,

$$E_{cell} = E^o + \frac{RT}{nF} \ln \frac{C_O^\infty}{C_R^\infty} \qquad (8)$$

where E^o is the standard potential of the redox couple, n is the number of electrons involved in the redox reaction, R is the gas constant, T is the temperature and F is Faraday's constant. This equation may then be extended to non-equilibrium conditions, and an expression for the resulting current may be derived, which will partly depend on the rate of the electron transfer process [54b].

Although this thesis is primarily concerned with the electrochemical response of systems in a qualitative way, it is important to outline what information can be gained from electrochemical studies. The current response is particularly informative when observed as a function of the potential sweep rate. The faster the sweep, the larger the current response, but the exact relationship between these two will depend upon whether the electrochemistry is diffusion controlled, or whether the redox species is adsorbed to the electrode surface. In this latter case no diffusion occurs. If the system is diffusion controlled with linear diffusion to a plane electrode, then Fick's first and second laws will apply, and the Randles-Sevcik equation for the peak current may be derived [57]

$$I_p = (\text{constant})n^{3/2}AD^{1/2}v^{1/2}C_O^\infty \qquad (9)$$

where A is the electrode area, D is the diffusion coefficient of the redox species, C_O^∞ is the bulk concentration of the oxidized species and v is the potential sweep rate in a voltammetric experiment. Thus, the current in a diffusion-controlled reaction varies with the square root of the potential sweep rate.

---

57. See for example, appendix of reference 54b.

On the other hand, if a species is adsorbed to the electrode, all forms of mass transport may be ignored, and the following expression can be derived for the cathodic current [58]

$$I = \frac{n^2F^2\Gamma_o v}{4RT} \qquad (10)$$

where Γ_o is the surface coverage of oxidized species. Thus, in this case, the current for the redox reaction of an adsorbed species varies linearly with the potential sweep rate. By monitoring the peak current as a function of sweep rate, adsorbed species may be distinguished from those in solution. Furthermore, as the total current from an adsorbed species will correspond to the oxidation of all adsorbed molecules, by calculating the total amount of current passing through the cell for each oxidation and reduction, and subtracting the capacitance current, the number of adsorbed molecules may be calculated, giving the surface coverage (Γ_o).

The reversibility of a redox couple in solution may be characterized by various techniques. The simplest technique involves measuring the peak separation, which refers to the difference between the oxidation and reduction potentials, ΔE. From the Nernst equation (8), it can be calculated that a perfectly reversible, diffusion limited species will have a peak separation of 59mV at 25°C for a one-electron process. Any irreversibility or other deviation from diffusion control will increase this value. An adsorbed species, on the other hand, will ideally show a peak separation that is equal to 0mV, providing the electrochemistry is reversible.

In addition to the various mass transport mechanisms, the kinetics of the electron transfer process must also be considered. These two factors may be separated and examined by judicious control of the experimental conditions. Furthermore, chemical processes may be occurring before, after, or in competition with the electrochemistry. Again, with proper experimental control, this can all be determined. An adsorbed species

---

58. See for example, appendix of reference 54b.

is easily distinguished from those in solution on the basis of its peak shapes and peak separation values. Finally, electrocatalysis is readily monitored with the appropriate combination of experimental conditions. In all of these cases, the specific electrochemical technique chosen will determine the type of information obtained.

Several techniques are used to study electrochemical systems. They may be classified as either galvanostatic or potentiostatic. The former involves maintaining a constant current while observing the resulting cell potential, and the latter involves applying a constant potential and monitoring the resulting current. The latter approach is more common, and will be used most frequently in this thesis. There are many potentiostatic techniques available. Figure 35 lists some of these, with the applied potential, E_{app}, as a function of time in one column, and a typical current reponse for a well-behaved redox couple in solution in the other column. In a constant potential experiment, current is recorded as a function of time, while a fixed potential is applied to the cell (Figure 35I). This may be extended to a pulse sequence, in which the potential is stepped over any number of fixed potentials, and held at each potential for a designated length of time (Figure 35II). Finally, a potential sweep technique may be used, in which the potential is swept over a designated range at a fixed rate. This technique is called voltammetry. Linear sweep voltammetry involves sweeping the potential in one direction over the chosen potential range (Figure 35III). Cyclic voltammetry involves sweeping over the potential range for a designated number of cycles (Figure 35IV). With these techniques, a redox couple may be completely characterized. These techniques are all standard and are accessible with commercial instruments.

With this in mind, it is necessary to again consider the problem of thiophene electropolymerization. With respect to the electrochemical technique employed, it has been reported that galvanostatic conditions give a better quality of polymer [59]. However, since it is not always easy to impose the correct galvanostatic conditions,

---

[59] For example Yassar, A.; Roncali, J.; Garnier, F., *Macromolecules*, **1989**, *22*, 804.

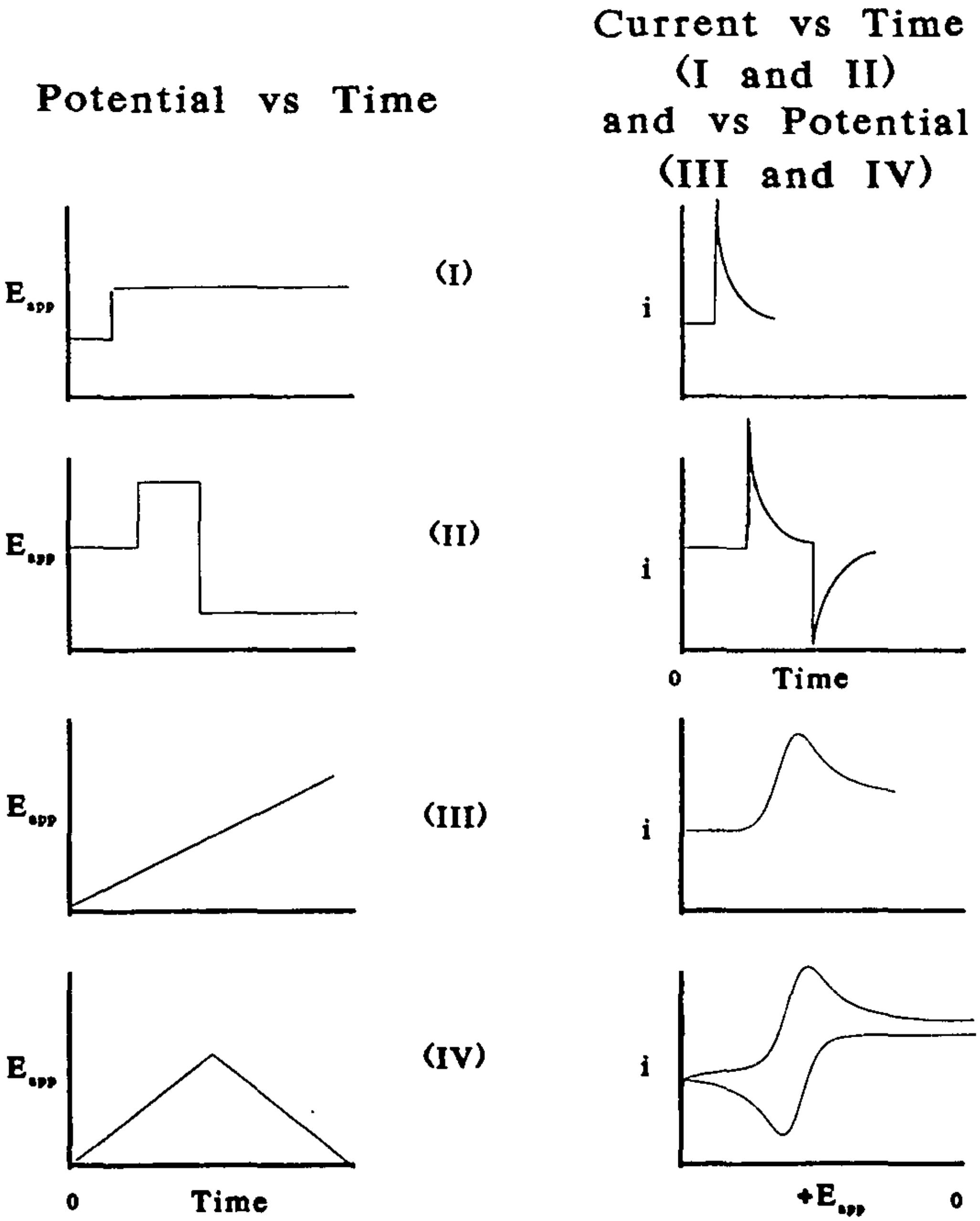

Figure 35. Potentiostatic techniques. The first column shows the applied potential (E_{app}) as a function of time, and the second column shows a typical current response to this applied potential for a well behaved redox couple in solution. I) constant potential II) potential step(s) III) linear sweep voltammetry IV) cyclic voltammetry.

potentiostatic conditions are often employed, with reasonable success. The current density is considered to be the critical experimental parameter, assuming the applied potential is adequate to oxidize the thiophene monomer. Recalling the competition between the formation of soluble oligomers and insoluble polymers, there is a minimum current density, below which the soluble oligomers will form to the exclusion of the insoluble polymer. To avoid this, high current densities that create a large number of initial reaction sites must be used. There is also an upper limit to the current density, mainly because of polymer destruction.

One relatively recent development in electrochemical studies of particular interest here has been the modification of traditional working electrode materials, through chemical or physical means, to give new working electrode surfaces [60]. The field of modified electrodes has greatly expanded opportunities in electrochemistry. There are two extreme approaches in this research. The underlying purpose of one approach involves the generation of novel electrochemical phenomena, such as electrocatalysis or selective electrochemical detection for application in novel electrochemical devices. In this approach, the material used to modify the electrode surface is chosen specifically for its ability to perform the required task, be it selection, catalysis, or simply alteration of the conductivity of the original surface. The other approach uses electrochemistry as a tool to probe the behaviour, on a molecular level, of given materials at the electrode surface. In this way, much can be learned about a material of interest. Often the two approaches are linked. That is, an electrode-modifying material of interest may be investigated extensively on a fundamental level by one group, and then used in some specific application by another group.

Conducting polymers are interesting materials with which to modify electrode surfaces. This is a category of polymer that has received extensive attention in the last

---

60. a) Murray, R.W., *Acc. Chem. Res.*, **1980**, *13*, 135. b) Abruña, H.D., *Coordination Chemistry Reviews*, **1988**, *86*, 135.

decade, and many excellent reviews have been written on the subject [61]. The polymers of particular interest in electrode modification are those that may be electropolymerized directly onto the electrode surface, offering a unique view of the resulting polymer's characteristics, including its conductivity, permeability, redox properties, selectivity towards other species and solubility. Conducting polymers may also act as a convenient "organic anchor" with which to attach various other groups to an electrode surface [2]. This may be achieved chemically, through modification of the polymer structure, or physically, wherein a molecule is adsorbed by the polymer on the electrode surface.

In this section, the electrochemistry of the thiophene/ferrocene compounds is described, as are attempts to electropolymerize these molecules.

II.3.2. Experimental

All electrochemical experiments were performed using a Bio-Analytical Systems (BAS) 100B electrochemistry workstation.

In a three compartment cell, the working electrode was a BAS Pt disk electrode, 1.8mm in diameter; the reference electrode was a BAS Ag/AgCl (3M KCl) and the auxiliary electrode was a Pt gauze. Early experiments were performed with an Au working electrode, but an interfering background oxidation at +800mV with these electrodes proved to be unavoidable, and they were not used in further studies.

An underpotential deposition (UPD) experiment was used to determine the active surface area of the Pt working electrodes. This entailed the deposition of Cu onto the bare Pt surface with a potential (+100mV vs Ag/AgCl) sufficient only to deposit a monolayer of the Cu atoms onto the Pt. This exploits the fact that Cu requires a more negative potential to deposit onto a Cu surface than onto surfaces such as Au and Pt, ensuring only monolayer deposition. After a 60sec pulse at +100mV vs Ag/AgCl in aqueous 0.001M $CuSO_4$ (J.T. Baker chemical Co.)/0.5M Na_2SO_4 (BDH Chemicals), the monolayer of Cu

---

61. Patil, A.O.; Heeger, A.J.; Wudl, F., *Chem. Rev.*, **1988**, *88*, 183.

was subsequently stripped by sweeping from +100mV to +650mV vs Ag/AgCl at 50mV/sec. The area under the resulting oxidation peak was used to calculate the number of Cu atoms deposited on the electrode surface. Figure 36 shows the current response to the potential sweep from +100mV to +650mV vs Ag/AgCl in the UPD experiment used to determine the active surface area of a Pt electrode. This trace has been corrected for the background current, so that the oxidative current is representative of the stripping of a monolayer of Cu atoms from the Pt surface exclusively. Reference 62, describing a similar experiment, determined the coverage of Cu on various Pt crystal faces. Using the data in this reference, the coverage of Cu on polycrystalline Pt is calculated to be 3.6×10^{-9} mol/cm^2. With this information, and the data shown in Figure 36, the active Pt electrode area is determined to be 0.011cm^2. Other techniques to measure the electrode area were also employed. These involved measurement of the electrode response to a well-characterized redox couple, $Fe(CN)_6^{3-/4-}$, by cyclic voltammetry, chronoamperometry and chronocoulometry, giving areas ranging from 0.010 to 0.021cm^2. All electrodes were polished manually with 0.3µm alumina (Buehler) prior to use.

II.3.2.1. Electrochemistry of Monomers in Solution

The TM-C_n-Fc series was studied at concentrations ranging from 0.005-0.1M in nitrobenzene (American Chemicals, Ltd.), CH_2Cl_2 (American Chemicals, Ltd.), and CH_3CN (Aldrich and American Chemicals, Ltd.), with several organic salts, including $LiClO_4$, tetrabutylammonium tetrafluoroborate (TBATFB) and tetrabutylammonium hexafluorophosphate (TBAHP) (all Aldrich). Cyclic voltammetry was performed between 0.0 and +2.5V. The importance of deaerating the electrolyte solution with N_2 was investigated, as was the necessity of drying the solvent and purifying the organic salt.

---

62. Kolb, D.M.; Kötz, R.; Yamamoto, K., *Surface Science*, **1979**, *87*, 20.

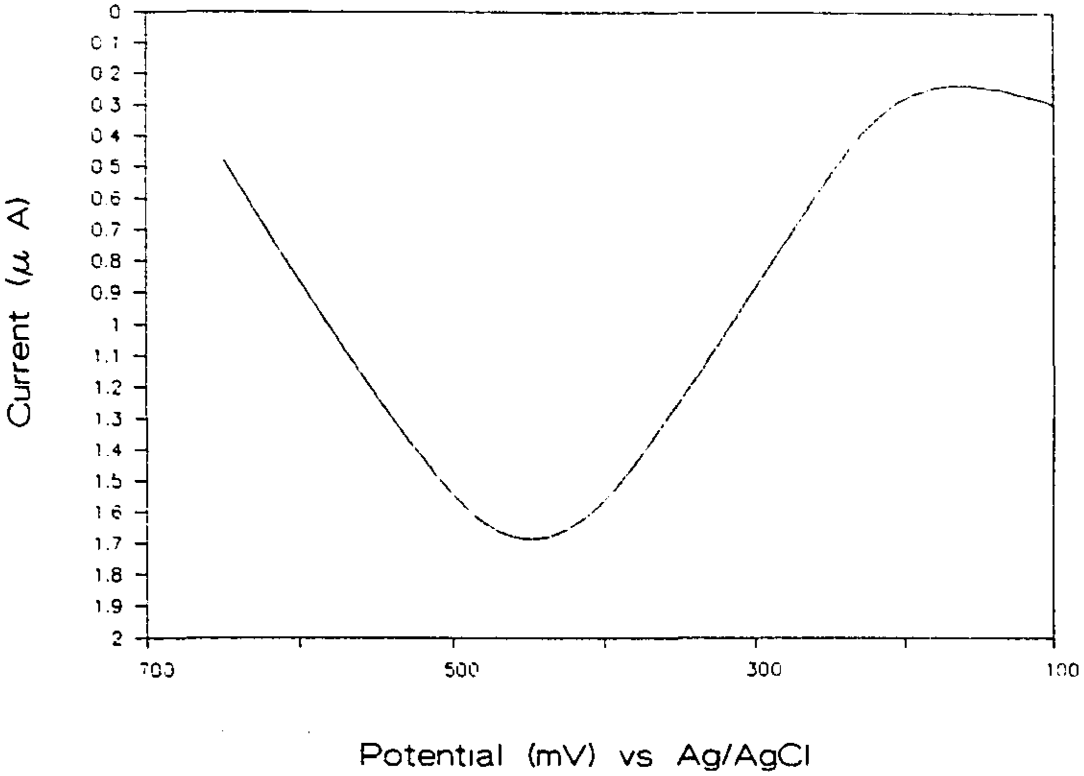

Figure 36. Linear sweep (+100mV to +650mV vs Ag/AgCl, 50mv/sec) used to strip a monolayer of Cu deposited in a UPD experiment (+100mV vs Ag/AgCl for 60sec) from an uncoated Pt electrode.

Solutions of the TE-C_n-Fc compounds were made only in 0.1M TBAHP (Aldrich, [63])/CH_3CN (Aldrich, HPLC grade). Although the oxidation potential of thiophene is lower in 0.1M $LiClO_4$/CH_3CN, such solutions were found to be unstable over the time period of the experiments. The electrochemistry of the ferrocene moiety was observed using cyclic voltammetry over a range of sweep rates. Care was taken to avoid polymerizing thiophene in these experiments; this was achieved by maintaining $E_{app} \leq 1.00V$. In a separate experiment, a cyclic voltammogram was performed to +2.5V to characterize the thiophene oxidation.

The three shortest chain monomers of the TE-C_n-Fc series - TE-C_6-Fc, TE-C_8-Fc and TE-C_{10}-Fc - were studied in solutions of approximately 10mM. The two longer chain monomers - TE-C_{12}-Fc and TE-C_{16}-Fc - were studied in solutions of not more than 2mM, due to their limited solubilities. TE-C_8-Fc was also studied at 2mM to investigate whether the bulk concentration affected the observed electrochemistry.

Compound I was dissolved in 0.1M TBAHP/CH_3CN at a concentration of 10mM. A cyclic voltammogram was performed between 0.0 and +2.0V.

II.3.2.2. Electropolymerization

The electropolymerizations were performed from the aforementioned solutions of the TE-C_n-Fc series and the model compound, I. Constant potential experiments for a defined time were used to effect polymerization. Polymerization was also attempted using cyclic voltammetry.

II.3.2.3. Electrochemistry of Polymers

Once the polymer was formed on the electrode, the electrode surface was thoroughly rinsed with CH_3CN and placed in a solution of 0.1M $LiClO_4$ [64]/CH_3CN. In

---

63. Tetrabutylammonium hexafluorophosphate (TBAHP) was recrystallized once from ethanol, and dried under vacuum at 78°C overnight.
64. $LiClO_4$ was dried under vacuum at 78°C overnight.

$LiClO_4$ the ferrocene couple was shifted to less positive potentials than in 0.1M $TBAHP/CH_3CN$, [37] making it easier to distinguish from the background current. At the higher potentials required to observe the ferrocene couple in TBAHP, the peaks of the ferrocene couple showed more overlap with the broad oxidation peak of the polymer backbone than in $LiClO_4$. The polymer modified electrodes were then examined by cyclic voltammetry and chronocoulometry. A UPD experiment was also performed as described in Section II.3.2. for the electrode area determination. In this case, it was used to determine the extent of polymer coverage of the Pt electrode.

II.3.3. Results and Discussion

II.3.3.1. Electrochemistry of the TM-C_n-Fc Series

An extensive electrochemical study of the TM-C_n-Fc series was undertaken primarily to optimize the electropolymerization conditions for these monomers. Of all the solvents and organic salts that were used, the electrolyte that gives the best conditions for polymerization is the 0.1M $TBAHP/CH_3CN$ solution. This solution has the best potential window, from 0.0 to +2.5V. It is important to deaerate the solution prior to polymerization to achieve the best solvent window and because the ferrocene has been reported to be unstable in the presence of oxygen [33]. It is also critical to remove all water from the CH_3CN (HPLC grade CH_3CN from Aldrich was sufficiently anhydrous), and to recrystallize and dry the salt, as the electropolymerization of thiophene has been reported to be inhibited by the presence of water [55].

These studies show that it is very important to maintain a low (≤10mM) concentration of monomer to effect good polymerization. At higher concentrations, ionic migration causes the ferricenium ions and the thiophene radical cations to migrate from the electrode surface before they can polymerize. This is not usually observed in electrochemical polymerization of thiophene, which is typically performed at monomer concentrations of 0.1M, even with only 0.1M electrolyte. It is thus assumed that it is primarily the electrochemically generate ferricenium moiety that causes ionic migration. In any case, polymerization is prohibited.

Although the exact oxidation potential of the thiophene moiety of this series of compounds varies substantially (±0.2V) with experimental conditions, it is found to be approximately +2.4V on the first sweep of a clean electrode. Subsequent sweeps cause this potential to decrease, and the reduction peak of the ferricenium ion to disappear. A typical CV of the first cycle for TM-C_6-Fc is shown in Figure 37.

Despite optimization attempts, the electropolymerization of TM-C_n-Fc compounds remained unsuccessful. Following one voltammetric sweep to +2.5V, the ferrocene couple is no longer reversible and the reduction peak appears much shorter and broader than the oxidation peak (Figure 37). In the electrochemical polymerization of aniline [43] a base is added to neutralize the acid produced by the polymerization reaction. However, the addition of a base to the thiophene reaction mixture did not improve the polymerization of the TM-C_n-Fc compounds, even when a sterically hindered base (2,6-di-*t*-butylpyridine, Aldrich) is used to accomodate the instability of ferricenium ions in the presence of a nucleophile. The inaccessibility of the electrochemical polymerization of the TM-C_n-Fc compounds is attributed to the high oxidation potentials required to oxidize the thiophene moiety of these compounds (Figure 37). At these potentials, neither the ferricenium ion nor the polythiophene backbone is stable, the solvent window is not reliable, and even trace amounts of water or oxygen could have deleterious effects.

In light of this and the "polythiophene paradox" [9], further attempts to polymerize these monomers were not made. Instead, the TE-C_n-Fc series was synthesized with two carbons separating the ether linkage from the thiophene ring. This was expected to lower the oxidation potential of the thiophene moiety sufficiently to avoid some of these aforementioned problems.

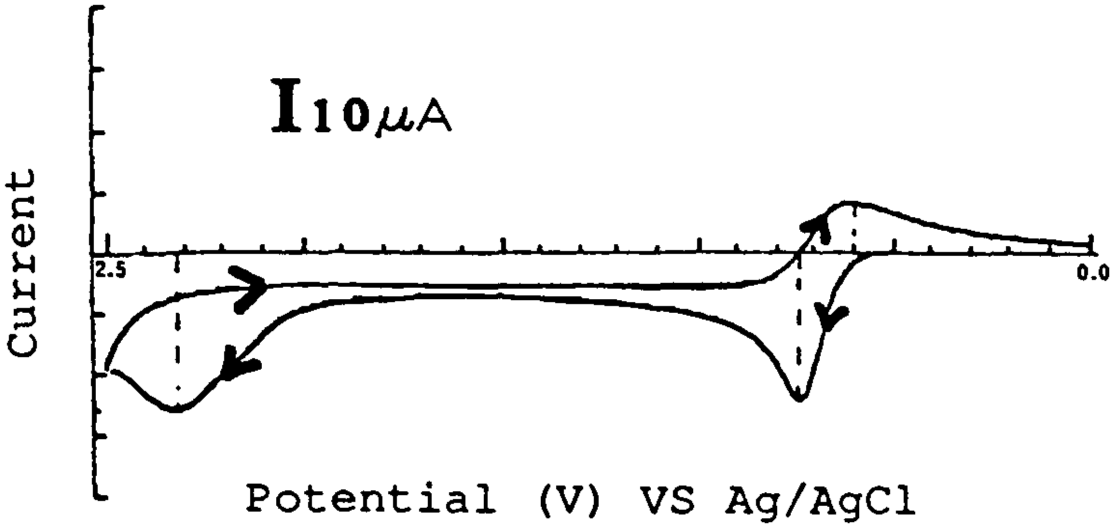

Figure 37. A typical CV of 0.005M TM-C_6-Fc (0.1M TBAHP/CH_3CN). The first sweep is shown, at a Pt working electrode, at a sweep rate of 100mV/sec and sweep limits of 0.0 to +2.5 vs Ag/AgCl.

II.3.3.2. Electrochemistry of the TE-C_n-Fc Series

The electrochemistry of the ferrocene-derivatized thiophene conjugates in bulk solution indicates that the ferrocene couple is quasi-reversible (Figure 38a). Cyclic voltammetry studies reveal a linear variation of peak currents with the square root of the sweep rate. Values of $E_{1/2}$ and ΔE for the ferrocene couple in all TE-C_n-Fc compounds are shown in Table 5. There is no obvious correlation between n and $E_{1/2}$.

An irreversible oxidative peak corresponding to the oxidation of the thiophene unit appears at more positive potentials. Again, as for the TM-C_n-Fc series, this potential varies greatly depending on factors such as the exact condition of the Pt electrode surface and the freshness of the monomer solution, but the oxidation potential of the thiophene moiety in the TE-C_n-Fc series is consistently lower than that of the TM-C_n-Fc series. These potentials range from +1.8V to +2.2V vs Ag/AgCl. A typical cyclic voltammogram of TE-C_{12}-Fc from 0.0 to +2.0V is shown in Figure 38b.

II.3.3.3. Electropolymerization of TE-C_n-Fc

In the first attempt to electropolymerize the TE-C_n-Fc series, a high concentration (10mM) of TE-C_6-Fc, TE-C_8-Fc and TE-C_{10}-Fc was used. At higher concentrations, ionic migration is observed once the potential is sufficiently positive to oxidize ferrocene to the ferricenium form.

Both constant potential (+2.0V) and cyclic voltammetric (sweep limits of 0.0 to +2.0) methods of polymerization successfully deposit a ferrocene species onto the electrode surface for each TE-C_n-Fc monomer under a variety of conditions. Chronocoulometry and cyclic voltammetry were used to characterize the deposition products. Chronocoulometry revealed that material oxidizable at +1.0V adheres to the Pt electrode after each polymerization experiment. This is presumably oxidation of the ferrocene moiety in the polymer, but could include a component of the oxidation of the polythiophene backbone. Cyclic voltammetry indicates the presence of a surface wave

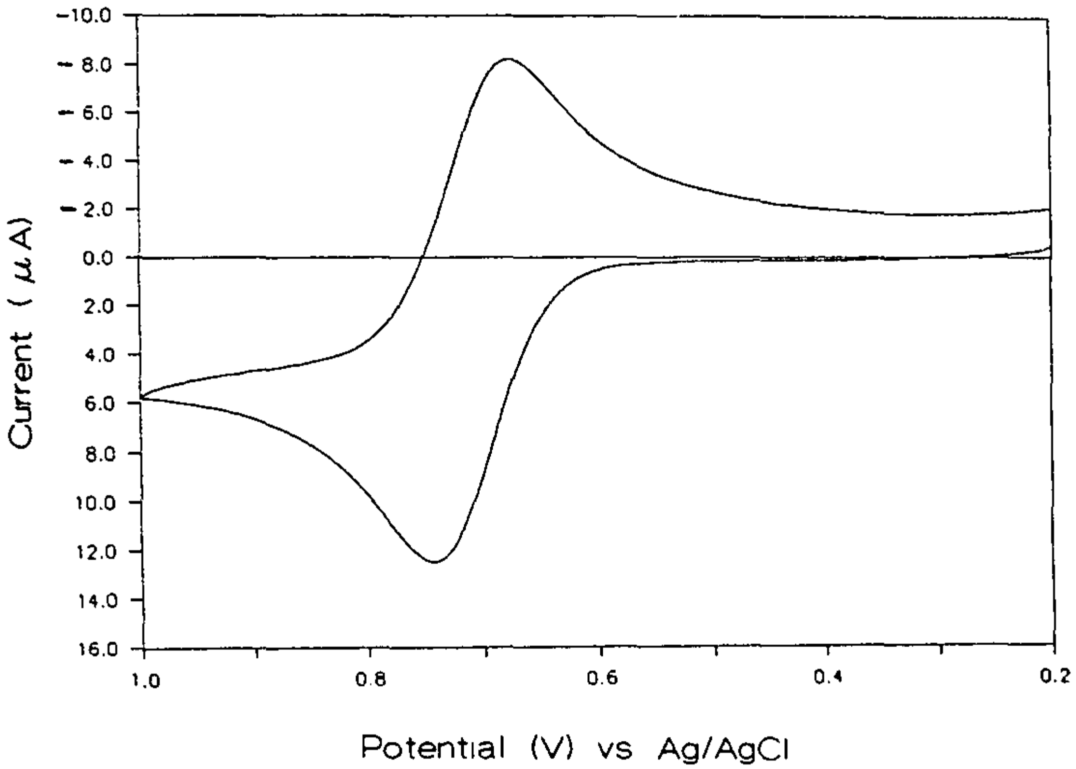

Figure 38a. CV of the ferrocene couple in 0.002M TE-C_{12}-Fc (0.1M TBAHP/CH_3CN), at a Pt electrode, at a sweep rate of 100mV/sec and sweep limits of +0.2 to +1.0 vs Ag/AgCl.

TABLE 5 Electrochemical data for ferrocene couple of TE-C_n-Fc monomers in 0.1M TBAHP/CH_3CN.

	$E_{1/2}$(mV)	ΔE(mV)*
TE-C_6-Fc (8.0mM)	650	90
TE-C_8-Fc (9.8mM)	650	100
TE-C_8-Fc (2.2mM)	680	70
TE-C_{10}-Fc (9.9mM)	670	100
TE-C_{12}-Fc (2.0mM)	710	70
TE-C_{16}-Fc (2.2mM)	660	70

* Values of ΔE are taken at a sweep rate of 100mV/sec.

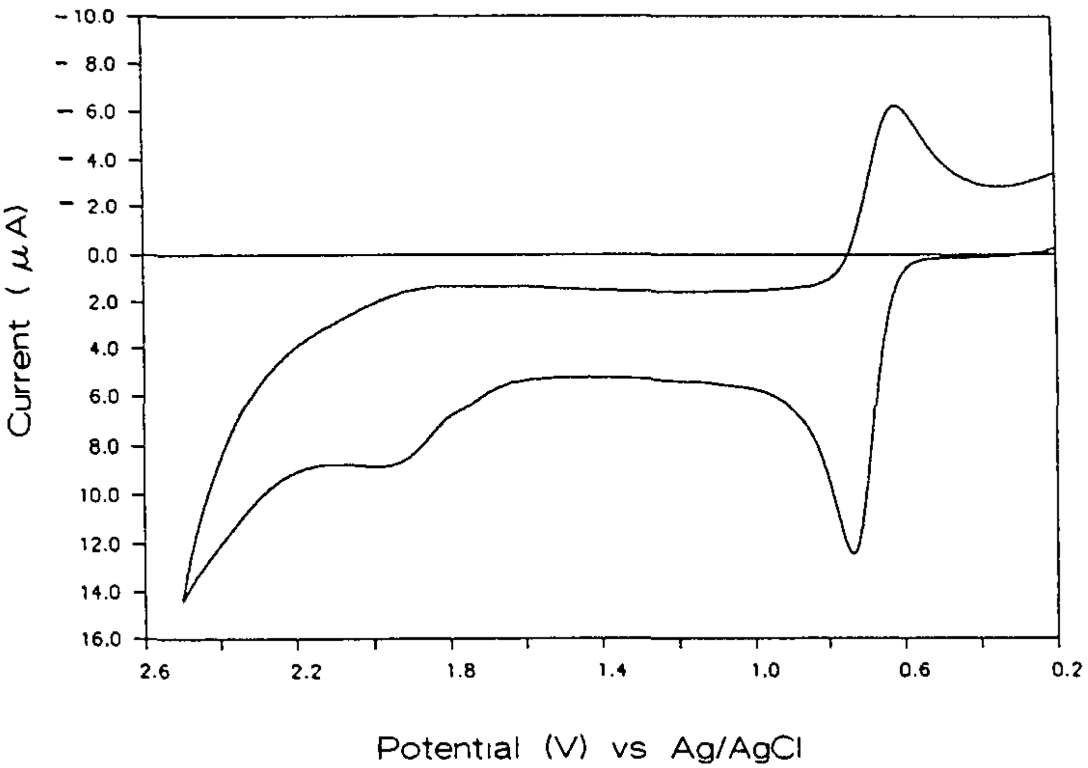

Figure 38b. CV in 0.002M TE-C_{12}-Fc (0.1M TBAHP/CH_3CN), with a Pt electrode, at a sweep rate of 100mV/sec and sweep limits of +0.2 to +2.5 vs Ag/AgCl.

centred at +600mV, corresponding to the oxidation and reduction of the ferrocene ester. Peak currents of these cyclic voltammograms show linear dependence on potential sweep rate, with some deviation at high sweep rates, confirming the presence of an adsorbed species. Peak separation is small, but increases at high sweep rates. A typical cyclic voltammogram, in this case of (TE-C_8-Fc)$_x$, is shown in Figure 39. Table 6 lists $E_{1/2}$ and ΔE values of the ferrocene couple for each polymer in the series. The $E_{1/2}$ values of the polymers are all less positive than the $E_{1/2}$ values of the monomers by 40-60mV. This is attributed to the presence of different electrolytes. The effect of the perchlorate ion on the surface-bound ferrocene has been studied in detail by Jönsson *et al* [37]. These authors speculate that the observed negative shift of E^{o} for the adsorbed ferrocene, which increases with increased perchlorate concentrations, is caused by ferrocenium/perchlorate complex formation.

In order to account for the behaviour of peak currents and peak separations at high sweep rates, the resistance of the polymer was measured, and was found to vary between 1 and 2kΩ. The iR drop associated with this resistance is <1mV, and is therefore a negligible contributor to peak separations. A slow rate of electron transfer is most probably the origin of non-ideal surface wave properties [53].

These observations confirm that the electropolymerization leads to the localization of ferrocene ester moieties onto the electrode surface. A surface coverage estimate using the electrode area obtained from the UPD experiments (0.011cm^2, Section II.3.2.) indicates that a surface coverage of about 40Å^2 per ferrocene moiety may be attained with a 10mM bulk solution. This is in the range of monolayer coverage [65]. The less concentrated solutions of TE-C_{12}-Fc, TE-C_{16}-Fc and TE-C_8-Fc lead to only a fraction of this coverage (30-40%) and the resulting materials are less stable to repeated cycling between 0.0 and +1.0V.

---

65. A report of Langmuir films containing ferrocene ester moieties gives an experimental value of the cross-sectional area of the ferrocene ester moiety to be 42Å^2. Effenberger, F.; Meller, P.; Ringsdorf, H.; Schlosser, H., *Adv. Mater.* **1991**, *3*, 555.

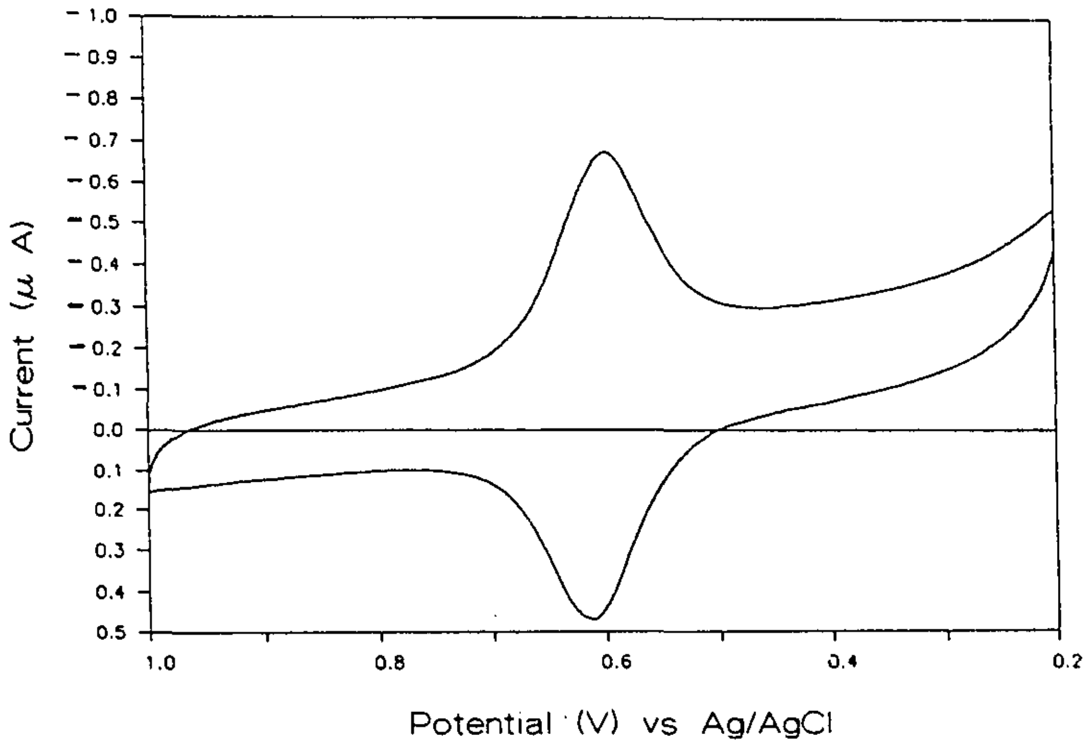

Figure 39. CV of the ferrocene couple in (TE-C$_8$-Fc)$_x$, adsorbed onto a Pt electrode, in 0.1M LiClO$_4$/CH$_3$CN, at a sweep rate of 100mV/sec and sweep limits of +0.2 to +1.0 vs Ag/AgCl.

TABLE 6 Electrochemical data for ferrocene couple of (TE-C_n-Fc)$_x$ polymers in 0.1M $LiClO_4/CH_3CN$.

	$E_{1/2}$(mV)	ΔE(mV)*
(TE-C_6-Fc)$_x$	600	40
(TE-C_8-Fc)$_x$	610	10
(TE-C_{10}-Fc)$_x$	610	20
(TE-C_{16}-Fc)$_x$	610	40

* Values of ΔE are taken at a sweep rate of 100mV/sec.

In order to distinguish between a uniform film of deposited material and clumps of material widely separated by bare electrode, a UPD experiment was performed. Any part of the electrode surface not covered by $(\text{TE-C}_n\text{-Fc})_x$ would allow for deposition of a monolayer of Cu atoms, whereas the polymer itself, which would be in its insulating state at +100mV, would block Cu deposition. Thus the area under the stripping peak was calculated to represent bare electrode present on a polymer-coated electrode surface. In keeping with the great variation in the quality of polymer coatings, as observed by cyclic voltammetry of the resulting ferrocene couple, a range of coverages were detected by UPD. For a successful polymerization, however, there is 19-34% bare electrode surface remaining after polymer has been deposited. This is calculated by comparing the stripping curves for polymer-coated electrodes with the same curve for bare electrodes (Figure 40). This, together with the surface coverage calculated from the cyclic voltammograms of the adsorbed ferrocene species, indicate the film to be of a fairly uniform thickness, on average one monolayer thick, and never more than two monolayers thick.

Assuming this material to consist of a polythiophene backbone with pendant ferrocene groups, one would expect to be able to detect redox activity from both the polymer and the ferrocene in this potential range. The polymer signal however is more difficult to detect, primarily because it overlaps to a certain extent with the ferrocene peaks. Moreover, as mentioned earlier, in a polythiophene backbone, only one electron is removed per four thiophene units [11]. The polymer oxidation and reduction peaks would therefore be only one quarter the area of the ferrocene peaks. Finally, the polymer oxidation and reduction peaks are characteristically broad, owing to a distribution of redox potentials resulting from a distribution of chain lengths, as described in Section II.1.2.2. Even subtracting the capacitance current of the bare Pt electrode, (as measured by cyclic voltammetry), from the cyclic voltammogram of the electropolymerized material is not conclusive, as the resistive properties of the bare electrode will be

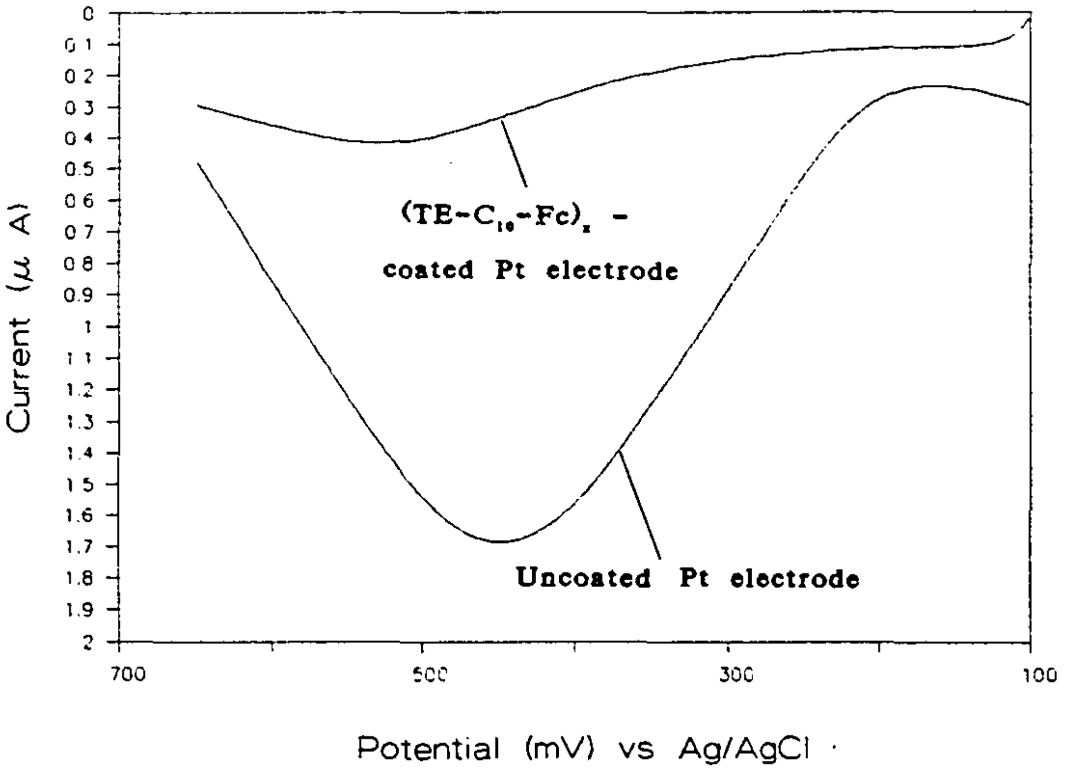

Figure 40. Linear sweep (+100mV to +650mV vs Ag/AgCl, 50mv/sec) to strip UPD layer of Cu deposited at +100mV vs Ag/AgCl for 60sec for a $(TE\text{-}C_{10}\text{-}Fc)_x$-coated electrode. The same sweep for a bare electrode (Figure 36) is included for comparison.

different from the coated electrode. It should be noted that, despite reports of the affinity of aromatic rings and sulfur for platinum surfaces, incubation of the electrode with monomer for 10 minutes (duration of a typical electropolymerization experiment) leads to no electrochemically detectable adsorbate. This observation rules out strong physisorption of the TE-C_n-Fc compounds as the origin of the surface wave at +600mV.

Attempts to increase surface coverage in this system by increasing the duration of the +2.0V pulse or increasing the pulse potential to +2.5V in the constant potential experiments were unsuccessful, and indeed ultimately resulted in the destruction of the original coating. The same is true for experiments involving either multiple sweeps in the cyclic voltammetry experiments or extension of the voltammetric sweep to +2.5V. Thus, the TE-C_n-Fc compounds do not favour formation of multilayers or large quantities of homopolymer.

The reproducibility of the polymerization experiment is poor. Although many variables were investigated, none seemed to be consistently successful. High potentials, long polymerization times, and low monomer concentrations (2mM and less) were consistently unsuccessful. Both constant potential and potential sweep experiments produce good polymer films, although neither do so in all attempts. Many factors may contribute to this. The gradual decomposition of the TE-C_n-Fc compounds in CH_3CN is observed over several days, but it was not practical to make fresh solutions up for every experiment. The presence of water, known to be deleterious to the polymerization process and the stability of the ferricenium ion, cannot be entirely eliminated, and will vary from experiment to experiment. The only other explanation rests with the state of the electrode surface. This could be the source of the inconsistencies, and should be investigated further to improve the success rate of these polymerizations.

In order to increase the number of ferrocene groups on the electrode surface, several copolymer systems were examined for the TE-C_n-Fc series. The electrochemical behaviour of compound I was also investigated, to verify the role of ferrocene in the deposited material.

II.3.3.4. Electrochemistry and Electropolymerization of I

The cyclic voltammogram of I is shown in Figure 41. In this experiment, multiple sweeps from 0.0 to +2.0 were performed. The first sweep, marked by arrows, shows no oxidative current until +1.8V. The peak for the irreversible oxidation of the thiophene moiety is at +1.85V, as for the other thienylethanol compounds. On subsequent sweeps, this peak broadens, and its maximum shifts to less positive potentials. Furthermore, the redox activity of the resulting polymer backbone becomes apparent in broad oxidation and reduction peaks at +1.2 and +1.0V, respectively. These peaks grow as the polymer is built up with successive sweeps.

This behaviour is typical of thiophene electropolymerization. It confirms that the limit in the polymerization of TM-C_n-Fc monomers to one monolayer is directly related to the presence of the ferrocene group, since the phenyl ring does not limit the extent of polymerization of I.

II.3.3.5. Bilayer Systems

The eventual destruction of the homopolymer $(TE\text{-}C_n\text{-}Fc)_x$ under continuous electropolymerization conditions cast doubt on the effectiveness of the adherence of the polymer to the Pt surface. Although simple polythiophenes should be well adsorbed onto Pt [56], the bulky ferrocene group may disrupt effective adsorption and packing. Attempts were made to alter the nature of the electrode surface by first forming a thin layer of a simple polythiophene derivative, poly-3-methylthiophene. Such an organic

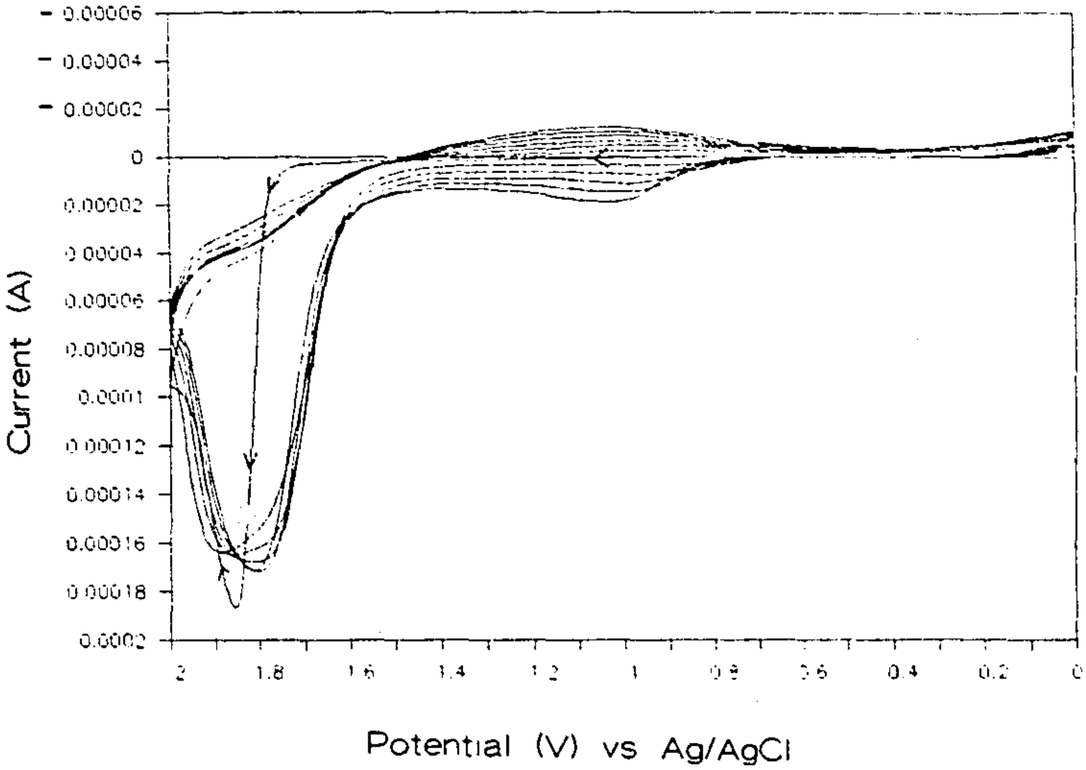

Figure 41. Mutiple sweep CV in 0.098M I (0.1M TBAHP/CH_3CN), with a Pt working electrode, at a sweep rate of 100mV/sec and sweep limits of +0.2 to +2.0 vs Ag/AgCl.

surface could be more amenable to the polymerization of the TE-C_n-Fc compounds than the bare Pt surface. The formation of a bilayer system was envisioned [66].

A bilayer system was formed by effecting the electropolymerization of 3-methylthiophene (3MT, Aldrich) from a 0.1M solution of this monomer by constant potential or cyclic voltammetry. The 3MT-coated electrode was rinsed and then immersed in a solution of TE-C_8-Fc, where again polymerization was effected electrochemically at +2.0V vs Ag/AgCl. Thus it is not a copolymerization, although arguably a copolymer may be formed.

The initial thin layer of poly-3-methylthiophene (P3MT) was characterized by cyclic voltammetry, as shown in Figure 42a. The layer of ferrocene-derivatized polythiophene ($(\text{TE-C}_8\text{-Fc})_x$ in this case) was then detectable by cyclic voltammetry of the bilayer, as shown in Figure 42b, where the ferrocene couple is evident. This ferrocene couple behaves in a fashion similar to that when it is attached directly to the platinum surface, in that the peak currents vary directly with potential sweep rate and the peak separation is small. Again, deposition of the $(\text{TE-C}_8\text{-Fc})_x$ is limited to a monolayer equivalent. Furthermore, excursions to +2.0V following the initial polymerization of TE-C_8-Fc destroy the bilayer, precluding any attempt at trilayer formation. Thus, this bilayer system exhibits similar but not enhanced electrochemical stability, between 0.0 and +1.0V, compared with the homopolymer deposited directly on the Pt electrode surface. Presumably, this marginal stability is also due to the presence of ferrocene.

II.3.3.6. Copolymer Systems

Given that polymerization of TE-C_n-Fc proceeds only up to some predetermined level (monolayer coverage), and that this phenomenon is observed whether the electrode surface is bare platinum or a thin layer of P3MT, it is apparent that the polymerized TE-

---

66. Abruña, H.D.; Denisevich, P.; Umana, M.; Meyer, T.J.; Murray, R.W., *J. Am. Chem. Soc.*, **1981**, *103*, 1.

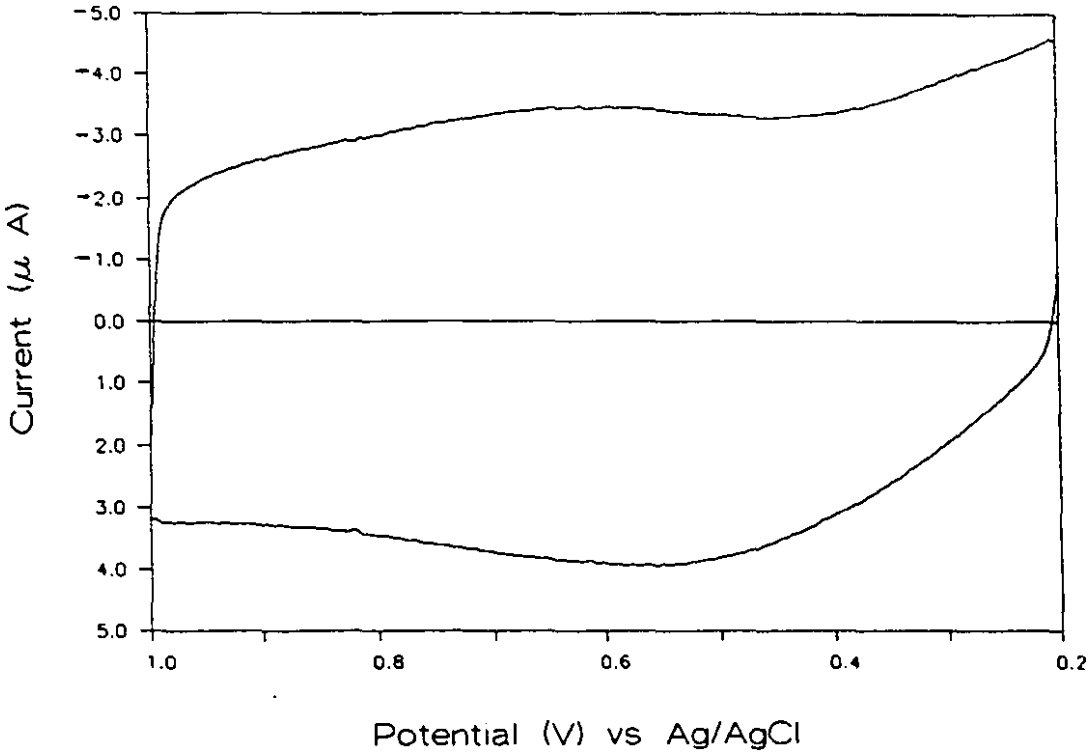

Figure 42a. CV of P3MT adsorbed onto a Pt electrode (P3MT deposited in a constant potential experiment, in 0.1M 3MT/0.1M TBAHP/CH_3CN) in 0.1M $LiClO_4$/CH_3CN, at a sweep rate of 100mV/sec and sweep limits of +0.2 to +1.0 vs Ag/AgCl.

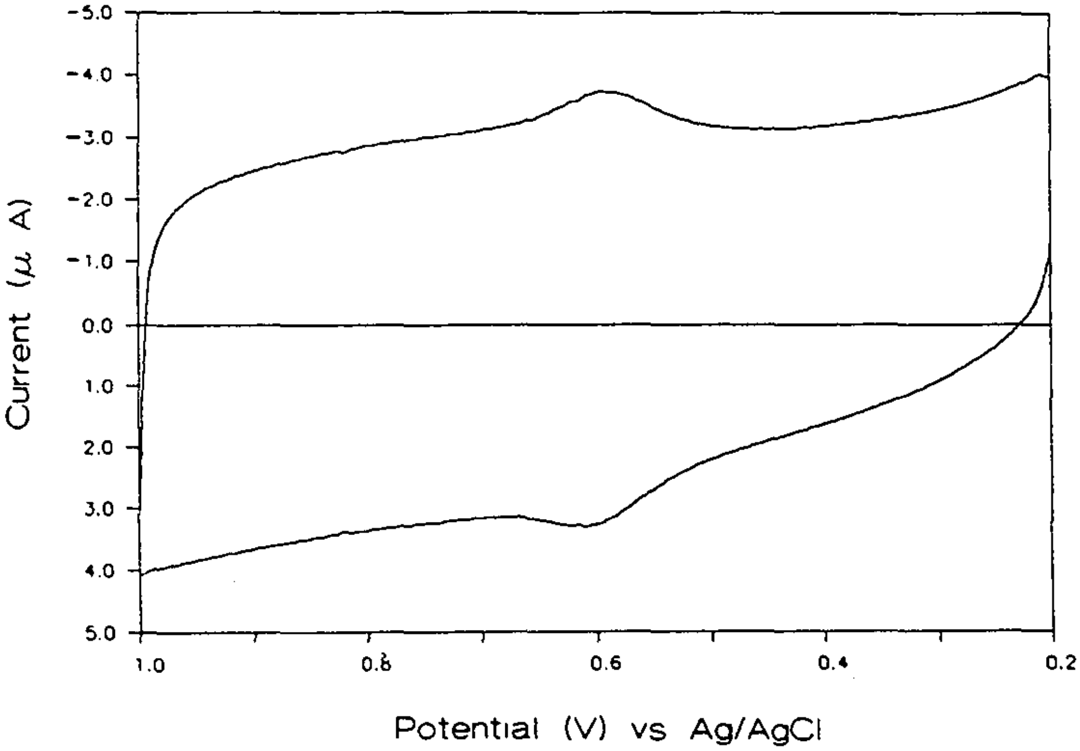

Figure 42b. CV of a (TE-C_8-Fc)$_x$/P3MT bilayer formed at a Pt working electrode in 0.1M $LiClO_4/CH_3CN$, at a sweep rate of 100mV/sec from +0.2 to +1.0 to +0.2V vs Ag/AgCl. The (TE-C_8-Fc)$_x$ was deposited on top of the P3MT in a constant potential experiment, in 0.005M TE-C_8-Fc/0.1M TBAHP/CH_3CN.

C_n-Fc compounds do not form a surface upon which subsequent layers of polymer are encouraged to form. Furthermore, from the studies of compound I, it is apparent that ferrocene is responsible for the inhibition of polymer formation past one monolayer equivalent. To understand this, the appearance of such a material to incoming monomer must be considered. Once a monolayer of polymer has been formed, incoming monomer is confronted with what is essentially a high local concentration of ferrocene molecules. Regardless of how permeable this ferrocene layer may be, at the potentials required to oxidize the thiophene unit the ferrocene groups will in fact be in their cationic ferricenium state. The ferrocene layer will therefore be positively charged. The thiophene radical cation intermediate through which the electropolymerization proceeds will therefore be repelled by this surface, and further chain growth will be inhibited.

It is interesting to note that when simple thiophene derivatives such as 3-methylthiophene and compound I are polymerized to give thick multilayer films, they are successfully building upon positively charged material, since the polymer backbone is in its oxidized state at the potential required to oxidize thiophene monomers. However, the polythiophene backbone only carries one positive charge for every four thiophene units [11], and the charge density on this material would therefore be substantially less than that on the ferricenium layer. Furthermore, the incoming oxidized TE-C_n-Fc molecules will carry a charge of +2, whereas the simple thiophene radical cation carries a charge of only +1, and thus the former will be repelled more strongly. Finally, there is a strong driving force for an oxidized chain to react with another oxidized chain through a radical-radical coupling polymerization mechanism, owing to the reactivity of the radical cations. Recalling the polymerization to form thick films from I, it is noted that one of the major differences between the ferrocene and the phenyl group is the redox activity of the ferrocene, which causes it to be charged at the potentials required to oxidize thiophene. The same is not true for the phenyl ring. This supports the idea of like-charge repulsion being the key factor in limiting polymerization of the TE-C_n-Fc monomers to one monolayer.

In order to circumvent this limit, and affix more ferrocene groups to the electrode surface, a copolymerization from a mixture of TE-C_n-Fc and 3-methylthiophene (3MT) was attempted. One such attempt involved a solution containing 3MT and TE-C_6-Fc in a 10:1 ratio. The total thiophene concentration was 0.055M, (much higher than the concentrations allowable of pure ferrocene-derivatized thiophene, due to the ionic migration limitations discussed earlier), which was thought to improve the chances of an increase in polymer deposition. Under these conditions, it is indeed possible, (using cyclic voltammetry and constant potential techniques), to form much more polymer on the electrode surface. Moreover, this material does contain ferrocene units, as evidenced by the cyclic voltammogram shown in Figure 42c. When compared to the cyclic voltammogram of P3MT in Figure 42a, this cyclic voltammogram shows that the material formed in this copolymerization is very different from pure P3MT. This difference is due in part to the presence of ferrocene, but it seems probable that the whole polymerization process will be changed by the presence of the ferricenium species. The morphological and electronic properties of the resulting copolymer and homopolymer backbones will be different as a result.

Since the electrochemistry of this unique copolymer cannot be measured in the absence of the ferrocene groups, there remains the problem of distinguishing the redox activity of the ferrocene from that of the polymer backbone, in order to calculate surface coverage. Calculating the total charge beneath the cyclic voltammogram curve in Figure 42c leads to an estimated surface coverage of approximately 100 monolayer equivalents of ferrocene [67]. The ferrocene peak currents vary directly with the sweep rate of the

---

67. It is assumed for the purposes of this calculation that the polymer consists of ferrocene and thiophene units in a ratio of 11:1. The total charge under the curve is then attributed to tetrathiophene [15] and ferrocene oxidation and reduction, and the number of ferrocene units adsorbed on the electrode surface can then be calculated.

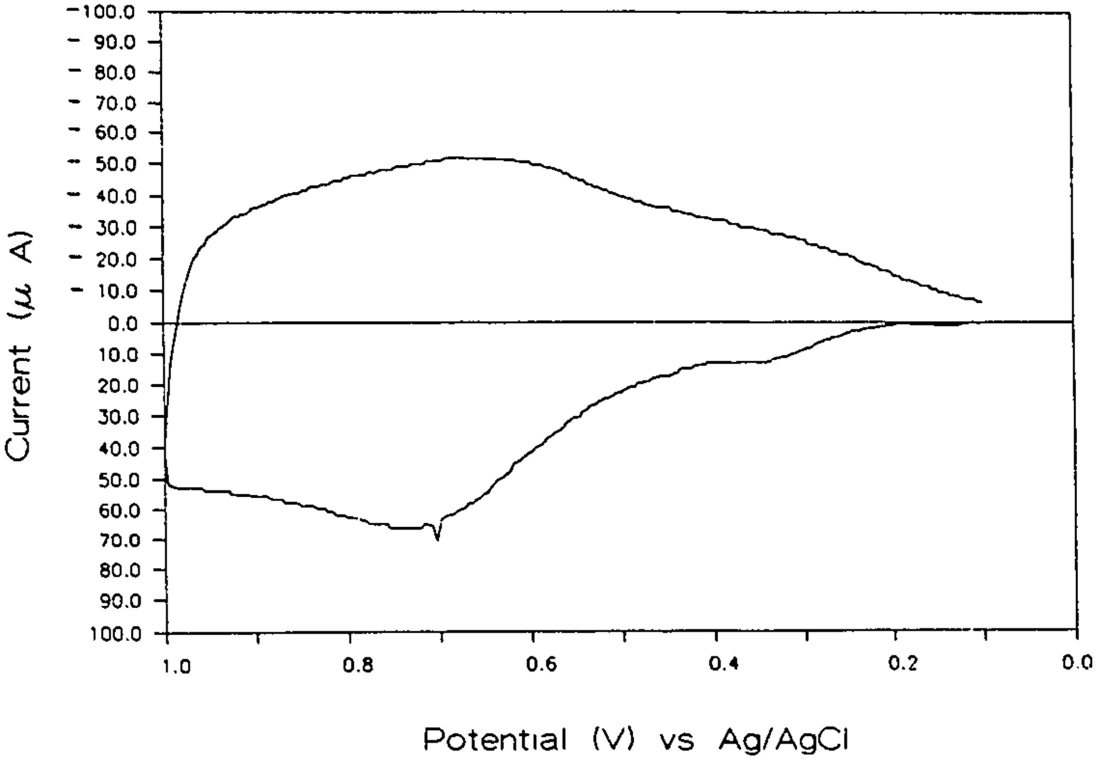

Figure 42c. CV of a $(TE\text{-}C_6\text{-}Fc)_x/P3MT$ copolymer (1:10) formed at a Pt electrode in 0.1M $LiClO_4/CH_3CN$, at a sweep rate of 50mV/sec from 0.1 to +1.0 to 0.1V vs Ag/AgCl. The copolymer was deposited by CV in 0.050M 3MT/0.005M $TE\text{-}C_6\text{-}Fc/0.1M\ TBAHP/CH_3CN$.

voltammograms, verifying the presence of a surface adsorbed species. The peak separations are not negligible, however, possibly indicating resistivity in the thicker polymer film, which could slow the electron transfer process.

Interestingly, an identical copolymerization procedure using a solution of 3MT and TE-C_6-Fc in a 4:1 ratio produces a surface adsorbed material with no more ferrocene units per thiophene unit than with a 10:1 ratio of the monomers. This must be an indication that the ferricenium ions begin to retard, (but not yet inhibit), further polymerization as their concentration in the polymer increases. Furthermore, 3MT may be preferentially electropolymerized compared with TE-C_6-Fc as ferrocene-containing polymer builds up on the electrode, since TE-C_6-Fc carries a net charge of +2 when oxidized, whereas 3MT carries only a charge of +1, as mentioned earlier. Thus the ratio of 3MT to TE-C_6-Fc may be more than 4:1 in the material deposited on the electrode. The assumption of a 10:1 ratio of 3MT to TE-C_6-Fc in the previous copolymer [67] is still reasonable, however. Copolymerization experiments with a 20:1 ratio of 3MT to TE-C_6-Fc produced material in which no ferrocene was detectable. There must therefore exist an optimum ratio of 3MT to TE-C_6-Fc, below which the effect observed at a 4:1 ratio prevails, but above which the 3MT to TE-C_6-Fc ratio in the co-monomer solution is preserved in the copolymer.

II.3.4. Summary

The electrochemical polymerization of the TE-C_n-Fc series of thiophene/ferrocene compounds successfully affixes a monolayer of ferrocene molecules to the electrode surface, presumably through a thiophene polymer backbone. This limit to one monolayer appears to be an inherent feature of the bifunctional molecules, arising from the simultaneous oxidation of ferrocene and thiophene, as the latter is polymerized.

Bilayers of P3MT and $(\text{TE-}C_8\text{-Fc})_x$ were deposited on the electrode surface, with the same control over film thickness being observed for the $(\text{TE-}C_8\text{-Fc})_x$. Copolymers of

3MT and TE-C_6-Fc do not exhibit such a limit to monolayer thickness, and were observed to result in approximately 100 monolayer equivalents of ferrocene being affixed to the electrode surface.

II.4. LANGMUIR FILMS AND LANGMUIR-BLODGETT FILMS

II.4.1. Introduction

The thiophene/ferrocene compounds that were examined by electrochemical methods in the previous section will be discussed with respect to their behaviour at the air/water interface, in Langmuir and LB films. The surface film balance was thoroughly described in Sections I.1.1.-I.1.4. Unconventional molecules used in surface film balance studies were examined and discussed. These molecules were primarily nonamphiphilic molecules, usually nonpolar, including fullerenes and aryl benzene dendrimers.

Another class of unconventional molecules that are studied at the air/water interface are bipolar molecules such as bolaforms [68], α,ω-diacids [69] α,ω-acid esters [70], and α,ω-acid alcohols [71]. Whereas the completely hydrophobic molecules have no "anchor" to provide for facile spreading on the water surface, these bipolar molecules have two "anchors". This leads to different compression-induced reorientation mechanisms than those observed for ordinary amphiphiles. By considering these compounds together, the criteria for Langmuir film-forming compounds may be reassessed once more, to accomodate the bipolar molecules as well as the nonpolar molecules.

Besides appearing to be somewhat bipolar, the TM-C_n-Fc and TE-C_n-Fc molecules have many potential applications, (outlined in Section II.1.2. and II.1.3), that would greatly benefit from the materials being assembled in the form of an ultrathin film. The electrochemical studies succeeded in making ultrathin films of polymer from these monomers by electrochemical polymerization. A chemical polymerization of these monomers would provide a material that could be compared to the electropolymerized film. If the bipolar nature of the monomers allowed them to be spread into an ordered

---

68. Furhop, J.-H.; Fritsch, D., *Acc. Chem. Res.* **1986**, *10*, 130.
69. Porter, N.A.; Ok, D.; Adams, C.M.; Huff, J.B., *J. Am. Chem. Soc.*, **1986**, *108*, 5025.
70. Vogel, V.; Möbius, D., *Thin Solid Films*, **1985**, *132*, 205.
71. Bader, H.; Ringsdorf, H., *Faraday Discuss. Chem. Soc.*, **1986**, *81*, 329.

Langmuir film, then polymerization could be effected within this film, possibly producing an ultrathin polymer film with a highly ordered molecular structure.

Other reactions have been performed *in situ* at the air/water interface. Polymerization is popular, particularly as it often results in a more durable LB film after deposition (Section I.1.4.1.). Besides the photochemical techniques used to polymerize diacetylene at the air/water interface [72], reagents may be added to the subphase to chemically initiate and/or propagate polymerization. For example, a condensation polymerization was effected by including one of the two monomers in an acidified subphase, and spreading the other monomer on the water surface, to produce wholly aromatic polymers [73]. It was believed that an oxidizing agent in the subphase might be sufficient to polymerize a Langmuir film of the thiophene/ferrocene compounds through the thiophene moiety. This would give unique Langmuir films, (and possibly LB films) of polythiophene derivatized with ferrocene.

Some thiophene polymers have been examined at the air/water interface [74], but all have been pre-polymerized in the bulk. Furthermore, in many cases they must be co-spread with a good amphiphile, such as a fatty acid [75]. α-Quinquethiophene has also been examined at the air/water interface, but with stearic acid as a co-spreadant [76]. To date, no thiophene monomer has proven to be sufficiently surface active to assemble at the air/water interface, and hence no *in situ* polymerization of a thiophene monomer on the surface film balance has been reported. However, pyrrole, which polymerizes through the same mechanism as thiophene, has been derivatized to form surface active compounds. These compounds have been examined at the air/water interface, and *in situ*

---

72. Tieke, B.; Lieser, G.; Wegner, G., *J. Polym. Sci.* **1979**, *17*, 1631.
73. Ueda, T.; Yokoyama, S.; Watanabe, M.; Sanui, K.; Ogata, N., *J. Polym. Sci.*, **1990**, *28*, 3221.
74. Callender, C.L.; Carere, C.A.; Daoust, G.; Leclerc, M., *Thin Solid Films*, **1991**, *204*, 451.
75. Watanabe, I.; Hong, K.; Rubner, M.F.; Loh, I.H., *Synth. Met.*, **1989**, *28*, C473.
76. Tasaka, S.; Katz, H.E.; Hutton, R.S.; Orenstein, J.; Fredrickson, G.H.; Wang, T.T., *Synth. Met.*, **1986**, *16*, 17.

polymerizations have been attempted [77]. These studies have not been entirely successful, as they have relied on a high concentration of pyrrole monomer in the water subphase to effect measurable reaction. These conditions ostensibly accomodated the steric requirements of the polypyrrole backbone. However, polymerization of a pyrrole derivative which first self-assembles into micelles [78] suggests that polymerization of these heterocyclic monomers may be achieved even when a high degree of order is imposed upon the molecules prior to polymerization.

The focus of the work presented below is the formation of Langmuir films from the bipolar TM-C_n-Fc and TE-C_n-Fc molecules. Providing that some surface activity of these derivatized thiophenes can be demonstrated, it may be possible to produce a Langmuir film of polymerizable thiophene units which has the feature of a reversible redox couple covalently bound to the thiophene by an alkyl tether. These films will be characterized at the air/water interface based on a detailed structure/property study, including data from the model compounds. The orientation of the molecules at the air/water interface will be discussed. The dynamic behaviour of the films at the air/water interface and the response to temperature variation will also be examined. Finally, attempts to polymerize the thiophene derivatives *in situ* will be presented.

II.4.2. Experimental

All surface film balance experiments were performed on either the LAUDA surface film balance (LAUDA Filmwaage Model D) equipped with a Langmuir torsion balance measuring device or the KSV 3000 surface film balance equipped with a Wilhelmy plate measuring device. These systems have already been described in detail (Section I.) The water was purified using a Millipore (Milli-Q, 18MΩ) filter system. Samples were manually applied to the water surface in 5-10μl drops from a μl Hamilton

---

77. Hong, K.; Rubner, M.F., *Thin Solid Films*, **1988**, *160*, 187.
78. Collard, D.M.; Fox, M.A., *J. Am. Chem. Soc.*, **1991**, *113*, 9414.

Syringe. Chloroform and isopropanol used to dissolve samples were both spectroscopic grade (American Chemicals Ltd.), and were used as received. Blank isotherms were run using neat solvent to ensure that they contained no surfactant impurities. 15 minutes was allowed for evaporation of solvent unless otherwise specified. Both the TM-C_n-Fc and TE-C_n-Fc series of compounds were examined, as were the model compounds I, II, III and IV. These are shown in Figures 24 and 25.

Polymerization studies employed an aqueous $FeCl_3$ (J.T. Baker Chemical Co.) subphase. Two types of polymerization experiment were performed. The first involved application of the sample solution to a subphase that already contained $FeCl_3$. Concentrations of this subphase ranged from 0.01mM to 0.01M $FeCl_3$. The second experiment involved application of the sample solution to a subphase containing no $FeCl_3$, and compressing the sample to a pre-determined surface density, with a corresponding degree of order and surface pressure. After this surface density was achieved, 20ml of a concentrated $FeCl_3$ solution (0.5M) was added to the subphase, in which a concentration of 0.01M was slowly established. Care was taken to distribute the concentrated solution in such a way as to avoid forming areas of high $FeCl_3$ concentration. Following the addition of $FeCl_3$, the change in surface pressure was monitored as a function of time.

LB films of monomers and polymers were formed using the KSV surface film balance, with dipping rates of 2 and 5mm/min. Evaporated gold on glass was used as the substrate. The gold was soaked in hot chloroform for at least 1 hour prior to deposition. The substrate was then immediately submerged into the subphase prior to the spreading of the sample. LB films were deposited upon withdrawal of the gold through the Langmuir film of the sample, which was effected at surface pressures ranging from 5 to 20mN/m. Atomic force microscopy (AFM), using a Digital Nanoscope III in height mode, was used to characterize all LB films.

II.4.3. Results and Discussion

II.4.3.1. Orientation of Molecules at the Air/Water Interface

The results from the isotherm studies are listed in Table 7. A typical isotherm from the thiophene series, that of TE-C_{12}-Fc, is shown in Figure 43, with the relevant parameters indicated. In both the TM-C_n-Fc and TE-C_n-Fc series the lift-off molecular areas (A_{on}) and the areas at which the phase transition begins (A_t) increased with increasing length of the alkyl spacer (n). The surface pressure at which the phase transition begins (π_t) decreased slightly with increased n. The limiting molecular areas (A_{lim}), on the other hand, exhibited no discernable trend with n.

The extensive plateau in the isotherm between A_t and A_{lim} suggests that considerable ordering occurs during the transition from an expanded phase to a condensed phase. Given this, and the generally large values of A_{on}, it is likely that the molecules are initially fully extended on the water surface in an anisotropic fashion, with both end groups interacting with the water surface. A rough determination of the area required for a horizontally oriented TE-C_{12}-Fc molecule using space-filling models gives 144Å^2, compared with an observed A_{on} for TE-C_{12}-Fc of 150Å^2. Only poor interaction between lipophilic chains would occur, as the relative bulkiness of the thiophene and ferrocene moieties would prevent good packing of these chains. Presumably, reduction of the area available per molecule results in extensive ordering. This would involve orienting the molecules perpendicular to the water surface at some critical surface pressure, π_t, to achieve a highly ordered monolayer. This description is consistent with the variation of A_{on} and A_t with alkyl spacer length, and the existence of a similarity in A_{lim} values amongst all of the thiophene/ferrocene compounds measured, since the chain length differences would only be manifested in the A_{on} and A_t values, and not in the A_{lim} values. It should be noted, however, that A_{lim} values are too small to be consistent with a monolayer at high compression values, and therefore some type of multilayering must occur. The A_{lim} value of another surface active ferrocene derivative has been reported to

TABLE 7 Data obtained from compression isotherms of TM-C_n-Fc and TE-C_n-Fc compounds.

Compound	A_{on} (Å^2/molecule)	A_t (Å^2/molecule)	A_{lim} (Å^2/molecule)	π_t (mN/m)
TE-C_6-Fc	57	37	8	4
TE-C_8-Fc	103	74	19	3.8
TE-C_{10}-Fc	137	97	17	3.8
TE-C_{12}-Fc	150	110	18	3.3
TE-C_{16}-Fc	160	123	16	3.2
TM-C_6-Fc	38	25	14	4.5
TM-C_8-Fc	102	68	12	3.2
TM-C_{10}-Fc	110	83	13	3.2
I	121	86	-*	3.5
II	97	79	25	3.5
III	80	25	16	11.7
IV	62	41	11	16

* A second phase transition to a highly condensed state was not observed.

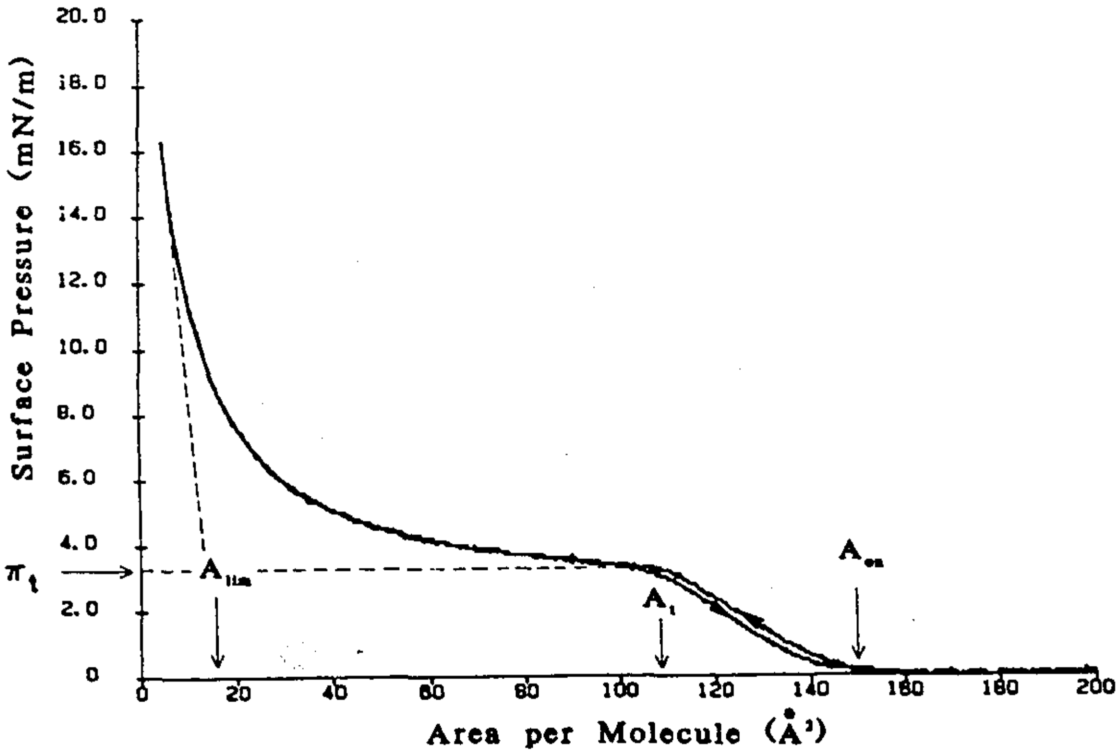

Figure 43. An isotherm of TE-C_{12}-Fc, which is typical for the TM-C_n-Fc and TE-C_n-Fc series. The onset area (A_{on}), area at which a transition occurs (A_t), limiting area (A_{lim}) and phase transition surface pressure (π_t) are indicated. Compression was followed by expansion, both with rates of 30mm/min at 25°C.

be 42Å^2 [65], further supporting the idea of multilayering in the present study. Another report of ferrocene ester derivatives in Langmuir films [79] suggests that, depending on the orientation of the ferrocene (with cyclopentadienyl rings parallel or perpendicular to the water surface), the limiting area will be 23 or 45-46Å^2/molecule, respectively. The latter area is difficult to reconcile, however, with an examination of simple space-filling models. The observed multilayering has the feature of being reversible, and is not like the catastrophic collapses that occur for molecules such as fatty acids [80]. It is largely the result of the poor interactions between lipophilic chains, caused by the bulky head groups.

The model compounds were examined to allow the specific thiophene and ferrocene functionalities to be studied independently, and thus to allow assignment of the various features in the isotherms of the TM-C_n-Fc and TE-C_n-Fc series. The data from these studies is included in Table 7. The isotherm of the thiophene/phenyl compound, (I), showed a similar shape to the isotherms for TE-C_{10}-Fc and TM-C_{10}-Fc, with comparable A_{on}, A_t and π_t values. The A_{lim} value for I was however smaller than those of TE-C_{10}-Fc and TM-C_{10}-Fc. The bis-ferrocene compound, II, on the other hand, had a π_t similar to the thiophene/ferrocene compounds, but has a larger A_{lim} than any of the other compounds reported here. Furthermore, the ferrocene alcohol and alkane derivatives (III and IV respectively) have much higher π_t values, but similar A_{lim} values to the thiophene/ferrocene compounds.

Given these observations, it is proposed that upon compression of the thiophene/ferrocene compounds, the ferrocene ester moiety of the compound remains on the water surface, while both the thiophene group and the linking alkyl chain are driven into the air phase. The hydrophilicity of the ester group and the lipophilic interactions between alkyl chains would serve to stabilize this configuration. Both TE-C_n-Fc and TM-

---

79. Nakahara, H.; Katoh, T.; Sato, M.; Fukuda, K., *Thin Solid Films*, **1988**, *160*, 153.
80. Langmuir, I., *J. Am. Chem. Soc.*, **1917**, *39*, 1883.

C_n-Fc would be expected to exhibit similar behaviour when they adopt this orientation, since the only difference between the two series is at the thiophene end of the molecules. This is, in fact, what is observed.

It is interesting to note the similar behaviour of I and the thiophene/ferrocene compounds. This suggests that the phenyl ester moiety has a similar hydrophilicity to the ferrocene ester moiety, although the small A_{lim} value for I suggests it has more of a propensity for multilayering at high compression than do the thiophene/ferrocene compounds.

In the case of the bis-ferrocene, II, the large A_{lim} suggests that multilayering does not occur as readily for these compounds. The small A_{on} value relative to TE-C_{12}-Fc suggests that at the onset of surface pressure, the alkyl chains are already looped into the air to some extent. The similar low values of π_t for the bis-ferrocene compound, II, and I, TE-C_n-Fc and TM-C_n-Fc, are probably a reflection of the poor lipophilic interactions between molecules, due to the two large head groups in all these molecules.

The ferrocene alcohol and alkyl derivatives (III and IV respectively) show A_{lim} values similar to the thiophene/ferrocene compounds. This suggests that III and IV also have a tendency to multilayering. On the other hand, III and IV show much higher π_t values. This indicates that the observed phase transition for these compounds involves different energies than those of II and I, TE-C_n-Fc and TM-C_n-Fc. The possible nature of their phase transitions is described below.

The alcohol group of III probably associates with the water phase upon compression, while the ferrocene group partitions into the air phase. The π_t is higher than for a compound such as the bis-ferrocene, II, however, because of stronger interactions between hydrocarbon chains on the water surface. The hydroxyl group is not large enough to inhibit these interactions, as do the larger head groups such as thiophene, phenyl and ferrocene.

Compound IV is most likely oriented with the alkyl group protruding from the water, and the ferrocene ester group at the water surface, as for TE-C_n-Fc, TM-C_n-Fc, and II. The high π_t required to achieve this orientation may also be explained by attractive interactions between the hydrocarbon chains in the expanded state, as for the ferrocene alcohol, III. The surface water molecules would then form a highly ordered phase around the resulting alkyl aggregates for both these compounds. This would add stability to the hydrocarbon chains, and make it more difficult to reorganize them in an ordered monolayer above the water surface. Intermolecular interactions between hydrocarbon chains is manifested not only in a higher π_t but in a smaller A_{on} for both compounds. Furthermore, it would not occur with I, TE-C_n-Fc, or TM-C_n-Fc because of their bulky thiophene groups.

II.4.3.2. Monolayer Dynamics

Hysteresis was observed in the isotherms of both TE-C_n-Fc and TM-C_n-Fc. This hysteresis was observed to vary with three experimental parameters: the compression rate, the time allowed for solvent evaporation, and the molecular weight of the thiophene/ferrocene compound.

The expansion of a compressed monolayer at an air/water interface often exhibits some hysteresis. Coherent films exhibit a hysteresis in their isotherms which becomes more pronounced as the target surface pressure is increased [81]. For the most part, the changes manifested in this hysteresis are reversible. In other cases, when compression is carried too far, multilayers are formed which cannot revert to monolayer dimensions upon expansion, probably due to strong three-dimensional interactions [80]. The thiophene/ferrocene compounds, on the other hand, exhibit a hysteresis which becomes more pronounced at decreased compression/expansion rates. Furthermore the changes indicated by this hysteresis are not reversible. This can be explained if the molecules

---

81. Crisp, D.J., *J. Colloid Sci.* **1946**, *1*, 161.

undergo a physical or chemical change (for example, aggregation) which is promoted by the compressed state, and which makes the re-expanded monolayer more condensed. The degree to which this type of change occurs would be related to the time the molecules spent in the compressed state.

To test whether this was indeed the case, two experiments were performed. In each case, TE-C_{12}-Fc in $CHCl_3$ was kept on the water surface for a total of 90 minutes. In one case (i) the solvent evaporation period was 60 minutes, and compression and expansion were 15 minutes each. In the second case (ii), the solvent evaporation period was 30 minutes, and compression and expansion processes were 30 minutes each (Figure 44). The compression isotherms show smaller A_{on} and A_t values for the 60 minute evaporation (i) than the 30 minute evaporation (ii). On the other hand, in the expansion isotherms the monolayer that spends the longest time in the compressed state (ii) has the smaller A_{on} and A_t values. If a physical or chemical change is responsible for the hysteresis, it would have to be a change that could occur in both the expanded and the compressed states, but which would favour the compressed state. Another explanation for this hysteresis is that the molecules leave the air/water interface over time. This process could only be accomplished by evaporation or dissolution. Although dissolution of such large organic molecules may seem unusual, it is worth noting that the resulting concentrations in the aqueous subphase would be on the order of only 0.1μM. Furthermore, if a chemical change were effected, it could render the molecules more soluble, and dissolution might then follow.

The hysteresis phenomenon was also observed to increase with decreasing molecular weight. This would support either an evaporation or dissolution mechanism, as both phenomena would be more prominent with smaller molecules. A physical or chemical change, on the other hand, might not be expected to show such a trend, and may perhaps be ruled out by these results.

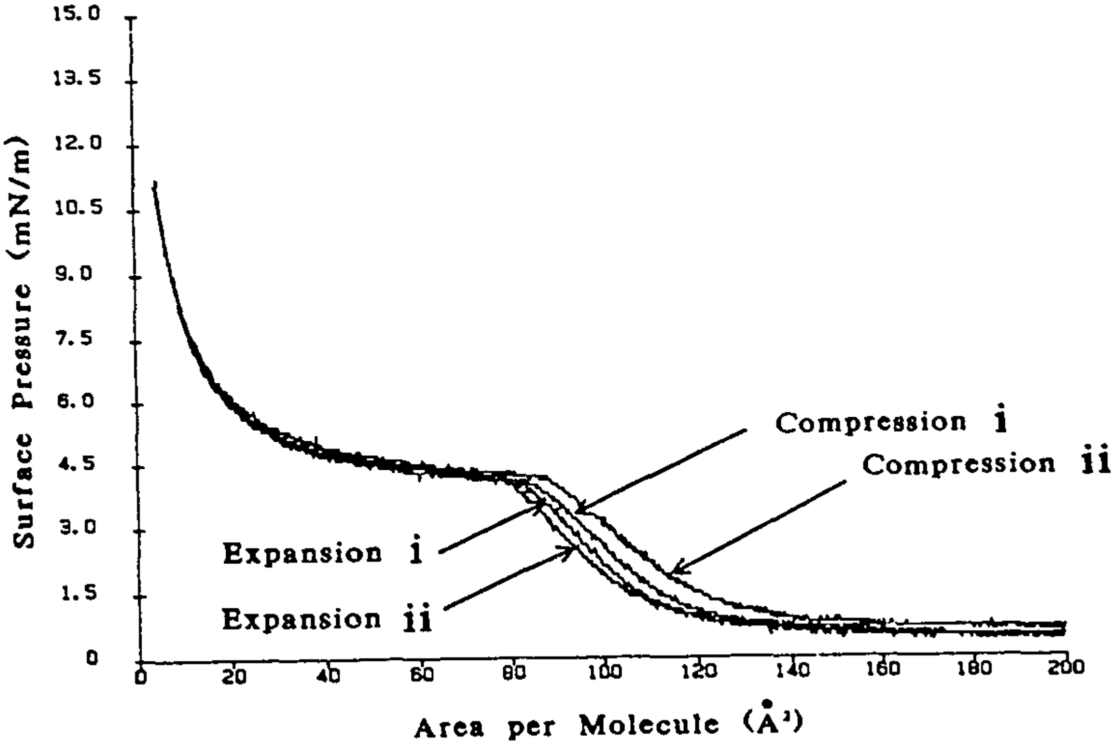

Figure 44. A compression rate/evaporation time study of TE-C_{12}-Fc. I) Solvent evaporation period of 60min, compression and expansion each 15min (30mm/min). II) Solvent evaporation period of 30min, compression and expansion each 30min (15mm/min).

To verify the stability of the films during compression, an isotherm of TE-C_{12}-Fc was recorded at a constant area. This involved adding known increments of sample solution to the water surface and allowing the surface pressure to stabilize between additions. In this way, surface pressures are recorded for a range of molecular areas. The results are plotted in Figure 45, along with the compression isotherm for comparison purposes. The constant area isotherm is similar to that measured by compression of a fixed number of sample molecules. The slight differences may indicate kinetic effects that cause a lag in reaching a stable surface pressure (for the constant area isotherm) and/or in reorganising the sample molecules (for the compression isotherm). Furthermore, the hysteresis described above, although minimal for TE-C_{12}-Fc, could also contribute to differences between the two isotherms. The fact that the constant area and compression isotherms are essentially the same indicates that the orientational phase transition observed for these compounds at the air/water interface is a reflection of the surface density of the molecules, and not an artifact brought about by the action of compression of the film on the water surface.

II.4.3.3. Temperature Effects

The effect of temperature on the isotherm of TE-C_{12}-Fc was examined to provide insight into the nature of the phase transition (Figure 46). An increase in temperature caused a decrease in π_t while the A_{lim} values increased as the temperature is increased. One result of this is the loss of the plateau region at high temperatures.

From this data the entropy and enthalpy of the phase transition involving reorientation of the thiophene/ferrocene molecules from the horizontal position to the vertical position may be calculated. Using the modified two-dimensional Clapeyron equation [82]

$$\Delta H = T\Delta A(d\pi/dT - d\gamma_o/dT) = T\Delta S \qquad (11)$$

---

82. Motomura, K., *Adv. Colloid Interface Sci.* **1980**, *12*, 1.

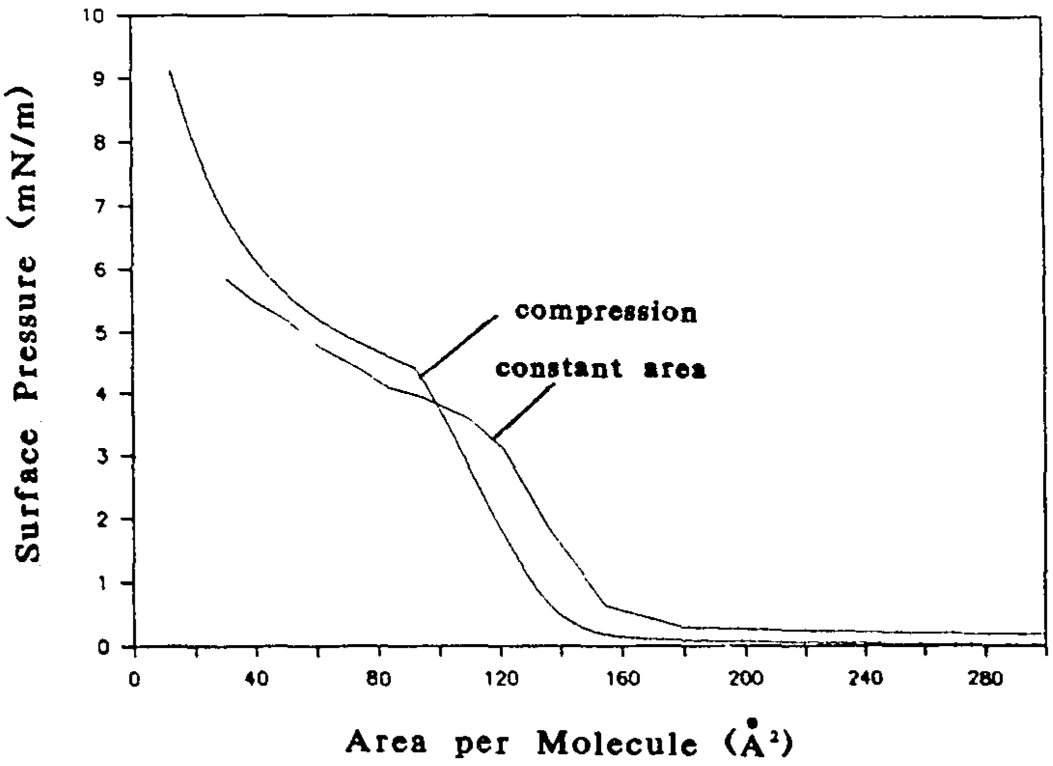

Figure 45. The isotherm of TE-C_{12}-Fc measured at a constant area (780cm²) at 25°C, by addition of defined increments (5-50µl) of sample stock solution (2mg/ml). The compression isotherm for the same compound with a compression rate of 10mm/min is shown for comparison.

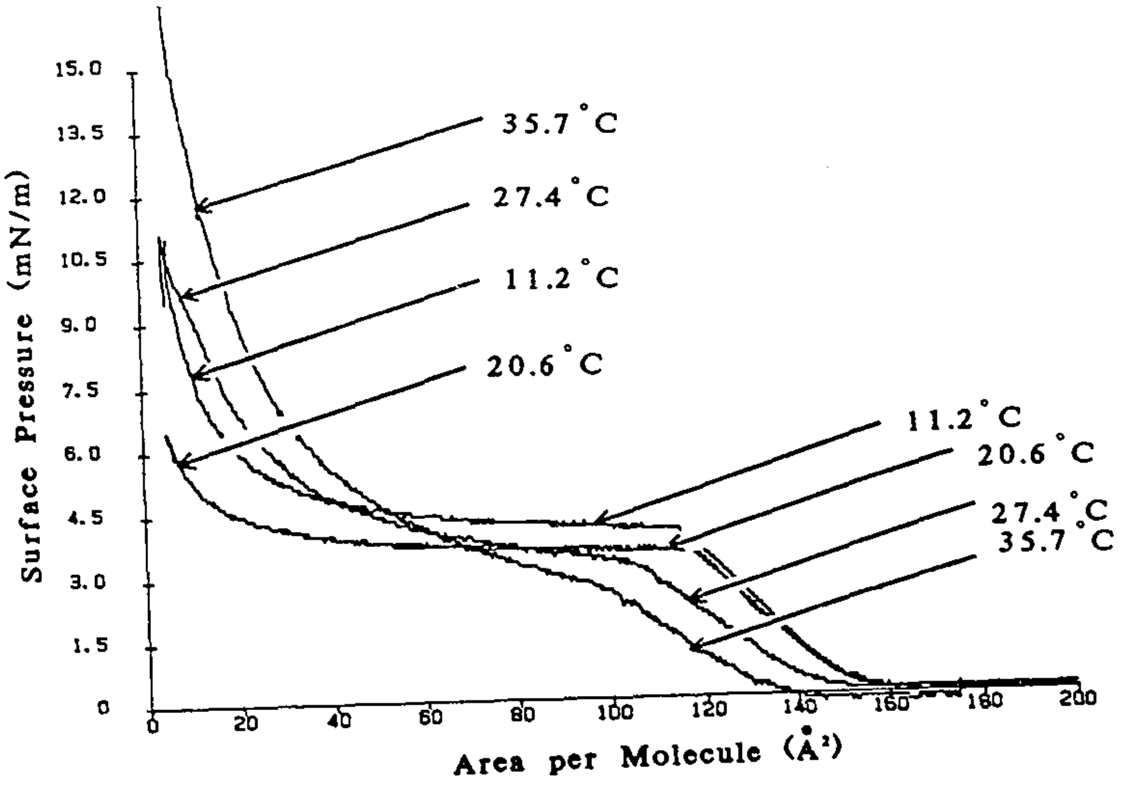

Figure 46. A temperature study of TE-C_{12}-Fc. Compression isotherms were collected at 11.2, 20.6, 27.4, and 35.7°C using compression rates of 30mm/min.

in which ΔA is the change in molecular area over the plateau of the phase transition (negative in sign), the first differential term is derived from a plot of π_t vs T, and the second differential term corrects for the temperature dependence of the surface tension of pure water, γ_o.

From this calculation we obtain $\Delta H = -3$kcal/mol and $\Delta S = -10$eu. Although π_t decreases slightly with increasing temperature, γ_o decreases even more sharply with increasing temperature and hence the entire expression in brackets is positive. Because ΔA is negative, the phase transition is slightly exothermic. The negative ΔS also suggests that the Langmuir film proceeds from a less ordered state to a more ordered state upon compression.

II.4.3.4. LB Films

Attempts to make LB films from the TE-C_n-Fc series were successful for the deposition of one monolayer upon withdrawal of the substrate. The best substrates are mica and gold evaporated onto glass. The transfer ratios were 1.0 ± 0.1, for depositions both before and after A_t. Deposition upon immersion was not successful.

When multilayers were attempted, the films deposited upon withdrawal were repeatedly lost upon immersion, as indicated by negative transfer ratios, usually -1.0 ± 0.2. Thus, neither **Y**, **X** nor **Z** multilayer LB films were possible.

The explanation for this lack of success is similar to that for the collapse and multilayering of the Langmuir films upon high compression. The lack of good packing, and thus the lack of strong attractive interactions between lipophilic chains for these molecules, results in an LB film that has very little cohesiveness, and thus it returns to the water surface upon its immersion into the subphase. It did not appear to improve the adhesion of the LB film to the substrate when the gold evaporated on glass was used as the substrate.

II.4.3.5. Polymerization at the Air/Water Interface

From the electrochemical studies described in Section II.3.3., it was established that the TE-C_n-Fc compounds can be electrochemically polymerized at a Pt electrode. The TM-C_n-Fc compounds, however, have a higher oxidation potential that is difficult to access experimentally. Hence, chemical polymerization at the air/water interface was attempted only with the TE-C_n-Fc series. $FeCl_3$ was used as the polymerizing agent, as it is the oxidizing agent of choice for thiophenes [83].

When TE-C_{12}-Fc was spread on a subphase of aqueous 0.01M $FeCl_3$, the resulting isotherm was very different from that observed on a pure water subphase. The two isotherms are shown in Figure 47 for comparison purposes. A_{on} for the Langmuir film on $FeCl_3$ was 20Å^2 less than A_{on} of TE-C_{12}-Fc on pure water. The phase transition feature was all but lost in the presence of $FeCl_3$, and at small areas, the film on $FeCl_3$ was much less compressible, indicating less propensity for multilayering behaviour. These films may be expanded and recompressed, resulting in an identical compression isotherm. Thus, these new compression isotherms are completely reversible.

The large change in the shape of the π-A isotherm was observed to occur very soon after the spreading of the sample solution. Compressions effected either immediately after sample spreading or 70min after sample spreading showed only slight differences, the former having a larger (+10Å^2) A_{on} value than the latter, while the latter exhibiting larger (+1mN/m) surface pressures at small areas (<40Å^2/molecule). Lower concentrations of $FeCl_3$ caused the same changes in the isotherm, but to a lesser extent.

LB films of the modified film of TE-C_{12}-Fc from the $FeCl_3$ subphase were deposited on evaporated gold at various surface densities, and compared to an LB film of TE-C_{12}-Fc deposited from a pure water subphase onto evaporated gold. The transfer ratios of the former films were poor (>1), indicating a constant condensation of the film

---

83. Leclerc, M.; Diaz, F.M.; Wegner, G., *Makromol. Chem.*, **1989**, *190*, 3105.

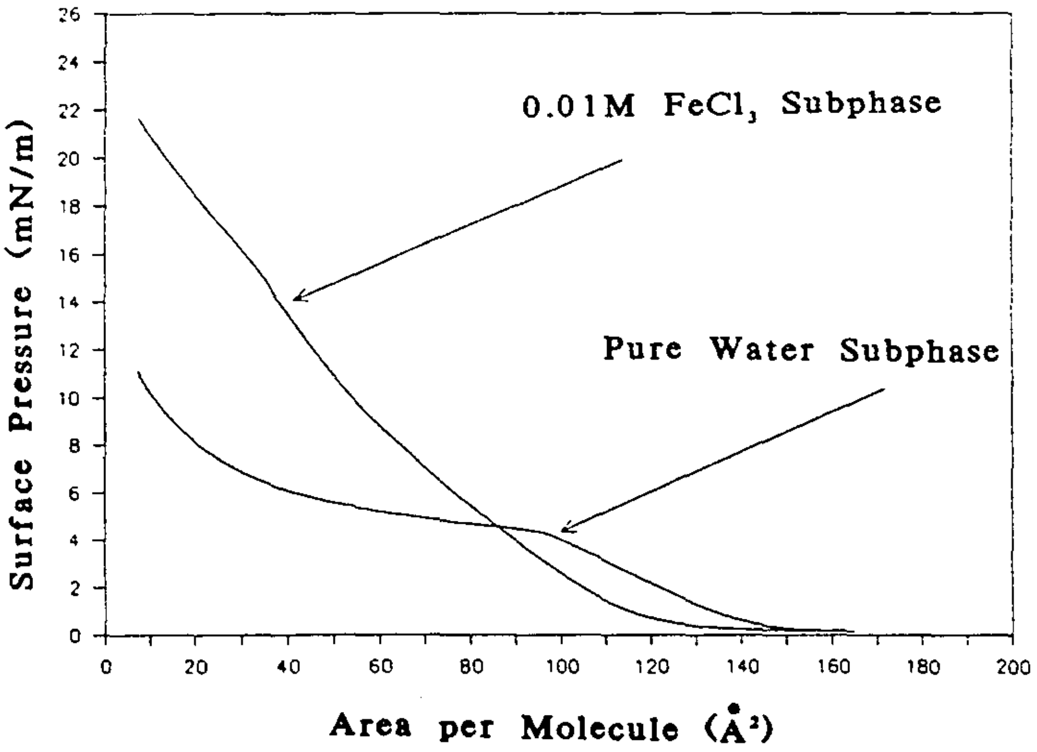

Figure 47. Compression isotherms of TE-C_{12}-Fc on pure water and 0.01M $FeCl_3$ at 25°C, at compression rates of 10mm/min.

as deposition is effected. The transfer ratio of the latter, on the other hand, is good (1 ± 0.1). AFM images of the TE-C_{12}-Fc from the $FeCl_3$ subphase indicate the presence of clumps of material. These clumps are very large (3-5μm in diameter), with well-defined edges, and separated by large areas of bare substrate, indicating that the clumps are several molecules thick. The AFM images indicate heights of 10-30nm for the clumps. Although the clumps are deposited as LB films, they appear to be arranged in no particular order. They consist, instead, of smaller particles (60-120nm), assembled into the larger clumps. The LB film of the TE-C_{12}-Fc deposited from the pure water was not amenable to characterization by AFM. This is probably because the material in this film is redistributed by the atomic force probe, and therefore cannot be readily imaged. These results do however confirm the presence of a new (presumably polymeric) material when TE-C_n-Fc compounds are applied to a subphase containing the oxidant $FeCl_3$.

The same chemical polymerizations were also attempted with a compressed Langmuir film of TE-C_{12}-Fc. Thus, TE-C_{12}-Fc was compressed to 3.6mN/m (just before A_t) and 5.3mN/m (just before A_{lim}), and $FeCl_3$ was then added to the subphase below these two films. In both cases, several hours elapsed before substantial surface pressure changes were recorded, unlike the immediate reaction observed in the expanded Langmuir film of the same compound. The surface pressures are shown in Figures 48a and 48b as a function of time for both of these films.

Despite the apparent lag time, these two films behave in the way expected, if the same process is occurring in the ordered film as in the expanded film. Thus, the surface pressure in the film of lower surface density (and order) decreases, and the surface pressure in the film of higher surface density (and order) increases. Furthermore, if either of these films are expanded and compressed after the aforementioned changes in surface pressure occur, the isotherm is virtually identical to that shown in Figure 47 for TE-C_{12}-Fc on 0.01M $FeCl_3$. More quantitative information, specifically regarding the kinetics of the reaction, is difficult to obtain, as it is impossible to achieve immediate and uniform

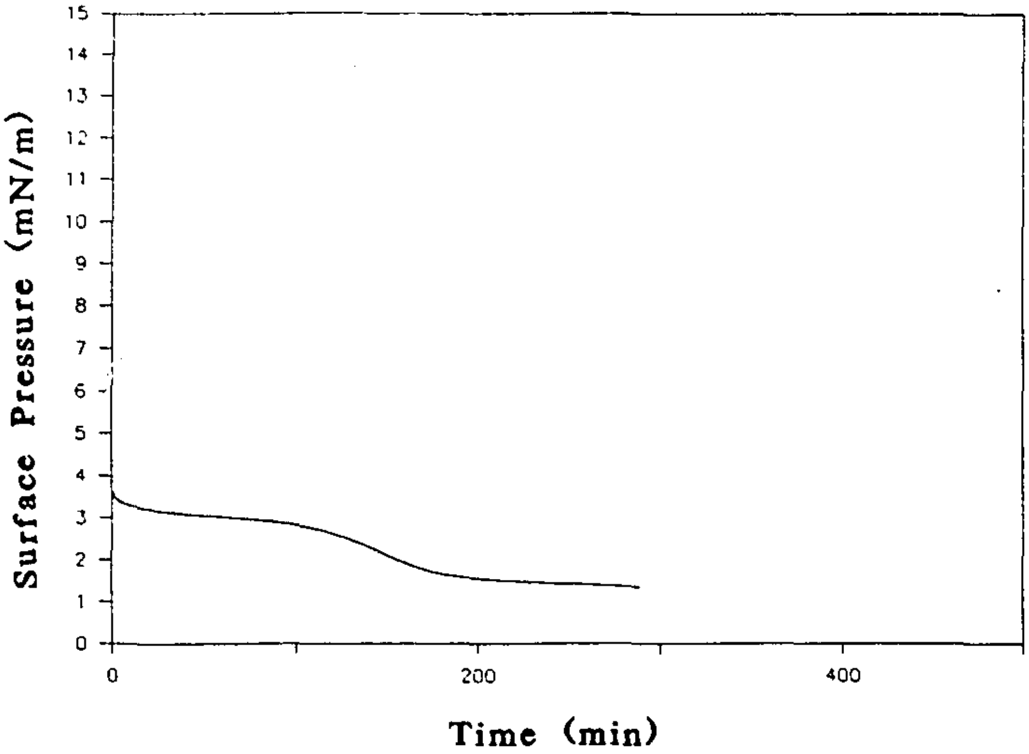

Figure 48a. Surface pressure as a function of time for a Langmuir film of TE-C_{12}-Fc on a 0.01M $FeCl_3$ subphase, which has an initial surface pressure of 3.6mN/m. The addition of FeCl3 to the subphase occurred at time=0min.

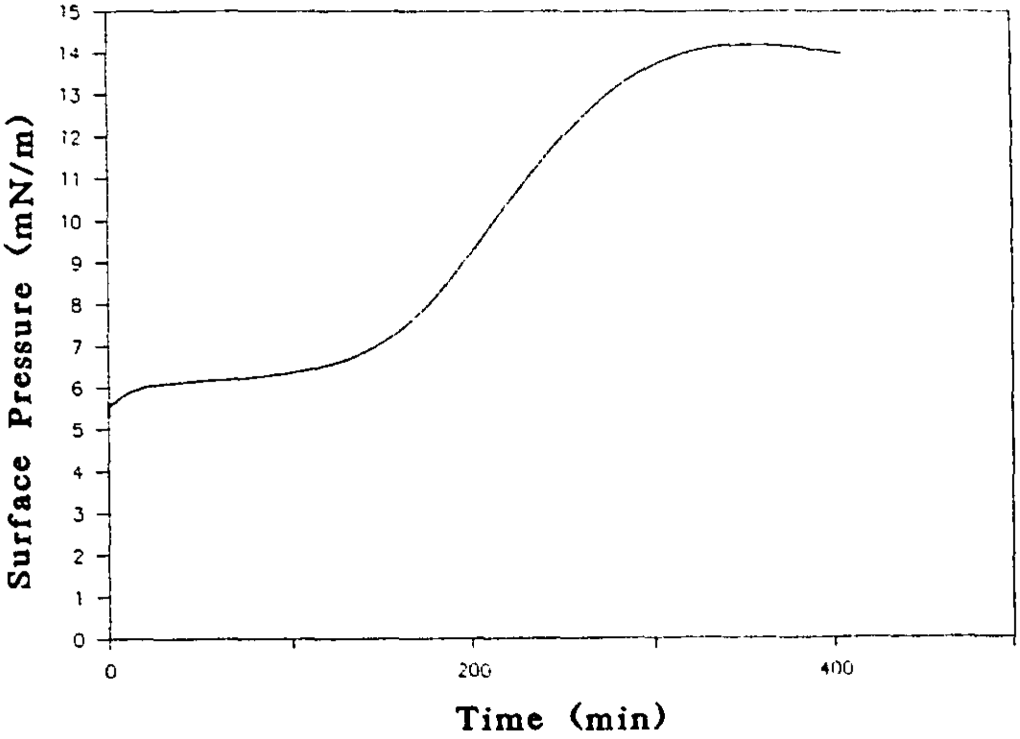

Figure 48b. Surface pressure as a function of time for a Langmuir film of TE-C_{12}-Fc on a 0.01M $FeCl_3$ subphase, which has an initial surface pressure of 5.3mN/m. The addition of FeCl3 to the subphase occurred at time=0min.

distribution of $FeCl_3$ in the subphase in these experiments. Nevertheless, the results suggest that the observed reaction is favoured when the TE-C_{12}-Fc molecules are entirely prone on the water surface instead of oriented in some fashion perpendicular to the surface.

Two of the model compounds (I and IV) were also spread onto the $FeCl_3$ subphase. The isotherm of I on the $FeCl_3$ subphase was no different from the isotherm on pure water. The isotherm of IV on the $FeCl_3$ subphase, however, was substantially different from that on the pure water, with an A_{on} value about 20Å^2 less than the A_{on} value on pure water. This is consistent with the ferrocene moiety being oxidized by the $FeCl_3$.

It is proposed that a new material is formed from the TE-C_{12}-Fc on an aqueous $FeCl_3$ subphase. The evidence for this is the dramatic change in the TE-C_{12}-Fc isotherm on the $FeCl_3$ subphase, and the AFM detection of clusters of material in the TE-C_{12}-Fc LB film from the same subphase. Presumably, this new material results from $FeCl_3$-mediated oxidation of TE-C_{12}-Fc. Specifically, the ferrocene unit is oxidized to the ferricenium ion by the $FeCl_3$ in the subphase, as is apparent from the data for IV. It is also believed that the thiophene units of TE-C_{12}-Fc are being oxidized, and subsequently polymerize to form the clusters that are detected by AFM. Since the isotherm of I is unchanged by the $FeCl_3$ subphase, the ferricenium moiety must somehow be involved in the thiophene polymerization. Whether this is a mediatory type of role, or whether the charge on the ferricenium unit simply induces aggregation and subsequent polymerization of the thiophene monomers, cannot be determined at the present. In any case, the clusters are believed to be oligomers or polymers of the thiophene/ferrocene molecules, with the pendant ferricenium units oriented in the water.

II.4.4. Summary

Two series of thiophene/ferrocene compounds have been shown to form Langmuir films at the air/water interface. These films undergo an orientational phase transition when their surface density is increased to a critical point (A_t). Upon further concentration at the air/water interface these molecules undergo a reversible multilayering process. The orientation of these compounds is believed to be one where the ferrocene ester moiety resides at the water surface, and the thiophene moiety protrudes from the water surface. The thermal properties of the films indicate that the reorientation results in an increase in the order of the system.

These molecules were spread on an oxidizing subphase, in order to polymerize them through the thiophene moiety. This resulted in the formation of a new, presumably polymeric material at the air/water interface, as evidenced by the different isotherm. The LB films of this new material indicated the presence of clumps that are not detectable in the monomer LB films, thus providing further evidence for a polymerization.

CONCLUSIONS AND FUTURE PLANS

This thesis has focused on the synthesis and characterization of ultrathin films, and the behaviour of various species when incorporated into an ultrathin film. Several routes to ultrathin films have been explored, each making use of different properties of the molecules involved to impose limits on the thickness of the films.

The air/water interface is often used as a template for monolayer formation, where molecules may align themselves according to the balance between their hydrophilicity and hydrophobicity. In this work, molecules with no such balance were nonetheless found to spread at the air/water interface, where they were observed to form well-defined multilayers. Fullerenes and dendrimers, both highly hydrophobic, form ultrathin films on the water surface, as evidenced by the change in surface tension of the water. This is believed to arise through the creation of a new interface, the fullerene/water or dendrimer/water interface, with a surface tension that is different than that of the air/water interface. This process is believed to occur through the formation of aggregates of hydrophobic molecules at the air/water interface, followed by the coalescence of these aggregates to form a continuous, hydrophobic film. This point of coalescence is significant, in that it marks the transition from an aggregate state to a film with properties of bulk material. The transformation of the air/water interface to the fullerene/water or dendrimer/water interface is thus a consequence of the transition from aggregates to bulk material. If a real nanotechnology is to develop, the intricacies of the "nanoscale", including this transition from aggregates to bulk, will be of paramount importance.

The polyimides studied at the air/water interface offer another type of "multilayer". Rather than aggregates, it is believed that the polyimides take on a secondary structure when spread at the air/water interface that allows them to form a coherent film on the water surface. Although these films are believed to consist of one layer of polymer molecules, and so are not strictly speaking multilayers, their compression isotherms indicate that the whole molecule is not located at the air/water interface, and thus their films must be considered to be three-dimensional. The rules that govern such "in-between" states are of crucial importance, as ultrathin films gain acceptance in practical applications.

Helices have been observed for some polypeptides spread at the air/water interface, and are a possible candidate for the polyimide secondary structure. Such a secondary structure may allow the formation of a Langmuir film from molecules that are not normally amenable to assembly at the air/water interface. The role of rigidity in the formation of Langmuir films and LB films has been explored here. Materials that do not behave as rigid rods in the bulk may still exhibit rigidity on the water surface, if they take on a new conformation with corresponding new mechanical properties.

A series of thiophene/ferrocene compounds was synthesized to provide the basis for a supramolecular structure: ultrathin films with redox activity and electroactivity. If a nanotechnology is to become viable, this approach of design on a molecular level will be imperative. The assembly of the molecules must be controlled by the molecules themselves, as it is only by creating a self-assembling system, through appropriate molecular design, that the "nanoscale" may truly be accessed.

Two approaches to the assembly of ultrathin films from the series of polymerizable thiophene/ferrocene compounds were taken. One approach used the air/water interface as a template, the other relied upon an electrochemical deposition process. At the air/water interface, a chemical polymerization was effected in two dimensions, and the resulting material was deposited in an ultrathin film by the Langmuir-Blodgett technique. Electrochemically, these molecules were found to be intrinsically limited in their electropolymerization to one monolayer. Electrostatic repulsion is believed to prevent polymer deposition beyond this thickness.

Ironically, it is most likely the electrochemical deposition that produces the more ordered film. LB deposition techniques generally rely upon highly ordered films at the air/water interface, and thus generally produce highly ordered films on a solid substrate. Once chemical polymerization is initiated at the air/water interface for these particular thiophene/ferrocene molecules, however, they appear to lose much of their initial order, as is evidenced by the resulting AFM images and deposition data. The electrochemically polymerized material, on the other hand, is known to exist in an ultrathin film that is on average one monolayer thick, with a Cu^{2+}-permeable area of approximately 20-30%. The number of ferrocene molecules affixed to the electrode surface, coupled with a knowledge of the polymer-coated Pt surface accessible to Cu UPD, is evidence for this assertion. It is reported that in the inital stages of polymerization, polythiophene is fairly ordered, as indicated by the high conductivities of ultrathin (200nm) polythiophene films [18]. Thus it may be postulated that these electropolymerized monolayer films of polythiophene are in a highly ordered configuration.

Further comparison of the two films made from the same material by different routes would be very informative. The surface film balance allows the concentration and configuration of the reactant molecules to be precisely controlled during the surface reaction. With this degree of control over experimental conditions, a better understanding of these particular polymerization reactions could be reached. This would lead to the ability to design materials much more precisely than is now possible.

The electrochemical polymerization of these bifunctional molecules, with the intrinsic limitation to the formation of one monolayer, opens up many possible avenues of research. The monolayer of functional groups offers the possibility of facile derivatization of the modified electrode surface. The coverage would be predetermined by the degree of coverage of ferrocene groups, which would provide the template for subsequent functionalities.

With the present knowledge of this self-limiting system, new molecules can be designed with this type of self-imposed constraint to their polymerization. The present system relies upon an electrochemical "switch", the ferrocene couple, to limit the polymerization to one monolayer. Other switches could be investigated, such as those controlled photochemically or through pH changes. This could lead to a modified resist strategy, in which a mask is used to render selected areas of a surface repulsive to incoming monomer, restricting polymer deposition to a desired pattern. It might also be profitable to start with a Langmuir-Blodgett film whose molecular composition may be controlled precisely, rather than a bare electrode surface. This could provide the ideal template on which to base this type of system.

Finally, the common thread through all of these ultrathin film systems is the fact that each allows for observation of the formation process of the film itself. The aggregates of fullerenes and the network of dendrimers at the water surface, the secondary structures adopted by the polyimides, the polymerization of thiophene on the electrode and on the water surface, all provide the opportunity to study the films from their <u>inception</u>. Their process of assembly of molecules to aggregates to bulk material is experimentally observable by the very means of their formation. For example, monitoring the surface tension of the water as the concentration of sample molecules is varied offers a wealth of information. AFM is useful in characterizing the topology of resulting LB films. Electrochemistry provides the means both to polymerize and to monitor the polymerization process. For future studies, there are still further techniques to apply to these challenges. Investigations at the air/water interface are amenable to such techniques as reflectance spectroscopy, surface potential measurements, and fluorescence microscopy. These may provide the means for tracking the films' formation from their earliest stages. Spectroelectrochemical studies can offer *in situ* information regarding the electropolymerization as well. Finally, elegant electrochemical techniques more complex than those used in this work may allow specific mechanistic details of the electropolymerization process to be gathered.

Before nanotechnology becomes a reality, there is extensive groundwork to be laid in "nanoscience". The development of absolute control over the molecular architecture of nanoscale systems is critical. The design and synthesis of self-assembling systems must be the goal of future work. In this thesis, progress has been made towards the design of self-assembling nanostructures. The concept of two-dimensional molecular architectures have been explored here. It is only through this type of fundamental approach to nanoscience that a nanotechnology may ever emerge beyond futuristic prophecies in scientific commentary.

CONTRIBUTIONS TO ORIGINAL KNOWLEDGE

Langmuir films of fullerenes C_{60} and C_{70} were formed at the air/water interface. These were shown to consist of multilayers of fullerenes with uniform and consistent thicknesses. A transition attributed to a reorientational process in the C_{70} multilayer film was observed and characterized. The work of compression for these films was also calculated.

Langmuir films of 1,3,5-phenylene-based hydrocarbon dendrimers were formed at the air/water interface. These films were shown to consist of a network of dendrimer molecules that relies upon interpenetration among these molecules to form a continuous film. Co-spread with a fatty acid, these dendrimer molecules were deposited in an LB bilayer film and characterized by AFM.

For both of these unconventional film-forming molecules, it was proposed that the observation of a change in surface tension of the water was a result of the transition from an air/water to a fullerene/water or dendrimer/water interface. This transition marks the point at which the film, previously a collection of aggregates, takes on bulk-like properties. This is the first time that such a measurement has been reported with the surface film balance.

Langmuir films of polyimides were formed from a series of highly amorphous polyimides. The polymers were believed to establish secondary structures when deposited on the water surface.

Two series of novel thiophene/ferrocene supramolecules were synthesized. These molecules are bifunctional, with a polymerizable functionality (thiophene) and a redox active functionality (ferrocene). These thiophene/ferrocene molecules were characterized electrochemically. Their electrochemical polymerization produced a surface(Pt)-adsorbed material with attached ferrocene functionalities. This new material is intrinsically limited to the formation of monolayers. Thicker film formation is impeded by the molecular architecture of the film. This is a new example of a self-regulated nanostructure. Copolymer and bilayer systems were investigated as means of further control over film thickness and composition.

These bifunctional molecules were found to form films at the air/water interface that exhibit a disorder to order phase transition upon compression. These Langmuir films were subjected to oxidative polymerization conditions in both their ordered and disordered states, and reaction was observed in both cases to produce a new, presumably polymeric material.

APPENDIX I
^{1}H NMR Data for TM-C_n-OH Series

^{1}H NMR [84]: **TM-C_6-OH** ($CDCl_3$, δ) 1.41-1.57 (8H, CH_2), 3.46 (2H, t, J=6.4Hz, OCH_2), 3.65 (2H, t, J=6.4Hz, C$\underline{H}_2$OH), 4.50 (2H, s, Th-CH2-O), 7.07 (1H, m, ThH), 7.20 (1H, s, ThH), 7.30 (1H, s, ThH); **TM-C_8-OH** ($CDCl_3$, δ) 1.34-1.60 (12H, CH_2), 3.49 (2H, t, J=6.4Hz, OCH_2), 3.65 (2H, t, J=6.4Hz, C$\underline{H}_2$OH), 4.50 (2H, s, Th-CH_2-O), 7.07 (1H, m, ThH), 7.20 (1H, s, ThH), 7.30 (1H, s, ThH); **TM-C_{10}-OH** ($CDCl_3$, δ) 1.31-1.63 (16H, CH_2), 3.49 (2H, t, J=7.2Hz, OCH_2), 3.65 (2H, t, J=7.2Hz, C$\underline{H}_2$OH), 4.50 (2H, s, Th-CH_2-O), 7.07 (1H, m, ThH), 7.20 (1H, s, ThH), 7.30 (1H, s, ThH).

---

84. For the reporting of all NMR and MS data, **Th** is used to designate the thiophene moiety, **Fc** is used to designate the ferrocene moiety, **Cp** is used to designate a cyclopentadienyl ring on the ferrocene moiety of the thiophene/ferrocene compounds, and **Ph** is used to designate a phenyl ring.

APPENDIX II
^{1}H NMR and Mass Spectrometry Data for TM-C_n-Fc Series

^{1}H NMR : **TM-C_6-Fc** ($CDCl_3$, δ) 1.28-1.66 (8H, CH_2), 3.49 (2H, t, J=6.4Hz, OCH_2), 4.20 (5H, s, CpH), 4.21 (2H, t, J=4.5Hz, CH_2-O-(CO)), 4.39 (2H, t, J=2.5Hz, (CO)CpH), 4.51 (2H, S, Th-CH_2O), 4.80 (2H, t, J=2.5Hz, (CO)CpH), 7.07 (1H, m, ThH), 7.20 (1H, s, ThH), 7.30 (1H, m, ThH); **TM-C_8-Fc** ($CDCl_3$, δ) 1.38-1.70 (12H, CH_2), 3.49 (2H, t, J=6.4Hz, OCH_2), 4.20 (5H, s, CpH), 4.21 (2H, t, J=4.5Hz, CH_2-O-(CO)), 4.39 (2H, t, J=2.5Hz, (CO)CpH), 4.51 (2H, S, Th-CH_2O), 4.80 (2H, t, J=2.5Hz, (CO)CpH), 7.07 (1H, m, ThH), 7.20 (1H, s, ThH), 7.30 (1H, m, ThH); **TM-C_{10}-Fc** ($CDCl_3$, δ) 1.38-1.76 (16H, CH_2), 3.49 (2H, t, J=6.4Hz, OCH_2), 4.20 (5H, s, CpH), 4.21 (2H, t, J=4.5Hz, CH_2-O-(CO)), 4.39 (2H, t, J=2.5Hz, (CO)CpH), 4.51 (2H, S, Th-CH_2O), 4.80 (2H, t, J=2.5Hz, (CO)CpH), 7.07 (1H, m, ThH), 7.20 (1H, s, ThH), 7.30 (1H, m, ThH).

Low resolution MS, 70eV (m/z, relative intensity, assignment): **TM-C_6-Fc** (T=30°C) 426, 35%, $M^{+\bullet}$; 230, 51%, $FcCOOH^{+\bullet}$; 97, 70%, $ThCH_2^+$: **TM-C_8-Fc** (T=30°C) 454, 100%, $M^{+\bullet}$; 230, 56%, $FcCOOH^{+\bullet}$; 97, 73%, $ThCH_2^+$: **TM-C_{10}-Fc** (T=30°C) 258, 100%, $FcCOOCH_2CH_2^{+\bullet}$; 230, 85%, $FcCOOH^{+\bullet}$; 213, 9%, $FcCO^+$.

APPENDIX III

^{1}H NMR Data for TE-C_n-OH Series

^{1}H NMR : **FcCOO-C_6-OH** ($CDCl_3$, δ) 1.47-1.73 (8H, CH_2), 3.68 (2H, t, J=7.0Hz, CH_2OH), 4.20 (5H, s, CpH), 4.21 (2H, t, J=4.3Hz, CH_2-O-(CO)), 4.39 (2H, t, J=2.5Hz, (CO)CpH), 4.80 (2H, t, J=2.5Hz, (CO)CpH): **FcCOO-C_8-OH** ($CDCl_3$, δ) 1.41-1.74 (12H, CH_2), 3.68 (2H, t, J=7.0Hz, CH_2OH), 4.20 (5H, s, CpH), 4.21 (2H, t, J=4.3Hz, CH_2-O-(CO)), 4.39 (2H, t, J=2.5Hz, (CO)CpH), 4.80 (2H, t, J=2.5Hz, (CO)CpH): **FcCOO-C_{10}-OH** ($CDCl_3$, δ) 1.33-1.71 (16H, CH_2), 3.68 (2H, t, J=7.0Hz, CH_2OH), 4.20 (5H, s, CpH), 4.21 (2H, t, J=4.3Hz, CH_2-O-(CO)), 4.39 (2H, t, J=2.5Hz, (CO)CpH), 4.80 (2H, t, J=2.5Hz, (CO)CpH): **FcCOO-C_{12}-OH** ($CDCl_3$, δ) 1.31-1.73 (20H, CH_2), 3.68 (2H, t, J=7.0Hz, CH_2OH), 4.20 (5H, s, CpH), 4.21 (2H, t, J=4.3Hz, CH_2-O-(CO)), 4.39 (2H, t, J=2.5Hz, (CO)CpH), 4.80 (2H, t, J=2.5Hz, (CO)CpH): **FcCOO-C_{16}-OH** ($CDCl_3$, δ) 1.26-1.73 (28H, CH_2), 3.68 (2H, t, J=7.0Hz, CH_2OH), 4.20 (5H, s, CpH), 4.21 (2H, t, J=4.3Hz, CH_2-O-(CO)), 4.39 (2H, t, J=2.5Hz, (CO)CpH), 4.80 (2H, t, J=2.5Hz, (CO)CpH):

APPENDIX IV

^{1}H NMR and Mass Spectrometry Data for TE-C_n-Fc Series

^{1}H NMR : **TE-C_6-Fc** ($CDCl_3$, δ) 1.44-1.73 (8H, CH_2), 2.91 (2H, t, J=7.5Hz, ThCH_2), 3.47 (2H, t, J=7.0Hz, $C\underline{H}_2$-O-CH_2CH_2Th), 3.65 (2H, t, J=7.7Hz, $C\underline{H}_2CH_2$Th), 4.20 (5H, s, CpH), 4.21 (2H, t, J=4.3Hz, CH_2-O-(CO)), 4.39 (2H, t, J=2.5Hz, (CO)CpH), 4.80 (2H, t, J=2.5Hz, (CO)CpH), 7.01 (2H, m, ThH), 7.28 (1H, m, ThH); ^{1}H NMR : **TE-C_8-Fc** ($CDCl_3$, δ) 1.38-1.71 (12H, CH_2), 2.91 (2H, t, J=7.5Hz, ThCH_2), 3.47 (2H, t, J=7.0Hz, $C\underline{H}_2$-O-CH_2CH_2Th), 3.65 (2H, t, J=7.7Hz, $C\underline{H}_2CH_2$Th), 4.20 (5H, s, CpH), 4.21 (2H, t, J=4.3Hz, CH_2-O-(CO)), 4.39 (2H, t, J=2.5Hz, (CO)CpH), 4.80 (2H, t, J=2.5Hz, (CO)CpH), 7.01 (2H, m, ThH), 7.28 (1H, m, ThH); **TE-C_{10}-Fc** ($CDCl_3$, δ) 1.31-1.71 (16H, CH_2), 2.91 (2H, t, J=7.5Hz, ThCH_2), 3.47 (2H, t, J=7.0Hz, $C\underline{H}_2$-O-CH_2CH_2Th), 3.65 (2H, t, J=7.7Hz, $C\underline{H}_2CH_2$Th), 4.20 (5H, s, CpH), 4.21 (2H, t, J=4.3Hz, CH_2-O-(CO)), 4.39 (2H, t, J=2.5Hz, (CO)CpH), 4.80 (2H, t, J=2.5Hz, (CO)CpH), 7.01 (2H, m, ThH), 7.28 (1H, m, ThH); **TE-C_{12}-Fc** ($CDCl_3$, δ) 1.30-1.74 (20H, CH_2), 2.91 (2H, t, J=7.5Hz, ThCH_2), 3.47 (2H, t, J=7.0Hz, $C\underline{H}_2$-O-CH_2CH_2Th), 3.65 (2H, t, J=7.7Hz, $C\underline{H}_2CH_2$Th), 4.20 (5H, s, CpH), 4.21 (2H, t, J=4.3Hz, CH_2-O-(CO)), 4.39 (2H, t, J=2.5Hz, (CO)CpH), 4.80 (2H, t, J=2.5Hz, (CO)CpH), 7.01 (2H, m, ThH), 7.28 (1H, m, ThH); **TE-C_{16}-Fc** ($CDCl_3$, δ) 1.28-1.70 (28H, CH_2), 2.91 (2H, t, J=7.5Hz, ThCH_2), 3.47 (2H, t, J=7.0Hz, $C\underline{H}_2$-O-CH_2CH_2Th), 3.65 (2H, t, J=7.7Hz, $C\underline{H}_2CH_2$Th), 4.20 (5H, s, CpH), 4.21 (2H, t, J=4.3Hz, CH_2-O-(CO)), 4.39 (2H, t, J=2.5Hz, (CO)CpH), 4.80 (2H, t, J=2.5Hz, (CO)CpH), 7.01 (2H, m, ThH), 7.28 (1H, m, ThH);

Low resolution MS, 70eV (m/z, relative intensity, assignment): **TE-C_6-Fc** (T=30°C) 440, 77%, $M^{+\bullet}$; 230, 100%, $FcCOOH^{+\bullet}$; 213, 17%, $FcCO^+$; 97, 43%, $ThCH_2^+$; 83, 49%, Th^+: **TE-C_8-Fc** (T=190°C) 468, 100%, $M^{+\bullet}$; 230, 50%, $FcCOOH^{+\bullet}$; 213, 8%, $FcCO^+$; 111, 12%, $ThCH_2CH_2^+$; 97, 15%, $ThCH_2^+$: **TE-C_{10}-Fc** (T=30°C) 497, 1.2%, $M^{+\bullet}$; 369, 100%, $FcCOOC_{10}H_{20}^+$; 230, 96%, $FcCOOH^{+\bullet}$; 213, 45%, $FcCO^+$; 111, 70%, $ThCH_2CH_2^+$; 97, 20%, $ThCH_2^+$: **TE-C_{12}-Fc** (T=210°C) 524, 100%, $M^{+\bullet}$; 230, 45%, $FcCOOH^{+\bullet}$; 213, 9%, $FcCO^{+}$; 111, 14%, $ThCH_2CH_2^{+}$; 97, 13%, $ThCH_2^{+}$: **TE-C_{16}-Fc** (T=250°C) 580, 100%, $M^{+\bullet}$; 230, 40%, $FcCOOH^{+\bullet}$; 213, 12%, $FcCO^{+}$; 111, 15%, $ThCH_2CH_2^{+}$; 97, 11%, $ThCH_2^{+}$.

APPENDIX V
^{1}H NMR Data for Compounds I, II, III and IV

^{1}H NMR : **I** ($CDCl_3$, δ) 1.33-1.75 (16H, CH_2), 2.91 (2H, t, J=7.5Hz, $ThCH_2$), 3.43 (2H, t, J=7.0Hz, $C\underline{H}_2$-O-CH_2CH_2Th), 3.63 (2H, t, J=7,7Hz, $OC\underline{H}_2CH_2Th$), 4.32 (2H, t, CH_2-O(CO)), 6.97 (2H, m, ThH), 7.25 (1H, m, ThH), 7.51 (3H, m, PhH), 8.05 (2H, d, J=5.1Hz, PhH): **II** ($CDCl_3$, δ) 1.31-1.73 (20H, CH_2), 4.20 (10H, s, CpH), 4.21 (4H, t, J=4.3Hz, CH_2-O(CO)), 4.39 (4H, t, J=2.5Hz, (CO)CpH), 4.80 (4H, t, J=2.5Hz, (CO)CpH): **III** (as for **FcCOO-C_{10}-OH**): **IV** ($CDCl_3$, δ) 0.89 (3H, t, J=6.0Hz, CH_3), 1.26-1.71 (30H, CH_2), 4.20 (5H, s, CpH), 4.21 (2H, t, J=4.3Hz, CH_2-O(CO)), 4.39 (2H, t, J=2.5Hz, (CO)CpH), 4.80 (2H, t, J=2.5Hz, (CO)CpH).